MAP-based Multifunctional Organocatalysts for Asymmetric *aza*- and Generic Morita–Baylis–Hillman Reactions

A thesis submitted in partial fulfillment of the requirements for the degree of

Master of Research

by

Sviatoslav Sergeevich Eliseenko

(MSc)

Department of Chemistry and Biomolecular Sciences

Macquarie University

Sydney, Australia

26 April 2016

Table of Contents

Abstract

MAP-based trifunctional organocatalysts, containing a phosphine Lewis base, amino Brønsted base, and phenol or *N*-tosyl Brønsted acid, have demonstrated highly proficient catalysis of asymmetric *aza*-MBH reactions with an acid additive. The phosphine nucleophile (Lewis base) initiates the *aza*-MBH reaction by addition to an activated alkene (e.g. MVK). The Brønsted base, activated by the acid additive, in conjunction with the Brønsted acid, promotes the subsequent aldol and proton-transfer elimination steps by H-bonding interactions to provide high rate and enantioselectivity. However, the reaction scope of this catalysis is limited to *aza*-MBH and not amenable to generic MBH reactions. In order to improve the proficiency and expand the substrate scope, new Brønsted acid motifs, such as substituted phenol, *N*-tosyl and pyrrole groups, were incorporated into the MAP-structure for testing in *aza*-MBH and generic MBH reactions. Change of Brønsted acidity in the phenol- and *N*-tosyl-containing catalysts did not improve on catalytic proficiency while pyrrole-containing catalysts provided the improvement in enantioselectivity in generic MBH reactions.

Declaration

I certify that in this work entitled "MAP-based multifunctional organocatalysts for asymmetric *aza*- and generic Morita–Baylis–Hillman reactions" has not been previously submitted as part of requirements for a degree to any other university or institution other than Macquarie University. I also certify that the thesis is an original piece of research, and it has been written by me. Any help and assistance that I have received in my research work and the preparation of the thesis itself have been appropriately acknowledged. Finally, I certify that all information sources and literature used are indicated in the thesis.

Sviatoslav Sergeevich Eliseenko

(S/N: 43492614)

26/04/2016

Acknowledgements

I would like to thank the following people, without whom this thesis would not have been possible:

My supervisor, Dr. Fei Liu, for the opportunity to work on this project and for the indispensable help and support.

My fellow lab mates: Ryan Kenny, Harry Spedding, Ivan Salazar Estrada, Alex Moore, Dr. Damian Moran and Umesh Gaikwad for their help in experimental techniques, advice, and comradery.

CBMS staff and fellow students for help in research method training: Ryan Kenny (chiral HPLC, NMR), Erika Davies (NMR), Harry Spedding (synthetic methods and equipment), Kavita Ragini (LCMS), Mark Tran (FT-IR), Anthony Gurlica (Safety and general requirement)

Ketan Ahire, for providing pyrrole aldehydes.

The Jamie, Karuso, Try, Piggot, and Messerle research groups for material supply and general assistance.

Macquarie University for a scholarship for this Masters of Research training.

My lovely mother, Galina Tikhonovna, for moral support, for her unquenchable love and care. Thank you for your faith in me.

Abbreviations

°	degrees
°C	degrees Celsius
Å	angstrom
Ac	acetyl
AcO	acetate
Alk	alkyl
Ar	aryl
atm	atmosphere
aza-MBH	*aza*-Morita–Baylis–Hillman
AZOP	2-(*N'*-arylazo)-2'-diphenylphosphino-1,1'-binaphthyl
BINAP	2,2'-bis(diphenylphosphino)-1,1'-binaphthyl
Bn	benzyl
Boc	*t*-butyl dicarbonate
Bu	butyl
BSA	*N,O*-bis(trimethylsilyl)acetate
Bz	benzoyl
BzOH	benzoic acid
cat.	catalyst
cod	1,5-cyclooctadiene
Cy	cyclohexyl
dba	dibenzylidenacetone
DCE	dichloroethane
DCM	dichloromethane
DMSO	dimethylsulfoxide
dppb	1,4-diphenylphosphino butane
dr	diastereomeric ratio
ee	enantiomeric excess
Et	ethyl
eq.	equivalent
h	hour
i	iso
L*	chiral ligand
m	meta
MAP	2-(dimethylamino)-2'-(diphenylphosphino)-1,1'-binaphthyl

MBH	Morita–Baylis–Hillman
Me	methyl
min	minute
mL	millilitres
MOM	methoxymethyl
MOP	2-(diphenylphosphino)-2’-methoxy-1,1’-binaphthyl
Ms	methane sulfonyl
MS	molecular sieve
MVK	methyl vinyl ketone
n	normal
NBS	*N*-bromosuccinimide
NCS	*N*-chlorosuccinimide
Nf	1,1,2,2,3,3,4,4,4-nonafluoro-butane-1-sulfonyl
NOBIN	2-amino-2’-hydroxy-1,1’-binaphthyl
Nu	nucleophile
OTMS	trimethylsiloxyl
o	ortho
p	para
pin	pinacolato
Ph	phenyl
Pr	propyl
rac	racemic
R	any functional group
re	stereochemical descriptor (as in the *re* face)
r.t.	room temperature
si	stereochemical descriptor (as in the *si* face)
S_N2	second-order nucleophilic substitution
t	tertiary
TEOS	tetraethyl orthosilicate
Tf	trifluoromethane sulfonyl
THF	tetrahydrofuran
TMEDA	tetramethylethylenediamine
Tol	tolyl
TS	transition state
Ts	toluene sulfonyl

List of Figures

List of Schemes

List of Tables

1. INTRODUCTION

1.1 1,1'-Binaphthyl representatives in asymmetric catalysis

Asymmetric catalysis is a prominent field in modern chemical research due to its wide range of applications in pharmaceutical and materials industry.[1] The main classes of asymmetric catalysts, namely enzymes, transition metal complexes and small organic molecules (organocatalysts), have been investigated thoroughly over the past century, and their advantages and disadvantages are well known.[2-7] Enzymes are very proficient catalysts but limited in substrate scope. Transition metal complexes can also be highly proficient but have issues in environmental impact, cost, and purification. Organocatalysts, in turn, are less proficient, but they are readily available, easy to handle, less toxic, easily modified and applicable to a wide range of reactions. For organocatalysts, the main issue remains the enhancement of catalyst proficiency,[8-11] primarily defined, by analogy to enzymatic proficiency, as concurrent enhancement of reaction rate and enantioselectivity.[11,12]

In order to improve on proficiency, a combination of main catalyst types, also known as "hybrid catalysis", has been investigated in the last decade.[13-19] Enzymes, transition metal complexes, and organocatalysts are used in combination or successively in a reaction for proficiency enhancement. The recent publications illuminate such areas as a chemoenzymatic synthesis that combines organo- and biocatalysis,[14,15] artificial metalloenzyme systems[16], the cooperativity of photoredox metal catalysis and organocatalysis,[13] silicon-mediated catalysis and organocatalysis,[18,19] and metal-templated organocatalysis.[17] Organocatalysts that are compatible with other domains of catalysis by enzymes or metals are particularly versatile in hybrid catalysis.

One of such "privileged" structures is the chiral 1,1'-binaphthyl scaffold. The main types of chiral 1,1'-binaphthyl scaffolds include phosphine, Schiff-base, and isoquinoline containing structures, nitrogen and oxygen derived 1,1'-binaphthyl compounds and also chiral Brønsted acids (Figure 1.1). Chiral 1,1'-binaphthyl-based structures have a wide range of applications and are used as organocatalysts[20-23] and chiral ligands complexed to alkali metals,[22] alkaline earth metals,[22,24] light metals,[22,25]transition metals,[22,23,25-29] and semimetals.[26]

The new generation of 1,1'-binaphthyl structures containing acids, ketones, and esters (Figure 1.1, Brønsted chiral acids section) have been used as organocatalysts predominantly.[30,31] Moreover, 1,1'-binaphthyl-based Brønsted chiral acids are used in organized catalysis as structures with the ability to accommodate Brønsted acid and Lewis acid motifs.[18,19,30,32-34]

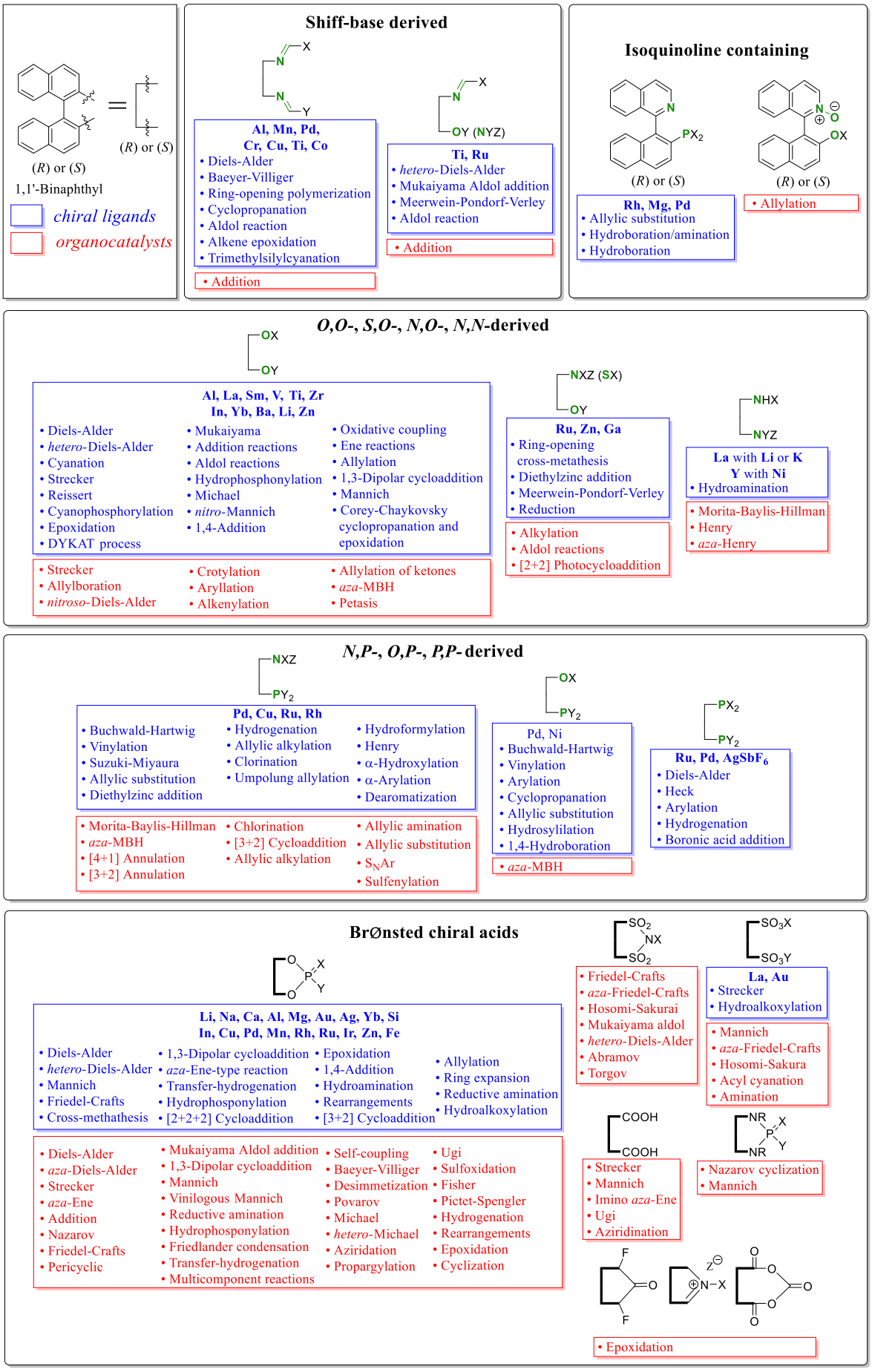

Figure 1.1 Range of applications of 1,1'-binaphthyl representatives.

1,1'-Binaphthyl organocatalysts and ligands have been investigated in various reactions such as cycloaddition, aldol addition, Strecker, Morita–Baylis–Hillman, addition, substitution, reduction, Reissert, Diels–Alder, Friedel–Crafts, Nazarov, Ugi, Henry, ene, Mannich, Michael, cross-methathesis, ring-expansion, Bayer–Villiger, and other pericyclic reactions.[20-23,25,26,28,29,35,36] Moreover, 1,1'-binaphthyl chiral ligands are privileged ones for metal-catalyzed coupling reactions.[37,38] This large collection of structural variants and applications makes the binaphthyl scaffold a good candidate for developing hybrid catalytic systems that use motifs such as Brønsted base, Brønsted acid, Lewis base, and Lewis acid for activation.[11,39]

Taking into account the above, it seems that derivatives of 2-amino-2'-posphino-1,1'-binaphthyl, also known as MAP derivatives with a phosphine as a Lewis base and an amino group as a Brønsted base, are good candidates for developing multifunctional catalysis (Figure 1.2). Modification of the amino group moiety can incorporate additional catalytic motifs such as a Brønsted acid and/or a Lewis acid. The cooperativity of these catalytic motifs may allow rate accelerate in only one enantiomeric pathway over other noncooperative or background pathways for developing organized catalysis in a wide range of asymmetric reactions.[11]

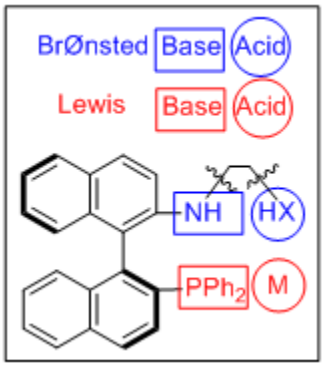

Figure 1.2 Potential systems combining multiple activation motifs in one structure.

The current literature review is devoted to MAP-based ligands and organocatalysts in asymmetric reactions in three parts: 1) the general overview of syntheses of the MAP scaffold; 2) MAP-based ligands in asymmetric reactions; and 3) MAP-based organocatalysts in asymmetric reactions. Due to the page limit of this training thesis, most of the existing literature is summarized in figures and tables with some reactions highlighted in more detail.

1.2 Synthetic pathways to MAP scaffolds

There were described three general approaches for obtaining MAP homologues (Scheme 1.1a–c). The first way is *triflate coupling*, described by Kočovský et al.,[40,41] that first converts a hydroxy group to a phosphino group by triflation, followed by coupling of triflate with diphenylphosphine oxide that affords a phosphine oxide for reduction with trichlorosilane to give the final MAP homologue in 57% yield over four steps (Scheme 1.1a). The sequence has enabled facile access of MAP for a wide range of applications.

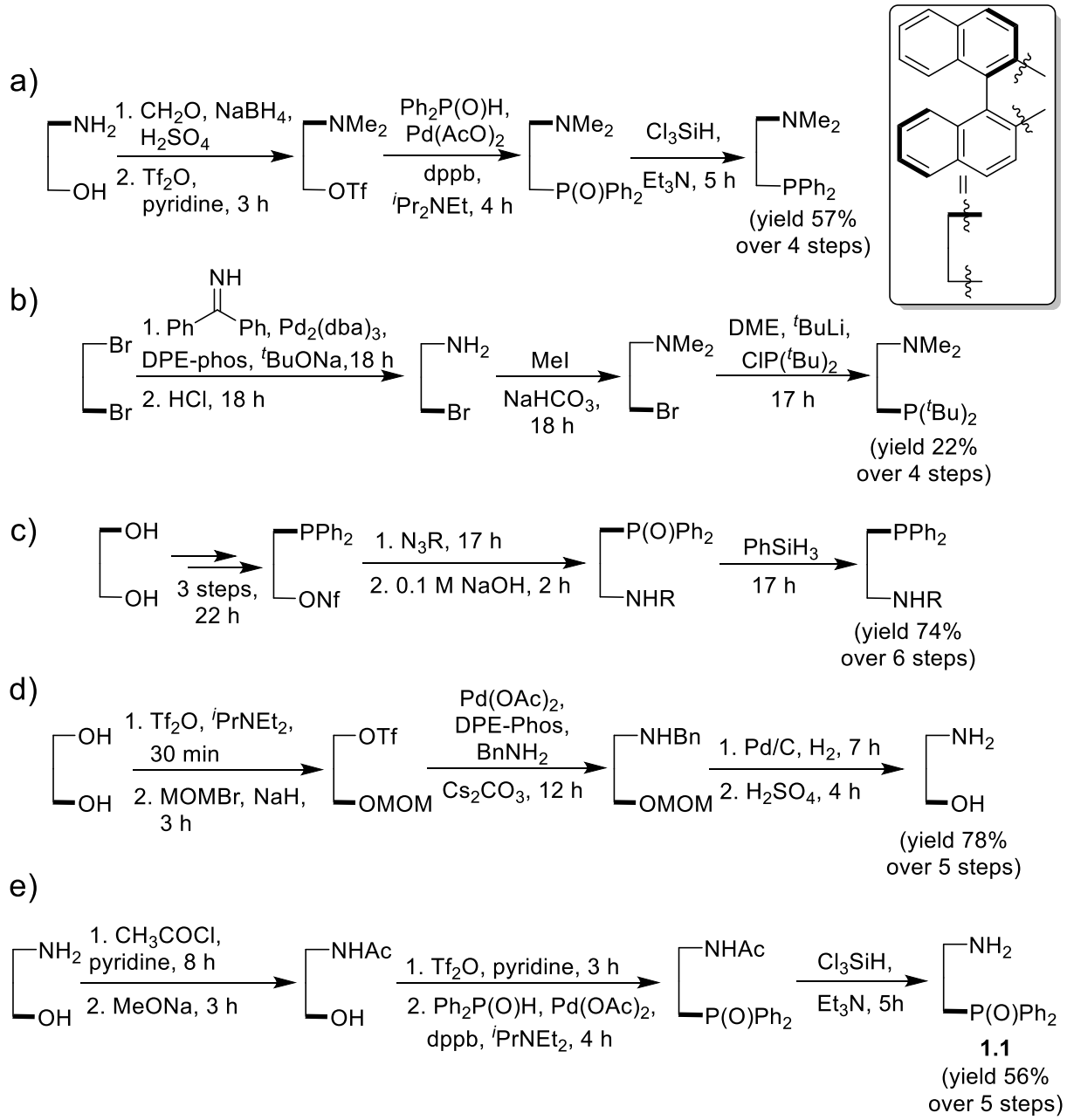

Scheme 1.1 General approaches to MAP homologues: triflate coupling (a);[40,41] lithiation (b);[42,43] Staudinger approach (c);[44] synthesis of NOBIN from BINOL (d);[45,46] synthesis of aminophosphine **1.1** from NOBIN (e).[41]

The *lithiation* approach, as described by Buchwald et al.,[42,43] employs di-*tert*-buthylchlorophosphine with in situ generated binaphthyllithium to synthesize MAP in 22% yield over four steps (Scheme 1.1b). The Staudinger ligation (Scheme 1.1c), described by Hiemstra and Maarseveen et al.,[44] is preceded by phosphonylation of BINOL before providing MAP oxide homologues for reduction to MAP. The total time of reactions for the Staudinger approach is 41 h with 88% yield over five steps. The triflate coupling sequence is a more rapid and reliable synthesis than the Staudinger and lithiation sequences but limited by the high cost of starting NOBIN. However, NOBIN could be readily obtained from cheap BINOL by combined Maruoka[46] and Brückner[45] procedures in 78% yield over five steps (Scheme 1.1d).

The synthesis of free amino MAP derivative **1.1** is more important to the study here. The synthesis of the aminophosphine **1.1** follows the triflate coupling method, as described by Kočovský et al.,[41] and includes initial protection of the amino group before triflate coupling and subsequent deprotection–reduction of *N*-acetyl phosphine oxide by trichlorosilane to provide aminophosphine **1.1** in 56% yield over five steps (Scheme 1.1e).

1.3 MAP derivatives in asymmetric metal-catalyzed reactions

1.3.1 MAP, its direct derivatives, and MAP-based *P,N*-ligands

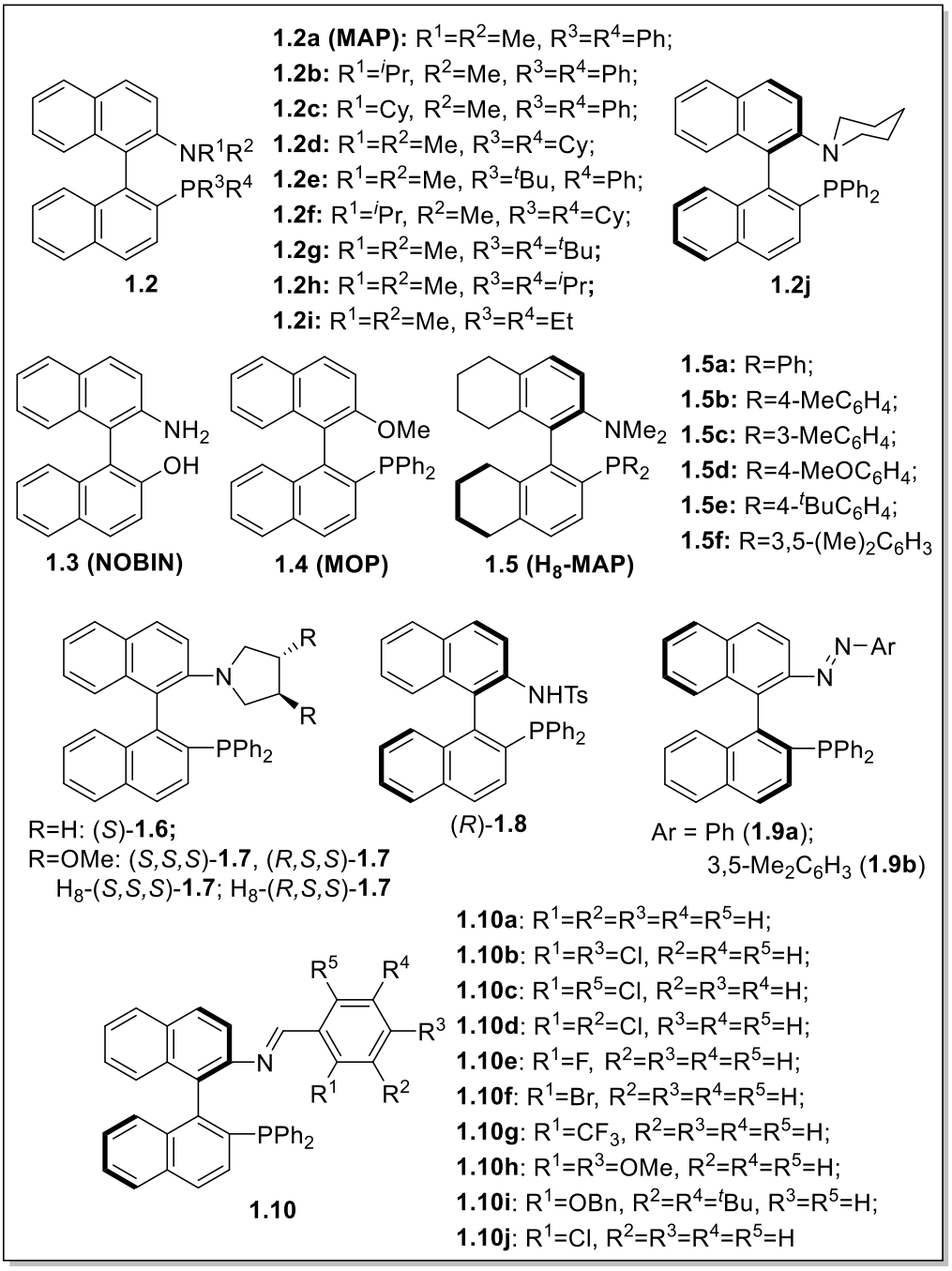

Figure 1.3 Representatives of MAP-based *P,N*-ligands in asymmetric catalysis.

Table 1.1 Application of MAP-based *P,N*-ligands.

Reactions	Catalysts	Metal	*yield, %*	*ee, % (dr)*	References
Allylic substitution	**1.2a**, **1.2b**, **1.2c**, **1.2j**	Pd	77–95	68–73	41
	1.5	Pd	89–99	73–84	47
	1.6, **1.7**	Pd	81–97	27–83	48
	1.9	Pd	37–98	42–88	49
Vinylation and Arylation	**1.2a**, **1.2d**, **1.2e**, **1.2g**	Pd	<10–99	5–97	42,50-52
Dearomatization	**1.2d**, **1.2e**, **1.2f**	Pd	62–99	50–93	53,54
Intramolecular cyclization	**1.2g**	Pd	83–95	98–99	55
Suzuki-Miyaura	**1.2a**, **1.2d**, **1.2g**, **1.2h**	Pd	56–96	40–94	56-58
Et_2Zn addition	**1.8**	Cu	44–63	84–98	59
Vinylogous Mannich	**1.10**	Ag	51–91	38–81 (3:1–99:1)	60

The first representative of *P,N*-type binaphthyl structures – (*R*)-(–)-2-(dimethylamino)-2'-(diphenylphosphino)-1,1'-binaphthyl **1.2a** (Figure 1.3) was reported in 1998 by Kočovský et al.[41] and synthesized by the triflate coupling approach from (*R*)-2-amino-2'-hydroxy-1,1'-binaphthyl **1.3**, also known as (*R*)-NOBIN (Figure 1.3). The acronym MAP, where "A" means for "amino", was proposed for compound **1.2a** by authors in analogy to 2-(diphenylphosphino)-2'-methoxy-1,1'-binaphthyl **1.4** also known as MOP[61] (Figure 1.3).

MAP-based ligands **1.2**, **1.6**–**1.10** were investigated in a wide range of reactions such as Pd-catalyzed asymmetric allylic substitution,[41,48,49] vinylation and arylation,[42,50-52] dearomatization,[53,54] intramolecular cyclization,[55] Suzuki-Miyaura[56-58] and also in Cu-catalyzed conjugative diethylzinc addition,[59] and Ag-catalyzed vinylogous Mannich[60] reactions, generally with good to excellent yields and enantioselectivity. H_8-MAP-based ligands **1.5** also were studied in Pd-catalyzed asymmetric allylic substitution[47] (Table 1.1).

Some representative reactions from Table 1.1 are discussed in more detail below to illustrate the high proficiency of the catalysts. Being the first representative of the *P,N*-binaphthyl class, (*R*)-MAP **1.2a** and some of its *N*-substituted derivatives (*R*)-**1.2b**, (*R*)-**1.2c** and **1.2j** (Figure 1.3) were examined in Pd(0)-catalyzed allylic substitution of racemic 1,3-diphenylprop-2-en-1-yls **1.11**. This reaction afforded substitution products (*S*)-**1.12** in 77–95% yields and 68–73% *ee* (Scheme 1.2).[41] 5,5',6,6',7,7',8,8'-Octahydro-1,1'-binaphthyl backbone (H_8-MAP) catalysts **1.5** (Figure 1.3) showed better proficiency than **1.2** and provided the desired product **1.12** in 89–99% yields with 73–84% *ee* in comparable conditions (Scheme 1.2).[47]

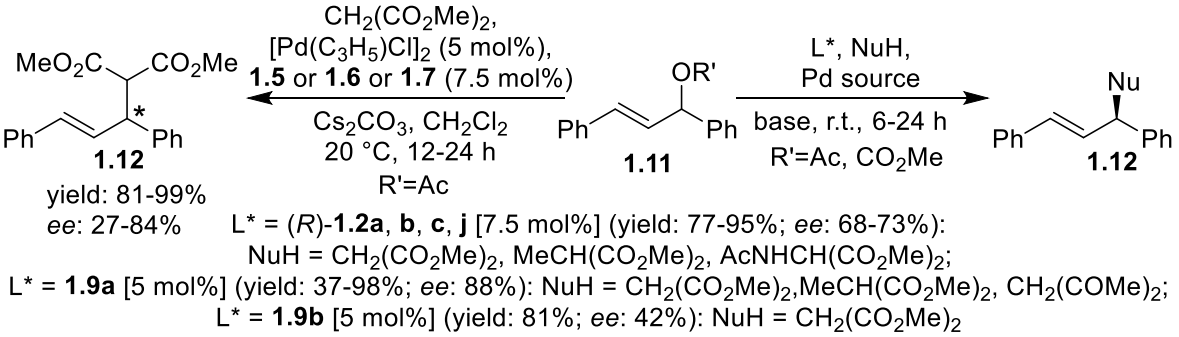

Scheme 1.2 Pd-catalyzed allylic substitution of 1,3-diphenylprop-2-en-1-yls **1.11**.[47,48]

Initially it was proposed that Pd coordinates to both phosphorus and nitrogen atoms,[41,47] but the single-crystal structure in complex with Pd showed that MAP acts as a bidentate *P,C*$_\sigma$-ligand (Figure 1.4a), rather than *P,N*-ligand (Figure 1.4b).[62-65] Similar results were obtained for the complex from (*R*)-**1.2a**, [Pd(Ph(η^3-C_3H_3)Ph)Cl]$_2$ with $AgPF_6$.[66] ^{1}H, ^{13}C, and ^{31}P NMR experiments corroborated the bidentate (*P,C*)-mode of coordination in solution.[63,66] Furthermore, MAP-ligands can also form monodentate monophosphine neutral complexes in the presence of different palladophilic anions such as a chloride (Figure 1.4c).[65]

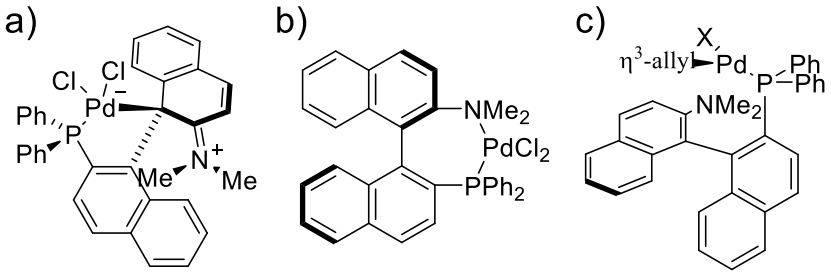

Figure 1.4 Coordination modes of a MAP-complex.

The sulfonylamino derivative of (*R*)-MAP **1.8** (Figure 1.3) was synthesized and examined in Cu-catalyzed enantioselective 1,4–addition of diethylzinc to enones **1.13**. The ligand **1.8** furnished 4-arylhexanones **1.14** in 44–63% yields and 84–98% *ee* in only a few hours (Scheme 1.3).[59]

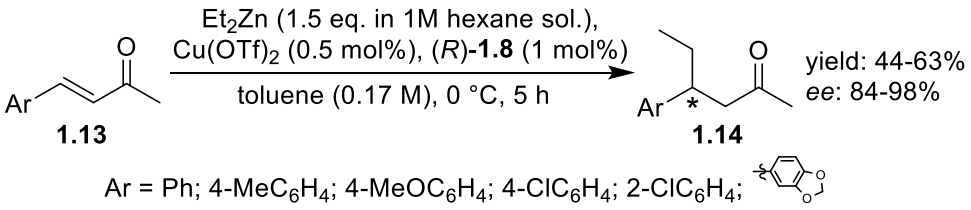

Scheme 1.3 Cu-catalyzed asymmetric 1,4-addition of diethylzinc to enones **1.13**.[59]

1.3.2 MAP-based *P,N,N*- and *P,N,O*-ligands

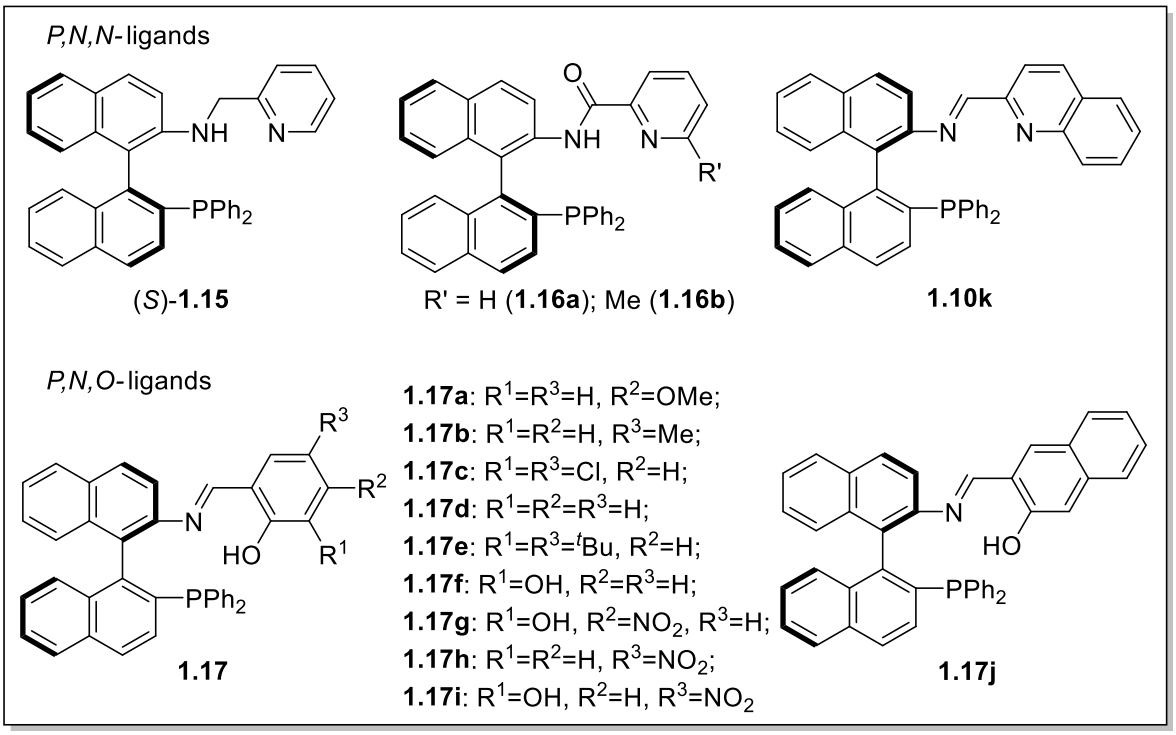

Figure 1.5 Representatives of MAP-based *P,N,N*- and *P,N,O*-ligands in asymmetric catalysis.

Table 1.2 Application of MAP-based *P,N,N*- and *P,N,O*-ligands

Reactions	Catalysts	Metal	yield, %	*ee*, %	References
Hydrogenation of ketones	**1.15**	Ru	91–98	52–98	[67]
Et_2Zn addition	**1.16**	Cu	69–97	83–98	[68]
Allylic substitution	**1.17**	Pd	21–99	0–76	[69]
Henry	**1.17a-e, j**	Cu	28–99	7–80	[70]
α-Hydroxylation and chlorination of β-keto esters	**1.17a-g, j**	Cu	78–99	39–82	[71,72]
Vinylogous Mannich	**1.17a, b**	Ag	50–53	33–35	[60]

The representative of MAP-based *P,N,N*- and *P,N,O*-ligands (Figure 1.5) and their typical applications are listed in Table 1.2. The novel type of 1,1'-binaphthyl ligands **1.16**, containing a pyridine ring linked via an amide bond (Figure 1.5),[68] were tested in Cu-catalyzed enantioselective 1,4-conjugate diethylzinc addition to enones **1.13** and provided **1.14** in 69–97% yield and up to 98% *ee*, although the reactions required long reaction time (Scheme 1.4).[68]

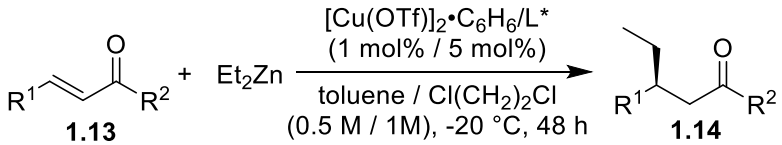

L* = (*R*)-**1.16a** (yield: 92%; *ee*: 83%): R^1=R^2=Ph;
L* = (*R*)-**1.16b** (yield: 69-97%; *ee*: 90-98%): R^1=Ph: R^2=Ph; 4-$MeOC_6H_4$; 4-ClC_6H_4; Me;
R^1=4-$MeOC_6H_4$, 4-ClC_6H_4: R^2=Ph

Scheme 1.4 Cu-catalyzed asymmetric 1,4-conjugate diethylzinc addition to enones **1.13**.[68]

The ligand **1.17g** (Figure 1.5) was found as the most proficient among the **1.17** group of ligands in Pd-catalyzed asymmetric allylic substitution of 1,3-diarylallyl acetates **1.11** at room temperature (Scheme 1.5).[69] It was proposed that the presence of hydroxyl at *ortho*-position and nitro group at *para*-position to imine in **1.17g** might be important for proficient catalysis.

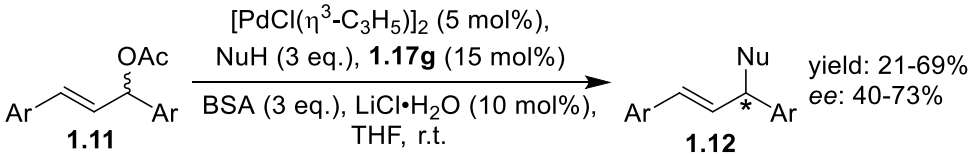

Ar = Ph: NuH = $CH_2(CO_2Et)_2$, $CH_2(CO_2Me)_2$, morpholine, $BnNH_2$;
Ar = 4-ClC_6H_4: NuH = $CH_2(CO_2Me)_2$

Scheme 1.5 Pd-catalyzed asymmetric allylic substitution of 1,3-diarylallyl acetates **1.11**.[69]

1.4 MAP derivatives in asymmetric organocatalyzed reactions

1.4.1 MAP-based *P,N*-organocatalysts

Table 1.3 Application of MAP-based *P,N*-organocatalysts.

Reactions	Catalysts	yield, %	*ee*, % (*dr*)	References
aza-MBH	**1.8**, **1.18**	0–99	*rac*–95	[73]
	1.19	69–98	35–91	[74]
Allylic substitution	**1.2a**, **1.18a**, **d**	25–99	*rac*–98 (51:49 – >95:5)	[75,76]
	1.20	47–97	85–99 (>95:5)	[77]

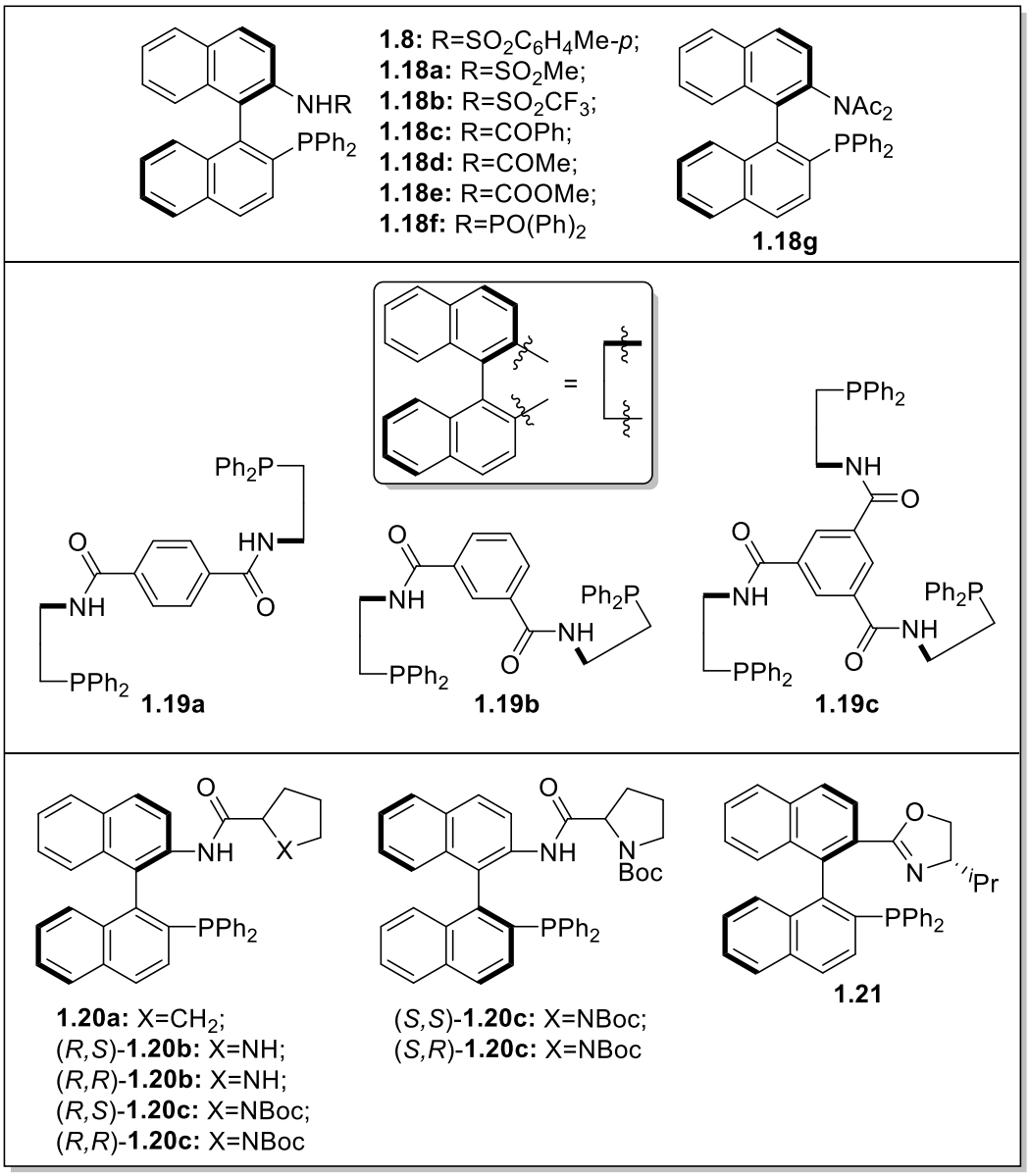

Figure 1.6 Representatives of MAP-based *P*,*N*-organocatalysts in asymmetric catalysis.

MAP-based *P*,*N*-organocatalysts **1.8**, **1.18**–**1.20** were extensively investigated in the *aza*-MBH reaction between aromatic *N*-Tosyl imines and MVK or ethyl vinyl ketone[73,74] and in allylic substitution of MBH adducts[75-77] providing up to 99% yields and 98% *ee*. The mechanism of an MBH reaction is complex, and a generalized mechanism using an enone and an aldehyde or imine is discussed in Scheme 1.6.[78-80] An MBH reaction is initiated by a reversible Michael addition of the nucleophilic catalyst to an activated alkene. The resulting zwitterionic intermediate **I** then undergoes the reversible aldol-type addition with an aldehyde (generic[81,82] MBH) or an imine (*aza*-MBH), followed by an irreversible proton-transfer-elimination step to produce the final product **1.24** with the generation of one chiral center.

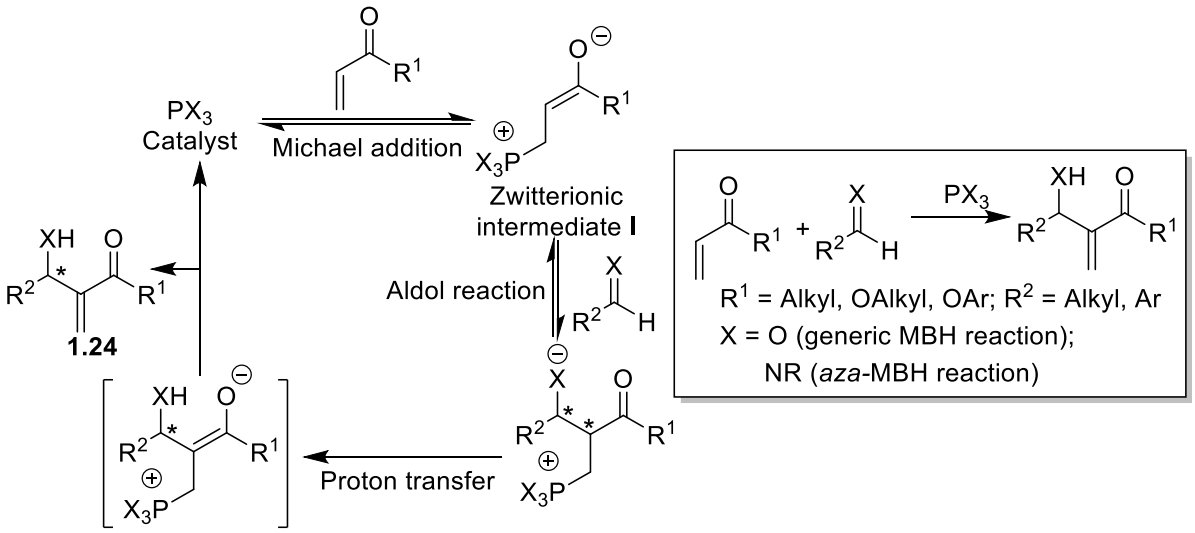

Scheme 1.6 Generalized mechanism of an MBH reaction.

Bifunctional (phosphine Lewis base and amide Brønsted acid) 1,1'-binaphthyl-based *P,N*-catalysts **1.8** and **1.18** (Figure 1.6) were studied in *aza*-MBH reactions (Scheme 1.7).[73] The organocatalyst **1.18d** demonstrated the highest proficiency in *aza*-MBH reactions between *N*-tosylimines **1.22** and vinyl ketones **1.23** (Scheme 1.7). Catalysts **1.18b** and **1.18g** did not give any product, suggesting that the presence and an adequate acidity of the amide proton were important for catalysis.[73]

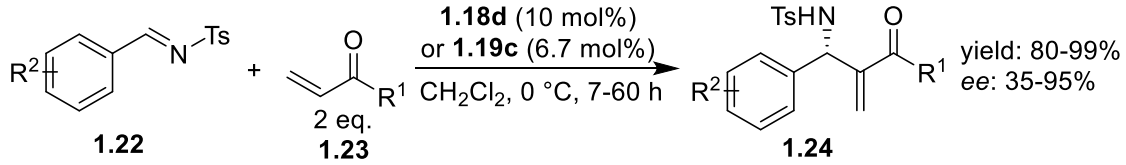

R^1=Me (**3.3a**): R^2=Ph, 2-Br, 4-Br, 2-NO_2, 3-NO_2, 4-NO_2, 2-Cl, 3-Cl, 4-Cl, 3-F, 4-F, 4-OMe, 4-Me;
R^1=Et (**3.3b**): R^2=Ph; 4-Br, 4-Cl

Scheme 1.7 *aza*-MBH reactions catalyzed by *P,N*-type organocatalyst **1.18d**,[73] and **1.19c**.[74]

Organocatalyst **1.19c** showed the highest proficiency compared to other catalysts **1.19** and **1.18c** and provided products **1.24** in 73–95% yield and up to 91% *ee* (Scheme 1.7).[74] Based on these results, it was proposed that steric interference could provide higher proficiency. However, the multivalency of the phosphorus Lewis bases and nitrogen Brønsted acids in **1.19c** structure could also influence catalytic proficiency. Therefore, the proposed steric influence seems tenuous. Organocatalyst **1.2a** (**MAP**) (Figure 1.3) was also tested in *aza*-MBH reaction but was not active without the amide proton that, in turn, could be considered as evidence for the important role of Brønsted acid function for *aza*-MBH catalysis.[74]

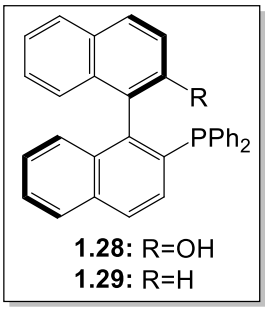

Figure 1.7 Representatives of 1,1'-binaphthyl structure **1.28** and **1.29**.

Catalysts **1.18a**, **1.18c**, **1.18d**, and **1.20a** (Figure 1.6) were also tested in the enantioselective substitution of MBH acetates **1.25** with 2-trimethylsilyloxy furan **1.26**, furnishing products **1.27** in up to 94% yield and 96% *ee*. (Scheme 1.8).[75] For this reaction, catalysts **1.18** were much more proficient than catalyst **1.2a** (**MAP**), **1.28** and **1.29** (Figure 1.7), suggesting the important role of the amide proton in asymmetric induction.[75]

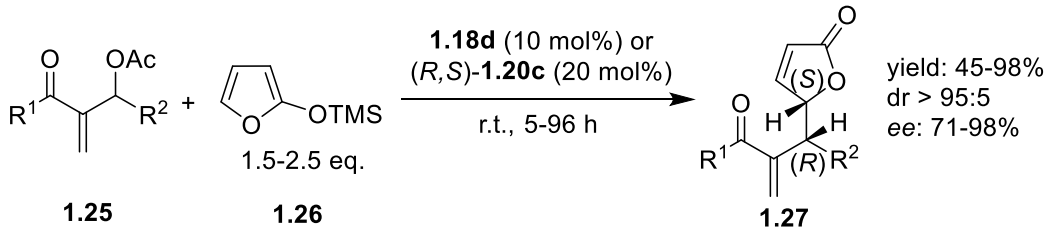

R^1=Me: R^2=4-FC_6H_4, 4-BrC_6H_4, 4-MeC_6H_4, 3-MeC_6H_4, 4-$CF_3C_6H_4$, 4-CNC_6H_4, Ph, 4-ClC_6H_4, 3-ClC_6H_4, 2-ClC_6H_4, 4-$NO_2C_6H_4$, 3-$NO_2C_6H_4$, furan-2-yl, thiophen-2-yl, $C_6H_4CH_2CH_2$, $Me(CH_2)_6$, C_3H_7; R^1=Et: R^2=Ph, 4-$NO_2C_6H_4$; R^1=OMe: R^2=Ph, 4-$NO_2C_6H_4$

Scheme 1.8 Enantioselective allylic substitution of MBH acetates **1.25** with 2-trimethylsilyloxy furan **1.26**.[75,77]

The proposed mechanism (Scheme 1.9) includes initial interaction between an asymmetric organocatalyst and an MBH acetate **1.25** that provides an enone intermediate **II**, which is stabilized by intramolecular H-bonding interaction. The siloxy furan then undergoes *endo*-selective Diels–Alder cycloaddition to **II** affording the intermediate **III**, which, in turn, undergoes Grob-type fragmentation to form a γ-butenolide **1.27**. It was found that the addition of water could improve proficiency of catalyst **1.18d**, but the role of water additive was not clear. However, it was proposed that the water may facilitate the Grobe-type fragmentation via H-bonding interactions in a pentacoordinated silicon intermediate **III**.

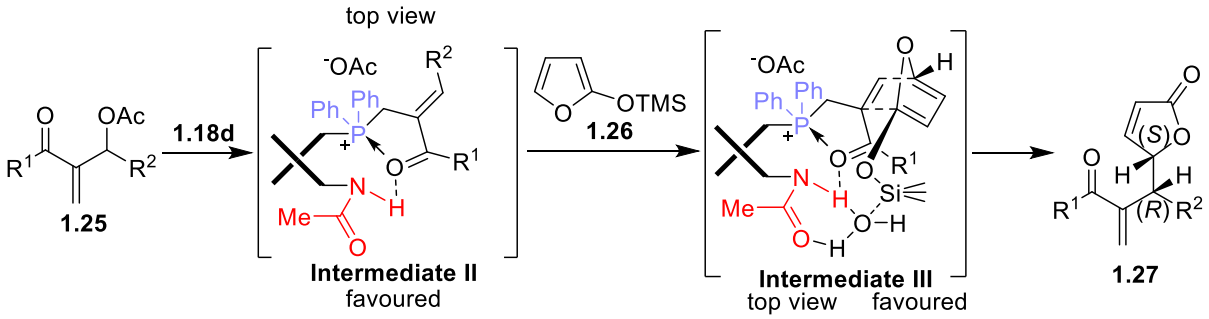

Scheme 1.9 The proposed mechanism of enantioselective substitution of MBH acetates **1.25** with 2-trimethylsilyloxy furan **1.26**.[75]

In attempts to develop organocatalysts for enantioselective substitution of MBH acetates **1.25** with 2-trimethylsilyloxy furan **1.26**, new 1,1'-binaphthyl-based organocatalysts **1.20** and **1.21** (Figure 1.6) were also prepared.[77] Organocatalyst **1.21**, which did not have an active amide proton, could not mediate this transformation. The comparison between **1.20b** and **1.20c** demonstrated a slightly better proficiency of Boc-substituted catalysts **1.20c** suggesting that

the amino proton of the proline moiety did not influence the enantiomeric excess (Scheme 1.8).[77]

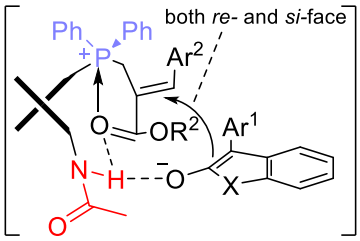

Figure 1.8 Proposed mechanism of asymmetric allylic alkylation of 3-substituted benzofuran-2(3*H*)-ones **1.30a** and oxindoles **1.30b**.

P,N-type organocatalyst **1.18d** was effective also in asymmetric allylic alkylation of 3-substituted benzofuran-2(3*H*)-ones **1.30a** and oxindoles **1.30b** to obtain the corresponding **1.31a**, **b** in 76–99% yields and 80–98% *ee*, but only moderate diastereoselectivity (Scheme 1.10).[76] The organocatalyst **1.18d** demonstrated the highest proficiency compared to catalysts **1.18a** and **1.20b** in these reactions for both substrates of furanones and oxindoles. A plausible transition state provided the addition product from both *re*- or *si*-face attacking (Figure 1.8).[76]

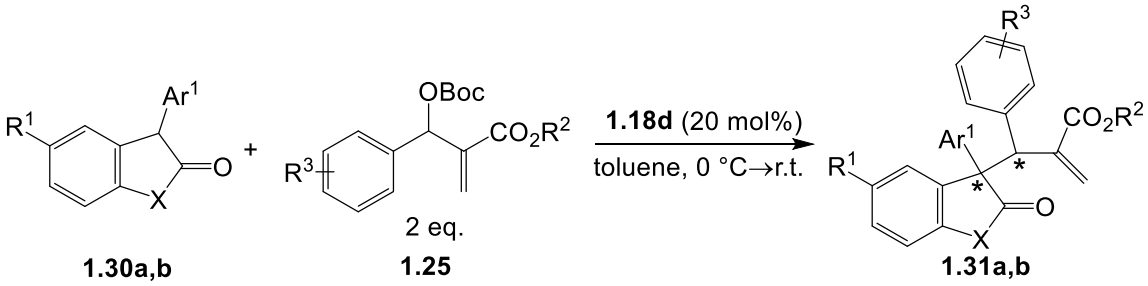

X=O: Ar^1=Ph (**1.30a, 1.31a**): (yield: 85-99%, *dr syn/anti:* 54:46-71:29, *ee*: 85-97%)
R^1=H: R^2=Me: R^3=H, 3-Cl, 3-CN, 4-F, 4-NO_2;R^2=Et: R^3=4-Me, 4-NO_2; R^2=^{t}Bu: R^3=4-NO_2;
R^1=Cl, Br, ^{t}Bu: R^2=Me: R^3=H;
X=NBoc, R^2=Me (**1.30b**, **1.31b**): (yield: 76-92%, *dr syn/anti:* 51:49-67:33, *ee*: 80-98%)
R^1=H: Ar^1=Ph: R^3=H, 4-NO_2, 3-CN, 3-Cl, 4-F, 4-Me; Ar^1=4-FC_6H_4, 4-MeC_6H_4: R^3=H;
R^1=F, Me: Ar^1=Ph: R^3=H

Scheme 1.10 Asymmetric allylic alkylation of 3-substituted benzofuran-2(3*H*)-ones **1.30a** and oxindoles **1.30b**.[76]

1.4.2 MAP-based *P,N,N*- and *P,N,O*-organocatalysts

Table 1.4 Application of MAP-based *P,N,N*- and *P,N,O*-organocatalysts.

Reactions	Catalysts	yield, %	*ee*, % (*dr*)	References
aza-MBH	**1.32a**, **1.33a,b**	50–98	64–97	83
Allylic substitution	**1.20b,c**	40–95	34–78	84
	1.18d, **1.32a**, **1.33c,d**, **1.34a–c**	76–95	85–98 (2:1 – 20:1)	85
	1.33a,b, **1.34c–j**; **1.35a**	20–99	26–90	86
	1.34c,f,i, **1.35a**, **1.37**	53–99	64–97	87

[3+2] Annulation	**1.35a**	92	74 (9:1)	88
[4+1] Annulation	**1.33b,f**, **1.34a,e,d**, **1.35**	29–99	7–98 (1:1 – 7:1)	89,90
[3+2] Cycloaddition	**1.32b,c**, **1.33f**, **1.34c**, **1.35a,c,d**, **1.36**	42–88	36–63	91

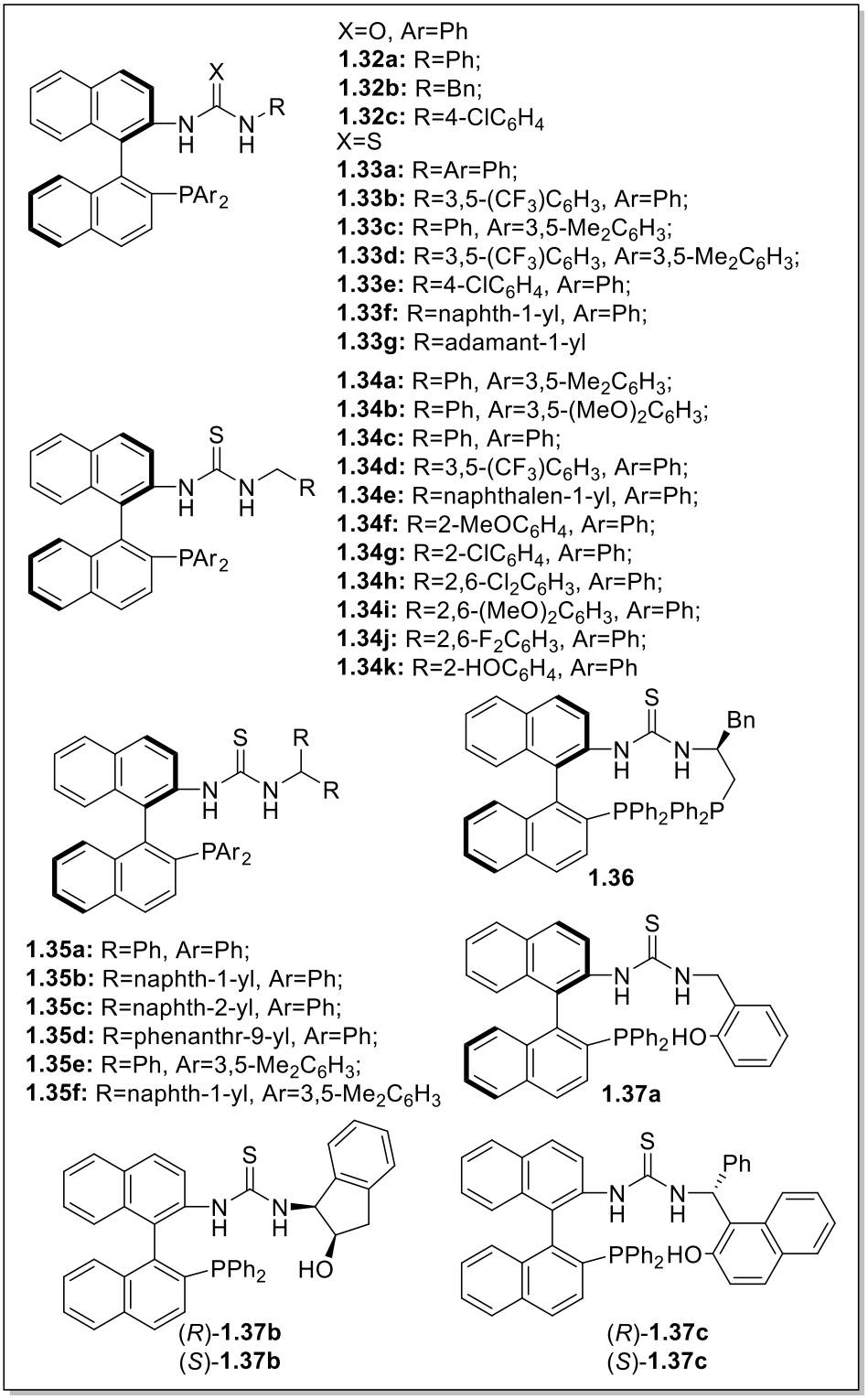

Figure 1.9 Representatives of MAP-based *P,N,N*- and *P,N,O*-organocatalysts in asymmetric catalysis.

MAP-based *P,N,N*-organocatalysts **1.32**–**1.37** (Figure 1.9) were studied in aza-MBH[83] reactions and allylic substitution of MBH adducts[85-87], [3+2] annulations[88] and cycloaddition[91] and in [4+1] annulation[89,90] providing products with excellent yields and *ee* values in all types of reactions except for [3+2] cycloaddition reactions (Table 1.4).[91]

As shown earlier, organocatalysts (*R,S*)- and (*R,R*)-**1.20b** (Figure 1.6) were considered as bifunctional (phosphine Lewis base and amide Brønsted acid) in enantioselective substitution of MBH acetates **1.25** with 2-trimethylsilyloxy furan **1.26** due to the absence of proficiency response to protection of pyrrolidine function.[77] However, the catalyst (*R,S*)-**1.20b** (Figure 1.6) was proposed as *trifunctional* (phosphine Lewis base, amide Brønsted acid and pyrrolidine Brønsted base) in enantioselective allylic amination of MBH acetates **1.25** (Scheme 1.11).[84] The Boc-protected catalyst (*R,S*)-**1.20c** was used as a control and showed reduced proficiency in comparison with (*R,S*)-**1.20b** that may suggest the indispensable role of an active amino proton in the proline moiety for the catalysis proficiency (Scheme 1.11).[84] However, this hypothesis seems tenuous because the Boc protection may act as a bulky fragment blocking the phthalimide approach to an MBH acetate. Moreover, the bifunctional (phosphine Lewis base and thiourea Brønsted acids) catalyst **1.34f** (Figure 1.9) was able to catalyze this reaction providing up to 99% yield with 90% *ee*.[86] Therefore, the actual mechanism of the catalyst (*R,S*)-**1.20b** in allylic amination remains unclear, without testing **1.20a** (Figure 1.6) in this reaction.

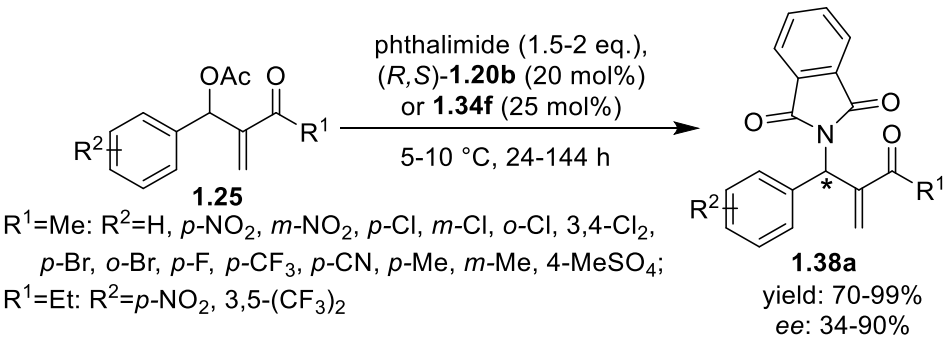

Scheme 1.11 Enantioselective allylic amination of MBH acetates **1.25**.[84,86]

The 1,1'-binaphthyl-based urea- and thiourea-derived organocatalysts **1.32a**, **1.33a**, and **1.33b** (Figure 1.9) were tested in *aza*-MBH reactions between *N*-tosylimines **1.22** and MVK **1.23** and proposed to be bifunctional (i.e. two distinct catalytic functionalities) *P,N,N*-organocatalysts (one phosphine Lewis base and two urea or thiourea Brønsted acids). The organocatalyst **1.33a** was found to be the best for this reaction, although no mechanistic explanations were provided (Scheme 1.12).[83]

It was found that the benzoic acid as an additive accelerated the reaction rate and increased *ee* for the product **1.24**. The screen of benzoic acid analogs showed that only additives with similar acidity (pK_a = 4.20) were successful. It was proposed that benzoic acid initially could protonate zwitterionic intermediate **IV** to form vinylic alcohol **V** that, probably, may be in rapid equilibrium with the initial zwitterionic intermediate **IV** (Scheme 1.12). The benzoic acid, being a source of a proton, may also promote the proton transfer step.[83]

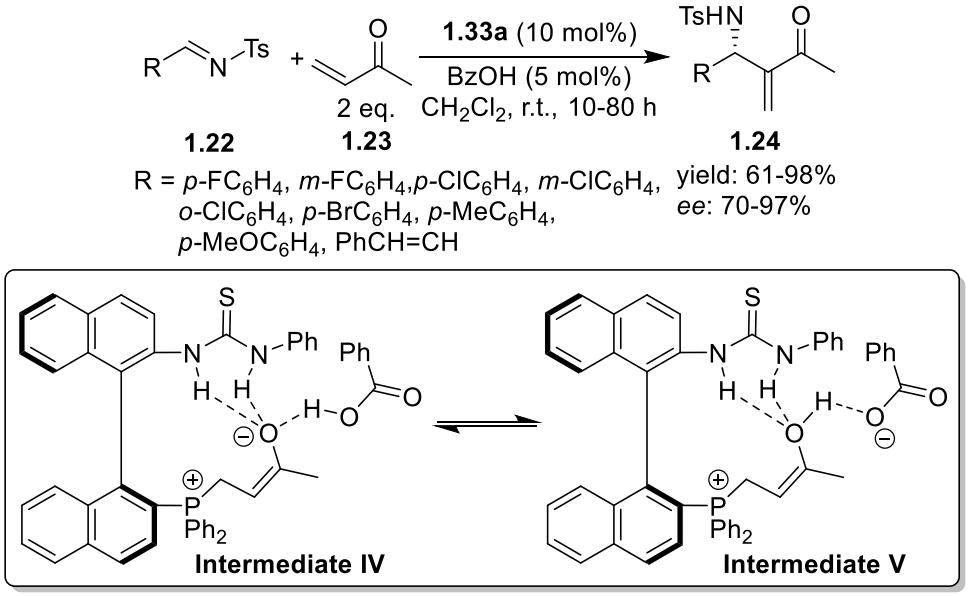

Scheme 1.12 *aza*-MBH reactions catalyzed by thiourea-derived organocatalyst **1.33a** and the proposed mechanism of benzoic acid stabilization.[83]

Catalysts **1.33c**, **1.33d**, and **1.34a**, **1.34b** (Figure 1.9), with modified nucleophilicity and the steric environment around the *P*-center, showed proficiency in enantioselective substitution of MBH adducts **1.25** with oxazolones **1.39.** The catalyst **1.34a** was found as most proficient, possibly providing the most effective intramolecular hydrogen bonding interactions (Scheme 1.13).[85]

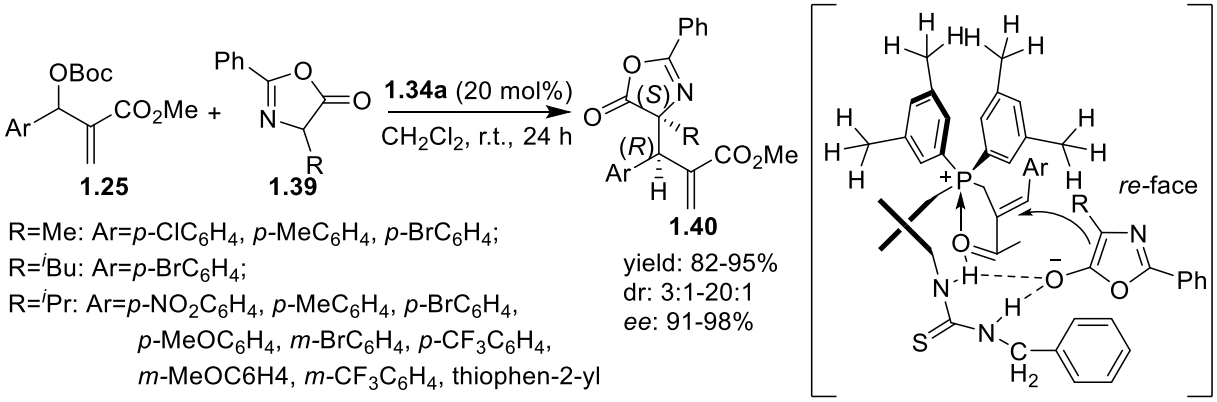

Scheme 1.13 Enantioselective substitution of MBH adducts **1.25** with oxazolones **1.39** and proposed reaction mechanism.[85]

1.4.3 MAP-based trifunctional *P,N,O*- and *P,N,N*-organocatalysts

Trifunctional organocatalysts **1.41** and **1.43** (Figure 1.10), combining phosphine as a Lewis base, amino group as a Brønsted base and phenol as a Brønsted acid, have been developed by our group and tested in *aza*-MBH and generic MBH reactions.[92-97]

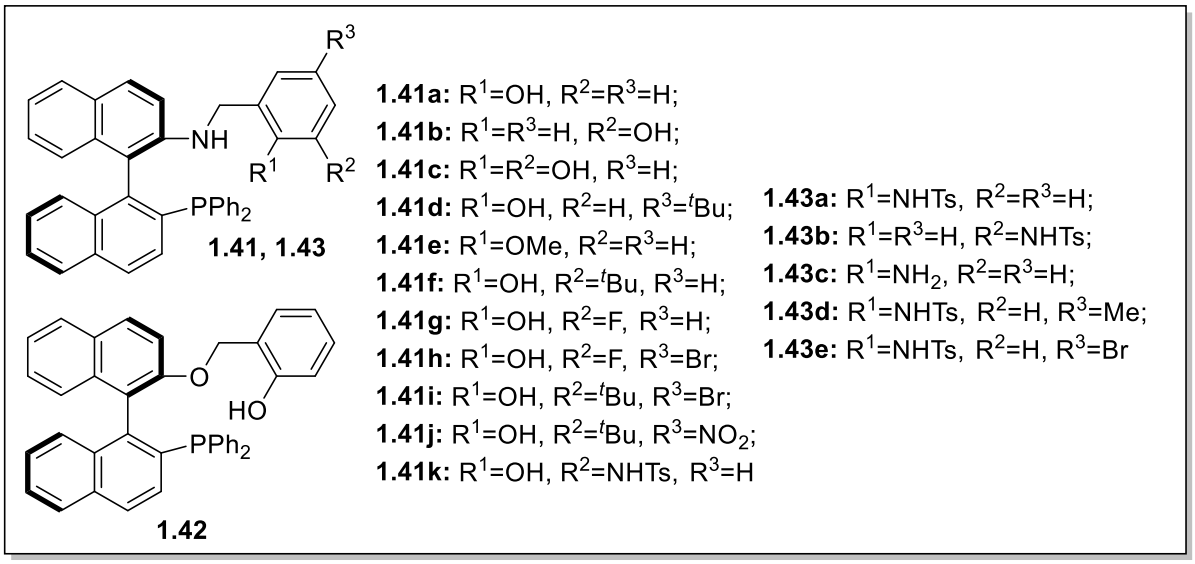

Figure 1.10 Representatives of trifunctional MAP-based organocatalysts **1.41**–**1.43** in asymmetric catalysis.[93-97]

The extension from bifunctional type (**1.42**) to a trifunctional type of catalysts was achieved by the inclusion of a Brønsted base function. This additional motif was thought to generate a secondary ammonium ion pair in the presence of an acid additive.[97] The trifunctional mechanism was established by comparing the activities of the bifunctional controls to that of the trifunctional catalyst. The trifunctional catalysts require the acid additive to provide very high *aza*-MBH reaction rates and enantioselectivity at ambient temperature while the bifunctional catalyst control is not responsive to acid activation.[97]

Table 1.5 Trifunctional catalyst **1.41a** compared to the bifunctional control **1.41e** and **1.42**.[97]

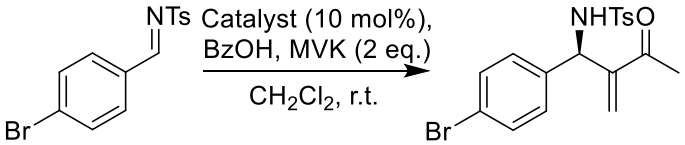

Entry	Catalyst	BzOH(mol%)	Time(h)	Conv[a](%)	*ee*[b](%)
1	**1.41a**[97]	50	3	>95	82
2	**1.41a**[97]	0	3	10	*rac*
3	**1.41e**[97]	50	4	81	46
4	**1.41e**[97]	0	6	49	17
5	**1.42**[97]	50	6	78	42

6	**1.42**[97]	0	6	66	71

[a]Calculated by ^{1}H NMR spectroscopy. [b]Determined by chiral HPLC analysis.

The cooperative participation of the three functional motifs in the catalysis mechanism was confirmed by a set of control experiments (Table 1.5). The bifunctional control catalysts, containing methyl-protected phenol (Brønsted acid control) **1.41e** or an isoelectronic oxygen instead of the Brønsted base (Brønsted base control) **1.42**, were synthesized and tested in an *aza*-MBH reaction. The proficiency of **1.41e** and **1.42** decreased sharply in comparison to the trifunctional catalyst **1.41a** (Table 1.5). The Brønsted acid control catalyst **1.41e** compared to trifunctional catalyst **1.41a** showed a significant loss in both reaction rate and *ee* value (Table 1.5, entry 1 and 3), confirming the key role of Brønsted acid function in proficient catalysis. Moreover, the Brønsted acid control catalyst **1.41e** showed positive response to acid activation (Table 1.5, entry 3 and 4). These results suggest that acid additive activates the catalyst via the Brønsted base function for proficient catalysis. Indeed, the Brønsted base control catalyst **1.42** behaved like a bifunctional catalyst that in the presence of benzoic acid additive loses enantioselectivity. In addition, the rate of reaction is not very responsive to acid activation (Table 1.5, entry 5 and 6). Based on these results, it was proposed that the addition of benzoic acid would form a secondary ammonium salt with the Brønsted base function that could stabilize a zwitterionic intermediate during the reversible Michael addition and the aldol steps. This salt may also favour one mode in the irreversible proton-transfer step (Figure 1.11a) and not the other (Figure 1.11b), providing both higher enantioselectivity and rate.[97] Moreover, the results of the control experiments showed the indispensable role of the Brønsted base and Brønsted acid motifs for proficient catalysis.[97]

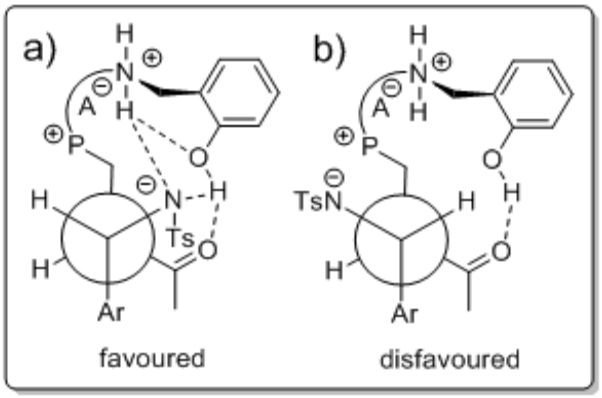

Figure 1.11 Plausible transitions structures of an *aza*-MBH reaction catalyzed by the *P,N,O*-organocatalyst **1.41a**.

It was proposed that the position of the Brønsted acid function could also be important for proficient catalysis due to H-bonding interactions (Figure 1.11). A control catalyst **1.41b** (Figure 1.10), containing Brønsted acid function at C3 of the aromatic ring, was synthesized and tested in an *aza*-MBH reaction (Table 1.6).

Table 1.6 Influence of a Brønsted acid position on the catalysis proficiency.[97]

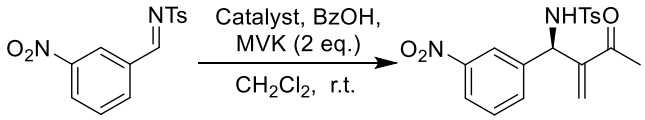

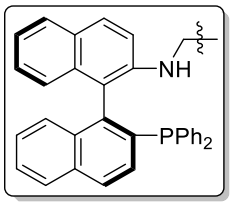

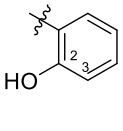

1.41a

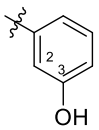

1.41b

Entry	Catalyst	Catalyst/BzOH loading (mol%)	Time (h)	Conv[a] (%)	*ee*[b] (%)
1	**1.41a**[97]	10/10	3	>95	82
2	**1.41a**[97]	10/0	3	16	*rac*
3	**1.41b**[97]	10/10	15	77	38
4	**1.41b**[97]	10/0	15	63	24

[a]Calculated by ^{1}H NMR spectroscopy. [b]Determined by chiral HPLC analysis.

Indeed, the control catalyst **1.41b** demonstrated significantly lower reaction rate and lower *ee* value than the trifunctional catalyst **1.41a** (Table 1.6, entries 1 and 3). Its response to acid activation is also limited (Table 1.6, entries 3 and 4). These results suggest that the Brønsted acid at C2 of the aromatic ring is necessary for catalysis by likely efficient H-bonding interactions.

The first generation catalyst **1.41a** was tested in *aza*-MBH reactions between a wide range of aromatic benzaldimines **1.22** and MVK **1.23** to furnish **1.24** in 86–96% yields with 59–92% *ee* (Scheme 1.14).[97] However, catalyst **1.41a** demonstrated very little activity in a generic MBH test reaction between 4-nitrobenzaldehyde and MVK, furnishing the product in 3 days in 86% yield with only 26% *ee* (Table 1.7, entry 7).[97]

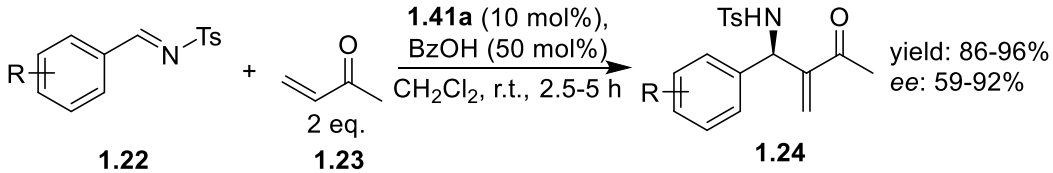

1.22 **1.23** **1.24**

R = *p*-F, *p*-Cl, *o*-Cl, *p*-Br, *p*-Me, *m*-MeO, *o*-MeO, *p*-NO_2, *m*-NO_2, *o*-NO_2,

Scheme 1.14 *aza*-MBH reactions catalyzed by the organocatalyst **1.41a**.[97]

It was proposed that acidity of phenol function might play an important role in the proficiency of a catalyst. Thus, the second generation trifunctional catalysts **1.41g**–**j** (Figure 1.10), containing additional electron-withdrawing substituents, and **1.41f** with a bulky electron-rich *tert*-butyl substituent in the position *ortho* to the hydroxy function, were synthesized and tested in *aza*-MBH reactions.[96]

As it was proposed, the addition of an electron-withdrawing fluorine atom into the aromatic ring afforded a dramatic rise of the reaction rate from 15% conversion for **1.41a** to 57% for **1.41g** in 15 minutes, but the *ee* value remained nearly the same (Table 1.7, entries 1, 2). The additional bromine at *para* to the phenolic Brønsted acid (catalyst **1.41h**) allowed for 87% conversion with 88% *ee* in comparable conditions (Table 1.7, entry 3). The catalyst **1.41f**, containing an electron donating bulky *tert*-butyl group, was less proficient than **1.41a**, but the tuning of the Brønsted acid acidity by a bromine at the *para*-position (catalyst **1.41i**) provided higher reaction rate without significant changes in *ee* values (Table 1.7, entries 1, 4, 5). Further increase in Brønsted acid acidity by replacement of bromine with a nitro group (catalyst **1.41j**) decreased reaction rate to 57% in 15 minutes with slightly better *ee* value (87%) (Table 1.7, entry 6). These results demonstrated that Brønsted acid acidity improves the catalytic proficiency up to a limit.[96] The second generation catalyst **1.41j** was also more proficient than the first generation catalyst **1.41a** in a generic MBH test reaction providing 85% conversion over 24 hours in 52% *ee* (Table 1.7, entries 7, 8).[96]

Table 1.7 Catalytic activity of catalysts **1.41a**, **f**–**j** in asymmetric *aza*-MBH and generic MBH reactions.[96,97]

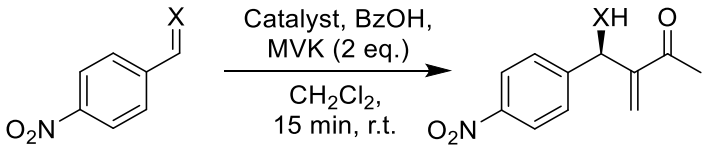

Entry	Catalyst	X	Catalyst/BzOH loading (mol%)	Conv[a] (%)	*ee*[b] (%)
1	**1.41a**	NTs	10/10	15(>95)[c]	80
2	**1.41g**	NTs	10/10	57	81
3	**1.41h**	NTs	10/10	87	88
4	**1.41f**	NTs	10/10	85[c]	73
5	**1.41i**	NTs	10/10	91	82
6	**1.41j**	NTs	10/10	57	87
7	**1.41a**	O	10/50	86[d]	26
8	**1.41j**	O	10/10	95[e]	52

[a]Calculated by ^{1}H NMR spectroscopy. [b]Determined by chiral HPLC analysis. [c]Reaction time 30 min. [d]Reaction time is 3 days. [e]Reaction time is 24 h.

To further investigate the role of the Brønsted acid motif in this trifunctional catalysis, the third generation catalysts with a different, NHTs Brønsted acid function **1.43** and a bivalent catalyst (two Brønsted acids) **1.41k** (Figure 1.10), were synthesized and tested in *aza*- and generic MBH reactions (Table 1.8).[94] The third generation catalysts also required an acid activation for proficient catalysis (Table 1.8, entries 3, 4, 9, 10).[94] The catalyst **1.43c** with a free amino group instead of NHTs Brønsted acid provided lower reaction rate and lower *ee*

value and negligible response to acid activation, confirming the importance of the NHTs Brønsted acid (Table 1.8, entries 1, 2, 3). The reduction of catalyst **1.43a** loading level from 10 mol% to 5 mol% allowed for higher *ee* from 82% to 88% without observable drop of the reaction rate. The further reduction of catalyst loading level to 2 mol% afforded a slightly lower reaction rate with 90% *ee* (Table 1.8, entries 3, 5, 6).

Table 1.8 Catalytic activity of catalysts **1.41k**, **1.43a**–**c**, **e** in Asymmetric *aza*-MBH and generic MBH reactions.[93,94]

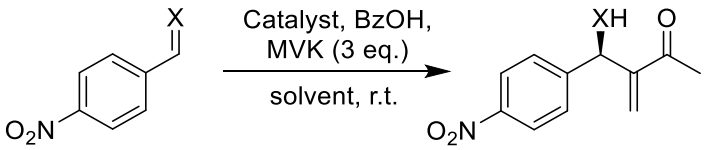

Entry	Catalyst	X	Catalyst/BzOH loading (mol%)	Time (h)	Conv[a] (%)	*ee*[b] (%)
1	**1.43c**	NTs	10/10	0.5	28	40
2	**1.43c**	NTs	10/0	0.5	9	32
3	**1.43a**	NTs	10/10	0.5	>95	82
4	**1.43a**	NTs	10/0	0.5	37	51
5	**1.43a**	NTs	5/5	0.5	>95	88
6	**1.43a**	NTs	2/2	0.5	89	90
7	**1.43b**	NTs	5/5	0.5	>95	40
8	**1.43b**	NTs	5/0	0.5	34	*rac*
9	**1.41k**	NTs	5/5	0.5	40	88
10	**1.41k**	NTs	5/0	0.5	17	*rac*
11	**1.43e**	NTs	5/5	0.5	>95	88
12	**1.43a**	O[c]	10/10	3	73	47
13	**1.43a**	O[c]	10/0	3	9	n.d.
14	**1.43b**	O[c]	10/10	6	95	54
15	**1.43b**	O[c]	10/0	6	30	*rac*

[a]Calculated by ^{1}H NMR spectroscopy. [b]Determined by chiral HPLC analysis. [c] Reaction performed in ether.

The catalyst **1.43b**, different from **1.43a** in the position of the NHTs Brønsted acid, demonstrated only 40% *ee* with similar reaction rate, confirming the key role of the Brønsted acid position for enantioselectivity (Table 1.8, entries 5, 7). The bivalent catalyst **1.41k** showed comparable enantioselectivity to that by **1.41a** and **1.43a** but provided lower reaction rate (Table 1.7, entry 1; Table 1.8, entries 5, 9).

The generic MBH test reactions catalyzed by **1.43a** and **1.43b** also demonstrated positive response of proficiency to the acid additive that is typical of a trifunctional mechanism, and the activity levels were comparable (Table 1.8, entries 12–15).[94] The most proficient catalyst **1.43a** in the third generation did not expand the MBH substrate scope, compared to the second generation catalysts **1.41g-j**, however the loading of the catalyst was reduced from 10 mol% to 2–5 mol% for *aza*-MBH reactions, providing products **1.24** in 91–97% yields with 54–86% *ee* (Scheme 1.15).[94]

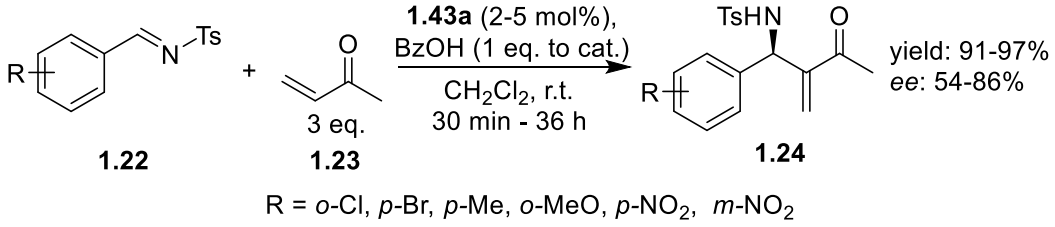

Scheme 1.15 *aza*-MBH reactions catalyzed by the organocatalyst **1.43a**.[94]

1.5 Summary and project aims

The MAP-derived structures are effective chiral ligands and asymmetric organocatalysts in a wide range of enantioselective reactions. The versatility of MAP scaffolds toward modification allows presentation of multiple activation motifs. The variety of ligands and organocatalysts obtained suggests that the MAP scaffold is an excellent candidate for developing hybrid catalytic systems.

Our MAP-based trifunctional catalysts, containing a phosphine Lewis base, a nitrogen Brønsted base (activated by benzoic acid), and various Brønsted acid functions in the structure, have shown good to excellent proficiency in *aza*-MBH reactions but limited activity in generic MBH reactions. The Brønsted acidity tuning of the third generation of catalysts **1.43** may improve further the catalytic proficiency or scope. The bivalent catalyst **1.41k** provided good *ee* value, but low reaction rate in MBH reaction. However, acidity tuning by at the addition of a bromine atom into the *para*-position to the phenolic Brønsted acid could increase its acidity and accelerate the reaction rate. Moreover, the acidity tuning could be investigated in generic MBH reactions as well. Therefore, the first aim of the MRes project is the catalyst **1.41m** (Figure 1.12) that may be readily synthesized and tested in *aza*-MBH and generic MBH reactions.

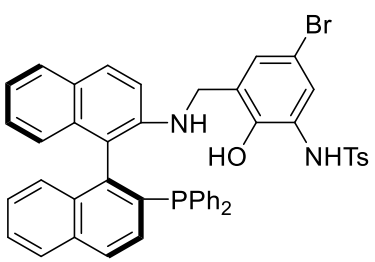

Aimed catalyst 1.41m

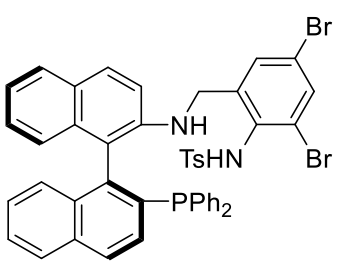

Aimed catalyst 1.43i

Figure 1.12 Aimed catalysts **1.41m** and **1.43i**.

In addition, the incorporation of potential metal chelating fragments into this trifunctional structure may lead to tetrafunctional catalytic systems. The tetrafunctional catalysts containing a metal atom as the Lewis acid function may afford hybrid catalysis from metal and organic activation.[13,17] The catalyst **1.43e** (Figure 1.10), containing a bromine *para* to the NHTs Brønsted acid, was synthesized and tested in *aza*-MBH reactions previously,[93] showing similar activities compared to that by catalyst **1.43a** (Table 1.8, entries 5, 11). The insertion of an additional bromine *ortho* to the NHTs Brønsted acid could provide a handle for further functionalization by cross-coupling reactions and additional information on increased Brønsted acidity on catalysis. Therefore, the second aim here is the synthesis and testing of **1.43i** (Figure 1.12) in *aza*-MBH and generic MBH reactions.

A pyrrole ring can coordinate a metal and is used as a key fragment in structures of chiral ligands.[98] The pyrrole nitrogen center has a different spatial position compared to that of phenol or NHTs Brønsted acids and could provide a different type of H-bonding interaction altering catalytic proficiency and substrate scope. Therefore, the synthesis and testing of catalysts **1.44a** and **1.44b** (Figure 1.13) became the third aim and the initial step in the development of pyrrole-containing multifunctional catalysts. It should be noted that attempts to introduce 2-indolyl ring as a Brønsted acid fragment into this type catalyst structure were made in our research group previously but the corresponding indole-containing catalyst was not obtained successfully.

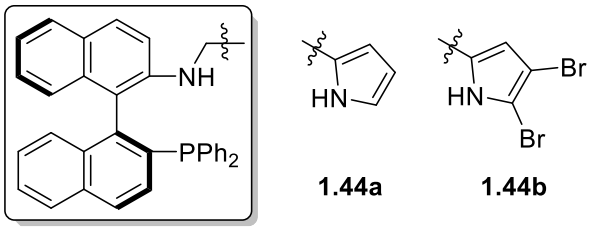

Figure 1.13 Aimed pyrrole-containing catalysts **1.44a** and **1.44b**.

2. EXPERIMENTAL SECTION

2.1 General information

(*S*)-BINOL was purchased from Combi-Blocks, Inc. UK. Diphenylphosphine oxide was purchased from Wako Chemical Ltd, Japan. Trifluoromethanesulfonic anhydride was purchased from Oakwood Products Inc. West Columbia, USA. 1,4-Bis(diphenylphosphino)butane was purchased from Strem Chemicals, USA. Bromine was purchased from BDH, UK. Sodium acetate trihydrate was purchased from M&B, Australia. Chloroform-*d* was purchased from Cambridge Isotope Laboratories, USA and stored over anhydrous potassium carbonate before use. All other reagents were purchased from Sigma-Aldrich Castle Hill. Unless specified, all commercially available reagents were used without further purification. Dichloromethane, chloroform, and toluene were distilled from calcium hydride and stored over 4Å MS. Tetrahydrofuran was distilled from sodium/benzophenone ketal and stored over 4Å MS. Methanol was distilled from sodium and stored over 3Å MS. Diisopropylethylamine and pyridine were distilled from potassium hydroxide and stored over 4Å MS. Trifluoromethanesulfonic anhydride was distilled from phosphorous pentoxide. Bromomethyl methyl ether was distilled from anhydrous sodium sulfate. Benzylamine was fractionally distilled at reduced pressure. DMSO was passed through a column of basic alumina, stored over 4Å MS for a week and fractionally distilled from calcium hydride at reduced pressure. Ethyl acetate was dried over anhydrous potassium carbonate, distilled and stored over 4Å MS. Acetonitrile was dried 24 hours over anhydrous potassium carbonate, 24 hours over 3Å MS then distilled. Methyl vinyl ketone was fractionally distilled before use. Cesium carbonate was flame-dried before reactions. Benzoic acid, 4-nitrobenzaldehyde, and *N*-bromosuccinimide were recrystallized from water. Diphenylphosphine oxide was treated with ethyl acetate to remove insoluble impurities and then filtered and concentrated *in vacuo*. Toluene and tetraethyl orthosilicate were degassed before use. Air and moisture sensitive reactions were performed under a nitrogen atmosphere. Reactions were magnetically stirred and monitored by thin-layer chromatography (TLC) using Merck silica gel 60 F_{254} aluminium pre-coated plates (0.25 mm). Flash column chromatography was performed on Merck silica gel 60 (0.015–0.040 mm). ^{1}H, ^{13}C, and 2D NMR experiments were performed at 298 K on either a Bruker DPX 400 MHz spectrometer equipped with a 5mm QNP probe, or a Bruker Avance II 600 MHz spectrometer equipped with a 5mm TXI cryoprobe. Chemical shifts were reported in ppm using the residual $CHCl_3$ peak as an internal reference (δ_H = 7.26 ppm, δ_C = 77.16 ppm). All ^{31}P NMR spectroscopy was performed on a Bruker DPX 400 MHz spectrometer at 298 K, and all spectra were referenced to H_3PO_4 (0 ppm). All spectra were processed using Bruker TOPSPIN software versions 1.3 and 3.2. Infrared spectra were taken

on Thermo Scientific Nicolet iS5FT-IR Spectrometer with an attenuated total reflectance (ATR) accessory and maximum absorption peaks were reported in cm^{-1}. Low-resolution mass analysis was acquired on an Agilent 6130 quadrupole LC/MS system with an electrospray ionization source (ESI) using the Zorbax SB-C18 column (2.1 x 50 mm, particle size 1.8 µm) or the Phenomenex Gemini C18 column (2.0 x 150 mm, particle size 3 µm); the mobile phase consisted of a gradient of 5–95% acetonitrile in water with 0.5% formic acid over 10 or 25 minutes (flow rate 0.5 mL/min, column temperature 40°C) and spectra were acquire in positive mode, scanning over the m/z range of 100–1000. HPLC analysis was performed using a Shimadzu Prominence system with either a Daicel Chiral Columns CHIRALPAK® AD–H column or a Regis Chiral Technologies Whelk-O1 column. HPLC grade solvents were degassed before use. Melting points were measured on Stuart Scientific Melting Point SMP 10.

2.2 Synthesis of aminophosphine 2.10 from (*S*)-BINOL 2.1

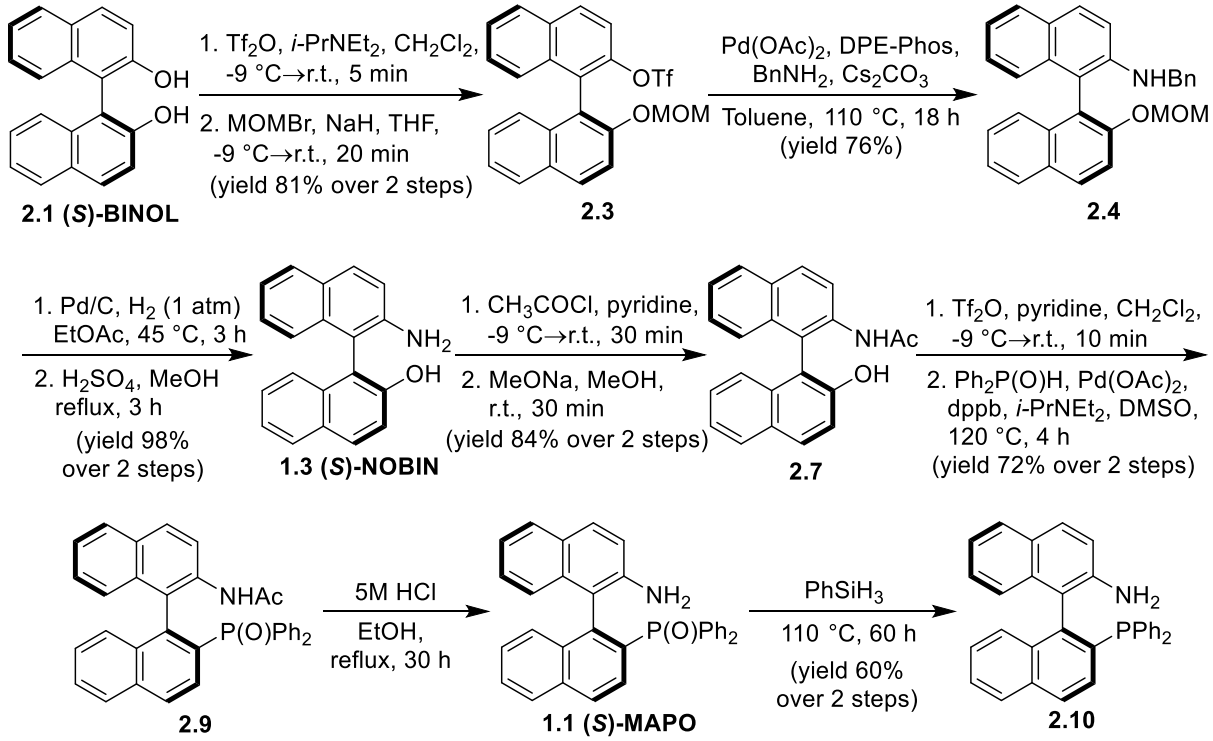

Scheme 2.1 Synthesis of aminophosphine **2.10** from **(*S*)-BINOL 2.1**.

(*S*)-2-trifluoromethanesulfoxy-2'-methoxymethoxy-1,1'-binaphthyl 2.3[46]

To a solution of **(*S*)-BINOL 2.1** (3 g, 10.5 mmol) and diisopropylethylamine (1.92 mL, 11 mmol) in dichloromethane (54 mL) was added triflic anhydride (1.85 mL, 11 mmol) over 40 minutes at -9 °C under nitrogen. After stirring at room temperature for 5 minutes, the reaction mixture was washed with saturated aqueous sodium bicarbonate and extracted twice with dichloromethane. The combined organic extracts were washed with brine, dried over anhydrous magnesium sulfate and evaporated under reduced pressure providing crude

monotriflate[99] as a white foam. **^{1}H NMR** (400 MHz, $CDCl_3$) δ 4.83 (bs, 1H), 7.00 (d, *J* = 8.5 Hz, 1H), 7.25 – 7.31 (m, 1H), 7.32 – 7.39 (m, 2H), 7.41 – 7.48 (m, 2H), 7.58 – 7.64 (m, 2H), 7.88 (d, *J* = 8.0 Hz, 1H), 7.98 (d, *J* = 9.0 Hz, 1H), 8.03 (d, *J* = 8.5 Hz, 1H), 8.14 (d, *J* = 9.0 Hz, 1H).

The crude monotriflate was dissolved in tetrahydrofuran (48 mL) under nitrogen and cooled to -9 °C whereby sodium hydride (0.66 g, 55% dispersion in mineral oil, 15.19 mmol) was added portion wise. After stirring for 30 minutes at -9 °C bromomethylmethyl ether (1.03 mL, 12.57 mmol) was added dropwise, and the mixture was left to stir at room temperature for 20 minutes. Then the reaction mixture was cooled down to -5 °C and *i*-propanol (0.36 mL, 4.72 mmol) was added dropwise. After stirring for 5 minutes at room temperature, dichloromethane (25 mL) was added to the reaction mixture, the precipitate was filtered and washed with dichloromethane (2 x 25 mL). The liquid phase was evaporated, and the residue was redissolved in dichloromethane, carefully washed with water. The aqueous layer was extracted with dichloromethane three times. The combined organic extracts were washed with brine, dried over anhydrous sodium sulfate and evaporated under reduced pressure. The crude product was purified by flash chromatography on silica gel with hexane:dichloromethane (2:1) to yield **2.3** (3.93 g, 81%) as a white solid. **^{1}H NMR** (400 MHz, $CDCl_3$) δ 3.23 (s, 3H), 5.03 (d, *J* = 7.0 Hz, 1H), 5.19 (d, *J* = 7.0 Hz, 1H), 7.04 (d, *J* = 8.5 Hz, 1H), 7.23 – 7.29 (m, 1H), 7.32 – 7.40 (m, 3H), 7.51 – 7.60 (m, 2H), 7.64 (d, *J* = 9.0 Hz, 1H), 7.89 (d, *J* = 8.0 Hz, 1H), 7.98 (d, *J* = 8.0 Hz, 1H), 8.00 – 8.08 (m, 2H).

(*S*)-2-(*N*-benzyl)amino-2'-methoxymethoxy-1,1'-binaphthyl 2.4[45,46]

A suspension of **2.3** (3.81 g, 8.25 mmol), palladium acetate (185 mg, 0.83 mmol), DPE-Phos (0.89 g, 1.65 mmol), cesium carbonate (3.23 g, 9.9 mmol) and benzylamine (1.08 mL, 9.9 mmol) in toluene (8.3 mL) was heated under nitrogen at 110 °C. After 18 hours, the reaction mixture was cooled, diluted with ethyl acetate, filtered through celite and evaporated under reduced pressure. The residue was redissolved in dichloromethane and washed with saturated aqueous sodium bicarbonate. The aqueous layer was extracted with dichloromethane three times. The combined organic layers were washed with brine. The brine layer was extracted with dichloromethane twice. The combined organic layers were dried over anhydrous sodium sulfate and evaporated under reduced pressure. The crude product was purified by flash chromatography on silica gel (neutralized by ammonia) with hexane:ethyl acetate (from 19:1 to 4:1) to yield **2.4** (2.63 g, 76%) as a white foam. **^{1}H NMR** (400 MHz, $CDCl_3$) δ 3.19 (s, 3H), 4.00 – 4.10 (m, 1H), 4.35 – 4.47 (m, 2H), 5.06 (dd, *J* = 21.0 Hz, 7.0 Hz, 2H), 6.95 (d, *J* = 8.0 Hz, 1H), 7.10 – 7.31 (m, 10H), 7.36 – 7.43 (m, 1H), 7.61 (d, *J* = 9.0 Hz, 1H), 7.72 – 7.77 (m, 1H), 7.80 (d, *J* = 9.0 Hz, 1H), 7.90 (d, *J* = 8.0 Hz, 1H), 7.98 (d, *J* = 9.0 Hz, 1H).

(*S*)-NOBIN 1.3[45]

A suspension of **2.4** (1.01 g, 2.41 mmol) and palladium (10% on carbon, 0.26 g, 0.246 mmol) in ethyl acetate (5.7 mL) was heated with hydrogen gas (1 atm) at 45 °C for 3 hours. A balloon was used to deliver hydrogen gas to the reaction mixture. After filtration through celite, the solvent was evaporated under reduced pressure to afford crude (*S*)-2-amino-2'-methoxymethoxy-1,1'-binaphthyl[92] as a slightly yellow solid which was used without further purification. **^{1}H NMR** (400 MHz, $CDCl_3$) δ 3.18 (s, 3H), 3.60 (bs, 2H), 5.05 (dd, *J* = 21.5 Hz, 7.0 Hz, 2H), 7.00 – 7.04 (m, 1H), 7.11 – 7.30 (m, 5H), 7.36 – 7.41 (m, 1H), 7.59 (d, *J* = 9.0 Hz, 1H), 7.77 – 7.83 (m, 2H), 7.88 – 7.92 (m, 1H), 7.99 (d, *J* = 9.0 Hz, 1H).

To a solution of crude (*S*)-2-amino-2'-methoxymethoxy-1,1'-binaphthyl in methanol (6 mL) and dichloromethane (6 mL) was added concentrated sulfuric acid (0.38 mL). After refluxing for 3 hours, the reaction mixture was cooled to room temperature, washed with saturated aqueous sodium bicarbonate (pH 8–9) and extracted three times with dichloromethane. The combined organic extracts were washed with brine and dried over anhydrous sodium sulfate and evaporated under reduced pressure to afford **(*S*)-NOBIN 1.3** (0.67 g, 98%) as a white solid which was used without further purification. **^{1}H NMR** (400 MHz, $CDCl_3$) δ 3.74 (bs, 2H), 5.13 (bs, 1H), 7.05 (d, *J* = 8.0 Hz, 1H), 7.13 – 7.41 (m, 7H), 7.81 (d, *J* = 7.5 Hz, 1H), 7.87 (t, *J* = 9.0 Hz, 2H), 7.93 (d, *J* = 9.0 Hz, 1H).

(*S*)-2-*N*-acetyl-2'-hydroxy-1,1'-binaphthyl 2.7[41]

To a solution of **(*S*)-NOBIN 1.3** (167 mg, 0.59 mmol) in pyridine (2.39 mL) was slowly added acetyl chloride (917 μL, 1.29 mmol) at -9 °C under nitrogen. After stirring at room temperature for 30 minutes, the reaction mixture was carefully poured onto ice cold water and extracted three times with dichloromethane. The extracts were washed twice with 5% aqueous hydrochloric acid, water, saturated aqueous sodium bicarbonate, brine, dried over anhydrous sodium sulfate and evaporated under reduced pressure to afford the crude *N*, *O*-diacetate[100]. **^{1}H NMR** (400 MHz, $CDCl_3$) δ 1.79 (s, 3H), 1.85 (s, 3H), 7.05 (d, *J* = 8.5 Hz, 1H), 7.11 – 7.54 (m, 7H), 7.90 (d, *J* = 8.0 Hz, 1H), 7.95 – 8.02 (m, 2H), 8.07 (d, *J* = 9.0 Hz, 1H), 8.35 (d, *J* = 9.0 Hz, 1H).

To a solution of crude diacetate in methanol (15.34 mL) was added sodium methoxide (50 μL, 25% in methanol). After stirring at room temperature for 30 minutes, the solvent was evaporated under reduced pressure and the residue redissolved in dichloromethane. The organic layer was washed with water, brine, dried over anhydrous sodium sulfate and evaporated under reduced pressure to afford **2.7** (0.18 g, 84%) as a white solid which was used without further purification. **^{1}H NMR** (400 MHz, $CDCl_3$) δ 1.84 (s, 3H), 5.20 (bs, 1H), 6.90 (bs, 1H), 7.01 (d, *J* = 8.5 Hz, 1H), 7.15 (d, *J* = 8.5 Hz, 1H), 7.24 – 7.32 (m, 2H), 7.35 –

7.41 (m, 2H), 7.42 – 7.47 (m, 1H), 7.89 – 7.95 (m, 2H), 7.98 (d, *J* = 9.0 Hz, 1H), 8.05 (d, *J* = 9.0 Hz, 1H), 8.56 (d, *J* = 9.0 Hz, 1H).

(*S*)-2-*N*-acetyl-2'-(diphenylphosphinoyl)-1,1'-binaphthyl 2.9[41]

To a solution of **2.7** (0.71 g, 2.16 mmol) and pyridine (0.53 mL, 6.49 mmol) in dichloromethane (11 mL) was slowly added triflic anhydride (0.4 mL, 2.38 mmol) at 0 °C under nitrogen. After stirring at room temperature for 10 minutes, the reaction mixture was diluted with dichloromethane (26 mL). The organic layer was washed with 5% aqueous hydrochloric acid, saturated aqueous sodium bicarbonate, water, dried over anhydrous sodium sulfate and evaporated under reduced pressure to afford the crude triflate[41]. **^{1}H NMR** (400 MHz, $CDCl_3$) δ 1.78 (s, 3H), 6.85 (s, 1H), 7.00 (d, *J* = 8.5 Hz, 1H), 7.25 – 7.40 (m, 2H), 7.41 – 7.48 (m, 2H), 7.58 – 7.65 (m, 2H), 7.92 (d, *J* = 8.0 Hz, 1H), 8.01 – 8.09 (m, 2H), 8.15 (d, *J* = 9.0 Hz, 1H), 8.36 (d, *J* = 9.0 Hz, 1H).

A suspension of the crude triflate, diphenylphosphine oxide (0.88 g, 4.32 mmol), 1,4-bis (diphenylphosphino)butane (0.18 g, 0.43 mmol), palladium acetate (97 mg, 0.43 mmol) and diisopropylethylamine (1.51 mL, 8.66 mmol) in dimethylsulfoxide (54 mL) was heated under nitrogen at 120 °C. After 4 hours, the reaction mixture was cooled to room temperature, diluted with dichloromethane (90 mL) and filtered through celite. The filtrate was washed with 5% aqueous hydrochloric acid, water, saturated sodium bicarbonate, brine, dried over sodium sulfate and evaporated under reduced pressure. The crude product was purified by flash chromatography on silica gel, toluene:ethyl acetate (2:1 to 0:1) to yield **2.9** (0.8 g, 72% calculated by ^{1}H NMR) as a white solid in mixture with diphenylphosphine oxide (the total mixture mass 0.902 g). **^{1}H NMR** (400 MHz, $CDCl_3$) δ 1.92 (s, 3H), 6.52 (d, *J* = 8.5 Hz, 1H), 6.61 – 6.66 (m, 2H), 6.77 (t, *J* = 7.5 Hz, 1H), 6.96 (t, *J* = 7.5 Hz, 1H), 7.12 (d, *J* = 8.5 Hz, 1H), 7.14 – 7.27 (m, 4H), 7.44 – 7.56 (m, 4H), 7.63 - 7.74 (m, 4H), 7.90 (d, *J* = 8.0 Hz, 1H), 7.93 – 7.99 (m, 3H), 9.74 (s, 1H); **^{31}P NMR** (162 MHz, $CDCl_3$) δ 30.77.

(*S*)-2-*N*-amino-2'-(diphenylphosphino)-1,1'-binaphthyl 1.1[93]

To a solution of **2.9** (0.9 g, 1.76 mmol, with ~10% of diphenylphosphine oxide impurity by NMR) in ethanol (18 mL) was added hydrochloric acid (4.47 mL, 5 M). After refluxing for 30 hours, the reaction mixture was cooled to room temperature, neutralized to pH 9 with sodium hydroxide (2 M) and extracted with dichloromethane. The combined organic extracts were washed with brine, dried over anhydrous sodium sulfate and evaporated under reduced pressure to afford **(*S*)-MAPO 1.1**[93] as a yellow foam which was used without further purification. **^{1}H NMR** (400 MHz, $CDCl_3$) δ 3.87 (bs, 2H), 6.51 (d, *J* = 8.5 Hz, 1H), 6.73 – 6.83 (m, 2H), 6.84 – 6.97 (m, 3H), 6.98 – 7.05 (m, 1H), 7.18 – 7.31 (m, 4H), 7.34 – 7.59 (m, 6H), 7.66 – 7.81 (m, 3H), 7.89 – 8.00 (m, 2H); **^{31}P NMR** (162 MHz, $CDCl_3$) δ 28.85.

A suspension of **(*S*)-MAPO 1.1** in phenylsilane (1 mL) was heated at 110 °C for 60 hours. The volatiles were removed *via* nitrogen blow down and the residue was purified by flash chromatography on silica gel with hexane:ethyl acetate (9:1) to yield aminophosphine **2.10** (425 mg, 60%) as a white foam. **^{1}H NMR** (400 MHz, $CDCl_3$) δ 3.29 (bs, 2H), 6.68 (d, *J* = 8.4 Hz, 1H), 6.93 – 6.99 (m, 1H), 7.03 (d, *J* = 8.5 Hz, 1H), 7.05 – 7.24 (m, 7H), 7.24 – 7.36 (m, 6H), 7.44 – 7.53 (m, 2H), 7.74 (d, *J* = 8.0 Hz, 1H), 7.81 (d, *J* = 8.5 Hz, 1H), 7.90 (d, *J* = 8.5 Hz, 2H); **^{31}P NMR** (162 MHz, $CDCl_3$) δ -11.33.

2.3 Synthesis of triflate phosphine oxide 2.12 from (*S*)-BINOL 2.1

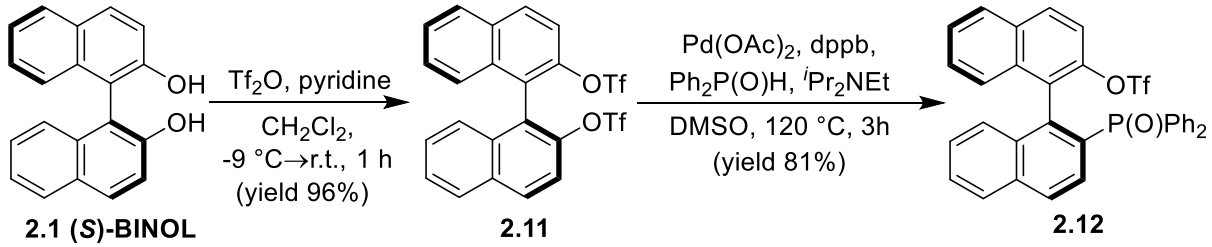

Scheme 2.2 Synthesis of triflate phosphine oxide **2.12** from **(*S*)-BINOL 2.1**.

(*S*)-2,2'-di(trifluoromethanesulfoxy)-1,1'-binaphthyl 2.11[93,101]

To a solution of **(*S*)-BINOL 2.1** (1 g, 3.49 mmol) and pyridine (847 μL, 10.48 mmol) in dichloromethane (20 mL) was slowly added triflic anhydride (1.47 mL, 8.73 mmol) at –9 °C under nitrogen. After stirring at room temperature for 1 hour, additional dichloromethane was added. The reaction mixture was washed with 5% aqueous hydrochloric acid (7.5 mL). The organic layer was washed by saturated sodium hydrogen carbonate aqueous solution (7.5 mL), and the aqueous layer was extracted with dichloromethane. The combined organic layer was washed with brine, dried over anhydrous sodium sulfate, and concentrated under reduced pressure to afford crude ditriflate **2.11** (1.84 g, 96%) as a white foam which was used without further purification. **^{1}H NMR** (400 MHz, $CDCl_3$) δ 7.26 (d, *J* = 8.5 Hz, 2H), 7.38 – 7.44 (m, 2H), 7.56 – 7.61 (m, 2H), 7.62 (d, *J* = 9.0 Hz, 2H), 8.01 (d, *J* = 8.5 Hz, 2H), 8.14 (d, *J* = 9.0 Hz, 2H).

(*S*)-2'-(diphenylphosphoryl)-1,1'-binaphthyl-2-yl trifluoromethanesulfonate 2.12[93,101]

A suspension of crude triflate **2.11** (1.84 g, 3.34 mmol), diphenylphosphine oxide (1.35 g, 6.68 mmol), 1,4-bis(diphenylphosphino)butane (285 mg, 0.67 mmol), palladium acetate (150 mg, 0.67 mmol) and diisopropylethylamine (2.91 mL, 16.7 mmol) in dimethylsulfoxide (20 mL) was heated under nitrogen at 120 °C. After 3 hours the reaction mixture was cooled to room temperature, diluted with ethyl acetate (45 mL) and filtered through celite. The filtrate was washed with 10% aqueous hydrochloric acid, water, saturated sodium hydrogen carbonate, brine, dried over sodium sulfate and evaporated under reduced pressure. The crude

product was purified by flash chromatography on silica gel, *n*-hexane:ethyl acetate (from 4:1 to 0:1) to yield **2.12** (1.63 g, 81%) as a white foam. **^{1}H NMR** (400 MHz, $CDCl_3$) δ 6.99 (d, *J* = 8.5 Hz, 1H), 7.13 – 7.20 (m, 2H), 7.22 – 7.52 (m, 13H), 7.58 (t, *J* = 7.5 Hz, 1H), 7.65 (dd, *J* = 11.5 Hz, 8.5 Hz, 1H), 7.84 (d, *J* = 8.5 Hz, 1H), 7.90 (d, *J* = 9.0 Hz, 1H), 7.94 (d, *J* = 8.0 Hz, 1H), 7.99 – 8.03 (m, 1H); **^{31}P NMR** (162 MHz, $CDCl_3$) δ 30.5.

2.4 Synthesis of aldehyde 2.19

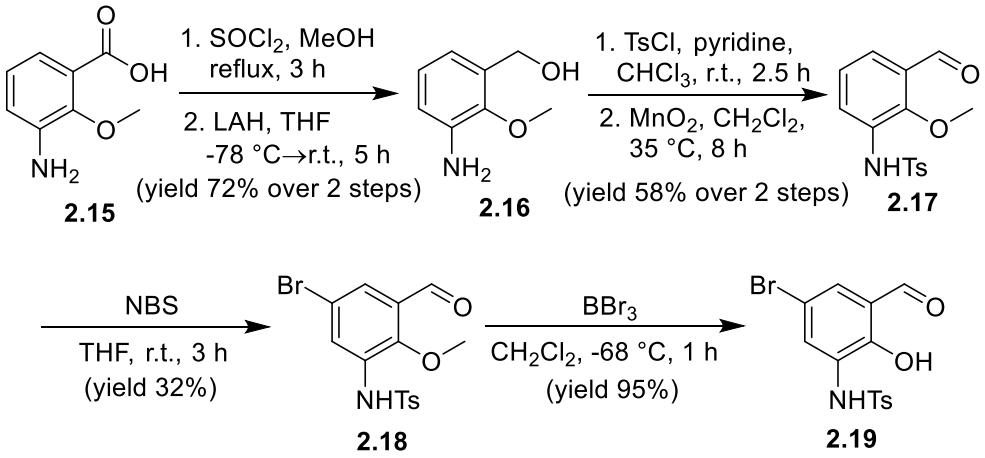

Scheme 2.3 Synthesis of aldehyde **2.19** from amino acid **2.15**.

(3-Amino-2-methoxyphenyl)methanol 2.16[94]

To a solution of 3-amino-2-methoxybenzoic acid **2.15** (0.5 g, 2.98 mmol) in methanol (5 mL) was added thionyl chloride (0.87 mL, 11.93 mmole) slowly at to 0 °C. After refluxing for 3 h, the reaction mixture was cooled to room temperature, washed with saturated aqueous sodium bicarbonate, and extracted three times with ethyl acetate. The organic layer was dried over anhydrous magnesium sulfate, filtered, and concentrated *in vacuo*. The resulting oil was dissolved in tetrahydrofuran (10 mL) and was added dropwise to a suspension of lithium aluminium hydride (453 mg, 11.93 mmol) in tetrahydrofuran (10 mL) at -68 °C (dry ice/*i*-propanol). The reaction mixture was allowed to stir for 40 minutes at 0 ºC and then was allowed to come to room temperature and left to stir for 4 hours. The reaction was washed with 0.1 M hydrochloric acid (40 mL) at -5 ºC diluted with ethylacetate, washed with water and brine. The organic layer was dried over anhydrous sodium sulfate, filtered, and concentrated *in vacuo* to yield the crude (3-amino-2-methoxyphenyl)methanol **2.16** (0.33 g, 72%) as a brown solid which was used without further purification. **^{1}H NMR** (400 MHz, $CDCl_3$) δ 3.81 (s, 3H), 4.69 (s, 2H), 6.70 – 6.75 (m, 2H), 6.93 (t, *J* = 7.5 Hz, 1H).

***N*-(3-Formyl-2-methoxyphenyl)-4-methylbenzenesulfonamide 2.17**[94]

To a solution of amino alcohol **2.16** (240 mg, 1.57 mmol) and pyridine (152 µL, 1.88 mmol) in dichloromethane (5.8 mL) was slowly added a solution of 4-toluenesulfonyl chloride (329 mg, 1.724 mmol) in dichloromethane (1.66 mL) at -5 ºC. After stirring at room temperature for 2 h, the reaction mixture was diluted in dichloromethane and washed with saturated aqueous ammonium chloride. The organic layer was dried over anhydrous sodium sulfate, filtered, and concentrated under reduced pressure to give the crude *N*-sulfonamide alcohol as green foam that was used without further purification. **^{1}H NMR** (400 MHz, $CDCl_3$) δ2.37 (s, 3H), 3.55 (s, 3H), 4.64 (s, 2H), 7.02 – 7.11 (m, 3H), 7.23 (d, *J* = 8.0 Hz, 2H), 7.49 – 7.54 (m, 1H), 7.73 (d, *J* = 8.0 Hz, 2H).

To a solution of crude alcohol in dichloromethane (8 mL) was added activated manganese dioxide (1.63 g, 18.80 mmol). After stirring at 35 ºC for 8 h, the reaction mixture was evaporated, redissolved in ethyl acetate, washed with water and filtered through a filter paper. The filtrate was concentrated *in vacuo*. The crude product was purified by flash chromatography on silica gel with hexane:ethyl acetate (from 9:1 to 3:2) to afford **2.17** (192 mg, 40%) as a white solid. **^{1}H NMR** (400 MHz, $CDCl_3$) δ 2.37 (s, 3H), 3.64 (s, 3H), 7.17 (bs, 1H), 7.20 (t, *J* = 8.0 Hz, 1H), 7.25 (d, *J* = 8.0 Hz, 2H), 7.49 – 7.55 (m, 1H), 7.72 (d, *J* = 8.0 Hz, 2H), 7.83 – 7.88 (m, 1H), 10.17 (s, 1H).

***N*-(5-Bromo-3-formyl-2-methoxyphenyl)-4-methylbenzenesulfonamide 2.18 (new compound)**

Solid *N*-bromosuccinimide (99 mg, 0.55 mmol) was added to a solution of the aldehyde **2.17** (154 mg, 0.50 mmol) in THF (2.5 mL) and the reaction mixture was stirred at the room temperature for 3 hours. The solvent was evaporated and reaction mixture was redissolved in dichloromethane and washed with water. The aqueous layer was extracted by dichloromethane. Combined organic layer was washed with brine, dried over anhydrous sodium sulfate and evaporate under reduced pressure. The crude product was purified by flash chromatography on silica gel, *n*-hexane:ethyl acetate (from 4:1 to 3:2) to yield *N*-(5-Bromo-3-formyl-2-methoxyphenyl)-4-methylbenzenesulfonamide **2.18** (62 mg, 32%) as a white solid. **^{1}H NMR** (400 MHz, $CDCl_3$) δ 2.37 (s, 3H), 3.58 (s, 3H), 7.23 (bs, 1H), 7.25 (d, *J* = 8.0 Hz, 2H), 7.37 (d, *J* = 9.0 Hz, 1H), 7.69 (d, *J* = 8.5 Hz, 1H), 7.70 (d, *J* = 8.5 Hz, 2H), 10.24 (s, 1H). **^{13}C NMR** (100 MHz, $CDCl_3$) δ 21.69, 63.80, 120.60, 125.04, 127.17, 127.25, 130.09, 130.10, 131.61, 135.95, 144.75, 151.09, 190.52; **IR** (ATR, cm^{-1}) ν 3237(m), 3085(w), 2853(w), 1694(s), 1574(w), 1462(m), 1418(m), 1334(m), 1168(s), 1091(m), 990(m).

***N*-(5-Bromo-3-formyl-2-hydroxyphenyl)-4-methylbenzenesulfonamide 2.19 (new compound)**

To a solution of 2-methoxybenzaldehyde **2.18** (51 mg, 0.134 mmol) in dichloromethane (3.3 mL) was added boron tribromide (129 µL, 1.34 mmol) dropwise at -68 °C (dry ice/*i*-propanol). After stirring at -68 °C for 1 h, the reaction mixture was warmed to room temperature and washed with water. The product was extracted with dichloromethane three times, the organic layer was dried over anhydrous magnesium sulfate, filtered and concentrated *in vacuo* to afford *N*-(5-Bromo-3-formyl-2-hydroxyphenyl)-4-methylbenzenesulfonamide **2.19** (47 mg, 95%) as a white solid. **^{1}H NMR** (400 MHz, $CDCl_3$) δ 2.37 (s, 3H), 7.06 (bs, 1H), 7.11 (d, *J* = 8.5 Hz, 1H), 7.19 – 7.25 (m, 2H), 7.62 – 7.70 (m, 3H), 10.18 (s, 1H), 12.21 (s, 1H); **^{13}C NMR** (100 MHz, $CDCl_3$) δ 21.71, 117.39, 121.87, 124.54, 126.16, 127.31, 127.75, 129.92, 135.97, 144.51, 153.87, 198.01; **IR** (ATR, cm^{-1}) ν 3241(m), 3086(w), 2918(w), 1646(s), 1597(m), 1435(s), 1418(m), 1399(w), 1335(s), 1268(m), 1238(s), 1163(s), 1091(m), 873(m). **LCMS (ESI)** $[M + H]^+$, *m/z* calculated for $(C_{14}H_{13}BrNO_4S)^+$ 369.97489, 371.97284, found 370.0, 371.9. **M.p.** 161–163 ºC.

2.5 Synthesis of aldehyde 2.23

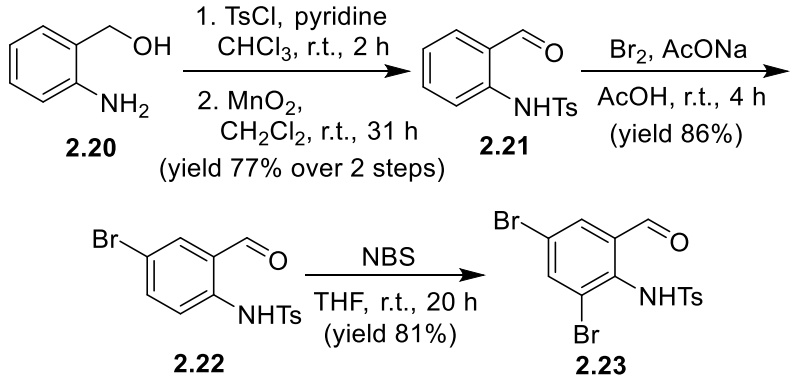

Scheme 2.4 Synthesis of aldehyde **2.23** from amino alcohol **2.20**.

***N*-(2-Formylphenyl)-4-methylbenzenesulfonamide 2.21**[94]

To a solution of amino alcohol **2.20** (500 mg, 4.06 mmol) and pyridine (394 µL) in chloroform (15 mL) was slowly added a solution of 4-toluenesulfonyl chloride (852 mg, 4.47 mmol) in chloroform (4.3 mL). After stirring at room temperature for 2 h, the reaction mixture was concentrated under reduced pressure, redissolved in dichloromethane and washed with saturated aqueous ammonium chloride. The organic layer was dried over sodium sulfate, filtered and concentrated under reduced pressure to give the crude *N*-sulfonamide alcohol,[102] which was used immediately without further purification. **^{1}H NMR** (400 MHz, $CDCl_3$) δ 2.04 (bs, 1H), 2.38 (s, 3H), 4.40 (s, 2H), 7.05 – 7.11 (m, 2H), 7.19 – 7.29 (m, 3H), 7.44 (d, *J* = 8.0 Hz, 1H), 7.65 (d, *J* = 8.2 Hz, 2H), 7.86 (bs, 1H).

To a solution of crude alcohol in dichloromethane (20 mL) was added activated manganese dioxide (8.5 g, 97.5 mmol). After stirring at room temperature for 1 h, the reaction mixture was filtered through a pad of celite and the filtrate was concentrated *in vacuo* affording **2.21** (0.861 g, 77%) as a white solid. **^{1}H NMR** (400 MHz, $CDCl_3$) δ 2.37 (s, 3H), 7.16 (t, *J* = 7.5 Hz, 1H), 7.24 (d, *J* = 8.0 Hz, 2H), 7.48 – 7.54 (m, 1H), 7.59 (d, *J* = 8.0 Hz, 1H), 7.69 (d, *J* = 8.5 Hz, 1H), 7.78 (d, *J* = 8.0 Hz, 2H), 9.83 (s, 1H), 10.78 (bs, 1H).

_N_-(2-Formyl-4-bromophenyl)-4-methylbenzenesulfonamide 2.22[103]

To a mixture of aldehyde **2.21** (145 mg, 0.53 mmol) and sodium acetate trihydrate (79 mg, 0.58 mmol) in 90% aqueous acetic acid (1.5 mL) was added bromine (53 µL, 2.11 mmol). After stirring at room temperature for 4 hours, 0.5 M aqueous sodium thiosulfate (1.5 mL) was added, and the stirring was continued for 30 minutes. The resulting solid was filtrated and washed with water to give brominated aldehyde **2.22** (0.16 g, 86%) as a pale yellow solid. **^{1}H NMR** (400 MHz, $CDCl_3$) δ 2.38 (s, 3H), 7.25 (d, *J* = 7.5 Hz, 2H), 7.57 – 7.65 (m, 2H), 7.68 – 7.71 (m, 1H), 7.75 (d, *J* = 8.0 Hz, 2H), 9.76 (s, 1H), 10.64 (bs, 1H).

_N_-(2,4-Dibromo-6-formylphenyl)-4-methylbenzenesulfonamide 2.23 (new compound)

Solid *N*-bromosuccinimide (208 mg, 1.17 mmol) was added to a cooled solution of the aldehyde **2.22** (69 mg, 0.19 mmol) in THF (975 µL) and the reaction mixture was stirred at the room temperature for 20 hours. The solvent was evaporated by nitrogen flow and reaction mixture was redissolved in dichloromethane and washed with water. The aqueous layer was extracted by dichloromethane. Combined organic layer was washed with brine, dried over anhydrous sodium sulfate and evaporate under reduced pressure. The crude product was purified by flash chromatography on silica gel, *n*-hexane:ethyl acetate (from 4:1 to 0:1) to yield **2.23** (206 mg, 81%) as a white foam. **^{1}H NMR** (400 MHz, $CDCl_3$) δ 2.42 (s, 3H), 6.75 (bs, 1H), 7.21 – 7.25 (m, 2H), 7.41 – 7.45 (m, 2H), 7.79 (d, *J* = 2.3 Hz, 1H), 8.09 (d, *J* = 2.3 Hz, 1H), 10.24 (s, 1H); **^{13}C NMR** (100 MHz, $CDCl_3$) δ 21.83, 121.91, 122.92, 127.73, 130.05, 131.60, 135.22, 135.34, 135.83, 139.47, 145.25, 187.55; **IR** (ATR, cm^{-1}) ν 3223(m), 3.060(w), 2958(w), 2881(w), 1685(s), 1572(w), 1439(m), 1372(m), 1338(s), 1227(m), 1165(s), 1148(s), 1088(s), 884(s). **LCMS (ESI)** $[M + H]^+$, *m/z* calculated for $(C_{14}H_{12}Br_2NO_3S)^+$ 431.89047, 433.88843, 435.88638, found 431.8, 433.9, 435.8. **M.p.** 152–154 ºC.

2.6 General procedure for synthesis of catalysts 1.41m, 1.43i, 1.44a, 1.44b[94]

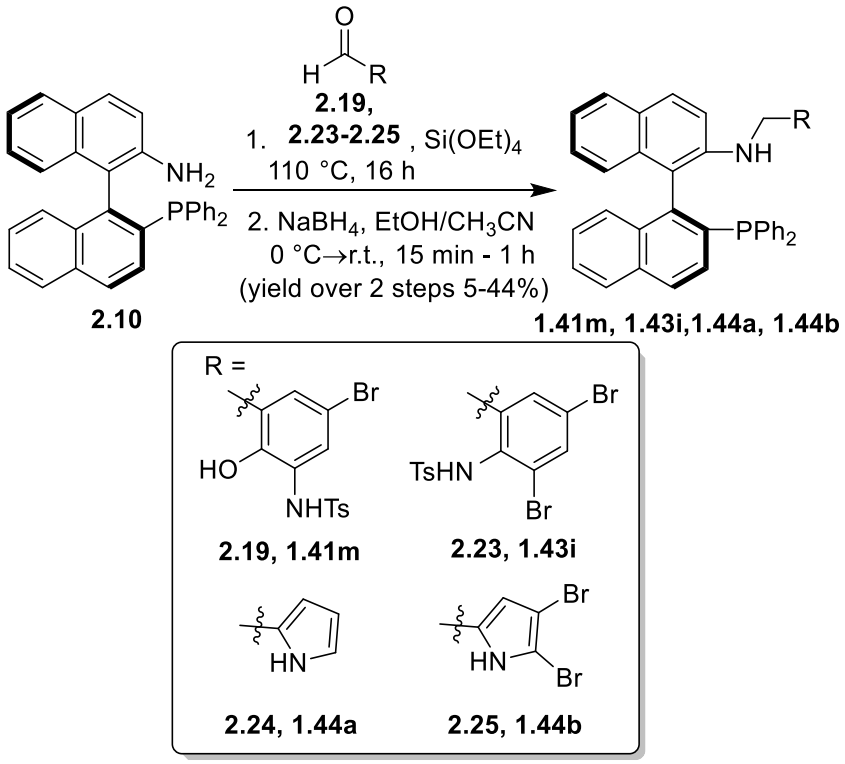

Scheme 2.5 Synthesis of catalysts **1.41m**, **1.43i**, **1.44a** and **1.44b** from aminophosphine **2.10**.

A suspension of aminophosphine **2.10** (25 mg, 0.055 mmol) and an aldehyde **2.19** or **2.23**–**2.25** (0.065 mmol) in tetraethylorthosilicate (250 µL) was heated in a sealed vial at 110 °C for 16 hours. After cooling to 0 °C, acetonitrile/ethanol (2:1, total 1 mL) then sodium borohydride (13 mg, 0.327 mmol) was added. After stirring at room temperature for 15 minutes or 1 hour, the reaction mixture was carefully washed with water and extracted three times with dichloromethane. The organic layer was washed with brine, dried over anhydrous magnesium sulfate and evaporated under reduced pressure. The crude product was purified by flash chromatography on silica gel, *n*-hexane : dichloromethane (from 1:1 to 1:2.5) to yield **1.41m**, **1.43i**, **1.44a**, **1.44b**.

(*S*)-*N*-(5-bromo-3-(((2'-(diphenylphosphanyl)-[1,1'-binaphthalen]-2-yl)amino)methyl)-2-hydroxyphenyl)-4-methylbenzenesulfonamide 1.14m (new compound)

Reduction time: 15 min; **Yield:** 44%; **^{1}H NMR** (400 MHz, $CDCl_3$) δ 1.96 (s, 3H), 3.36 (bs, 1H), 3.60 (d, *J* = 16.5 Hz, 1H), 3.89 (d, *J* = 16.5 Hz, 1H), 6.71 (bs, 1H), 6.79 (d, *J* = 9.0 Hz, 1H), 6.87 – 6.97 (m, 4H), 7.00 – 7.06 (m, 3H), 7.16 – 7.43 (m, 12H), 7.45 (dd, *J* = 8.5 Hz, 2.7 Hz, 1H), 7.47 – 7.52 (m, 2H), 7.53 – 7.95 (m, 1H), 7.83 – 7.89 (m, 2H), 7.93 – 7.98 (m, 2H), 10.20 (bs, 1H); **^{13}C NMR** (100 MHz, $CDCl_3$) δ 21.21, 49.53, 114.86, 118.11, 121.07, 121.70, 121.78, 121.99, 123.95, 124.14, 124.93, 125.01, 125.35, 126.95, 127.09, 127.59, 127.61,

128.11, 128.44, 128.50, 128.57, 129.13, 129.20, 129.47, 129.54, 129.61, 130.21, 130.43, 133.07, 133.26, 133.37, 134.19, 134.36, 134.57, 136.40, 136.52, 136.66, 137.07, 137.56, 138.68, 139.46, 139.79, 142.26, 142.28, 143.76, 149.11; **^{31}P NMR** (162 MHz, $CDCl_3$) δ -12.53; **IR** (ATR, cm^{-1}) ν 3052(w), 2919(w), 1619(w), 1597(m), 1495(w), 1431(s), 1377(m), 1333(s), 1304(m), 1258(w), 1155(s), 1089(s), 1022(m), 906(m), 862(m), 809(s). **LCMS (ESI)** $[M + H]^+$, *m/z* calculated for $(C_{46}H_{37}BrN_2O_3PS)^+$ 807.1446, 809.14255 found 807.0, 809.0.

(*S*)-*N*-(2,4-dibromo-6-(((2'-(diphenylphosphanyl)-[1,1'-binaphthalen]-2-yl)amino)methyl) phenyl)-4-methylbenzenesulfonamide 1.43i (new compound)

Reduction time: 1 h; **Yield:** 19%; **^{1}H NMR** (400 MHz, $CDCl_3$) δ 2.41 (s, 3H), 3.67 (bs, 1H), 4.22 (d, *J* = 17.5 Hz, 1H), 4.40 (d, *J* = 17.5 Hz, 1H), 6.28 (s, 1H), 6.66 (d, *J* = 8.5 Hz, 1H), 6.85 (d, *J* = 9.0 Hz, 1H), 6.95 (t, *J* = 8.0 Hz, 1H), 7.05 – 7.55 (m, 21H), 7.72 (d, *J* = 8.0 Hz, 1H), 7.80 (d, *J* = 9.0 Hz, 1H), 7.89 – 7.95 (m, 2H); **^{13}C NMR** (100 MHz, $CDCl_3$) δ 21.80, 45.06, 113.14, 116.56, 116.64, 122.00, 122.29, 123.65, 124.30, 126.17, 126.19, 126.38, 127.03, 127.29, 127.34, 127.45, 128.24, 128.30, 128.35, 128.61, 128.67, 128.74, 128.93, 129.54, 129.82, 129.92, 130.38, 130.55, 131.42, 131.50, 133.61, 133.78, 133.81, 133.91, 134.12, 134.33, 136.65, 138.23, 138.35, 142.65, 143.91, 144.49; **^{31}P NMR** (162 MHz, $CDCl_3$) δ -11.42; **IR** (ATR, cm^{-1}) ν 3051(w), 2918(w), 2849(w), 1620(w), 1595(m), 1452(m), 1433(m), 1393(m), 1336(s), 1161(s), 1090(s), 1021(m), 907(m), 861(m), 808(s). **LCMS (ESI)** $[M + H]^+$, *m/z* calculated for $(C_{46}H_{36}Br_2N_2O_2PS)^+$ 869.06019, 871.05815, 873.0561, found 868.9, 870.9, 872.9.

(*S*)-*N*-((1H-pyrrol-2-yl)methyl)-2'-(diphenylphosphanyl)-[1,1'-binaphthalen]-2-amine 1.44a (new compound)

Reduction time: 15 min; **Yield:** 5%; **^{1}H NMR** (400 MHz, $CDCl_3$) δ 3.71 (t, *J* = 5.5 Hz, 1H), 4.21 (d, *J* = 5.5 Hz, 2H), 5.95 (bs, 1H), 6.04 – 6.09 (m, 1H), 6.43 – 6.48 (m, 1H), 6.52 (d, *J* = 8.5 Hz, 1H), 6.87 – 6.93 (m, 1H), 6.96 – 7.03 (m, 2H), 7.05 – 7.19 (m, 6H), 7.22 – 7.37 (m, 6H), 7.44 (dd, *J* = 8.5 Hz, 3.0 Hz, 1H), 7.47 – 7.54 (m, 1H), 7.69 (d, *J* = 8.0 Hz, 1H), 7.81 (d, *J* = 9.0 Hz, 1H), 7.87 – 7.93 (m, 2H), 8.22 (bs, 1H); **^{13}C NMR** (100 MHz, $CDCl_3$) δ 41.61, 104.82, 108.45, 113.60, 116.99, 121.90, 124.24, 126.27, 126.38, 127.10, 127.37, 127.91, 128.25, 128.32, 128.36, 128.52, 128.66, 128.69, 128.79, 128.85, 129.96, 130.70, 133.58, 133.66, 133.77, 133.87; **^{31}P NMR** (162 MHz, $CDCl_3$) δ -11.55; **IR** (ATR, cm^{-1}) ν 3729(w), 3050(w), 2847(w), 1618(w), 1596(m), 1491(m), 1430(m), 1335(w), 1299(m), 1214(w), 1152(w), 1091(m), 1024(m), 907(m), 810(m). **LCMS (ESI)** $[M + H]^+$, *m/z* calculated for $(C_{37}H_{30}N_2P)^+$ 533.21466, found 533.2.

(*S*)-*N*-((4,5-dibromo-1H-pyrrol-2-yl)methyl)-2'-(diphenylphosphanyl)-[1,1'-binaphthalen]-2-amine 1.44b (new compound)

Reduction time: 15 min; **Yield:** 9%; **^{1}H NMR** (400 MHz, $CDCl_3$) δ 3.91 (bs, 1H), 4.18 – 4.37 (m, 2H), 6.00 – 6.06 (m, 1H), 6.35 (d, *J* = 8.5 Hz, 1H), 6.72 – 6.80 (m, 1H), 6.93 – 7.13 (m, 7H), 7.20 – 7.38 (m, 7H), 7.41 (dd, *J* = 8.5 Hz, 3.0 Hz, 1H), 7.48 – 7.54 (m, 1H), 7.62 (d, *J* = 8.0 Hz, 1H), 7.78 (d, *J* = 9.0 Hz, 1H), 7.91 (d, *J* = 8.5 Hz, 1H), 7.92 (d, *J* = 8.0 Hz, 1H), 9.71 (bs, 1H); **^{13}C NMR** (100 MHz, $CDCl_3$) δ 29.85, 41.10, 108.22, 113.26, 122.00, 124.29, 126.08, 126.10, 126.21, 127.23, 127.37, 127.44, 127.73, 128.20, 128.27, 128.38, 128.73, 128.86, 128.90, 128.92, 130.08, 130.20, 131.71, 133.58, 133.77, 134.09, 134.29, 141.69; **^{31}P NMR** (162 MHz, $CDCl_3$) δ -10.37; **IR** (ATR, cm^{-1}) ν 3052(w), 2955(m), 2917(s), 2849(s), 1736(w), 1618(w), 1596(m), 1493(m), 1463(m), 1432(m), 1376(m), 1339(m), 1296(m), 1257(m), 1187(m), 1152(m), 1083(m), 1023(m), 967(m), 908(m), 808(s). **LCMS (ESI)** $[M + H]^+$, *m/z* calculated for $(C_{37}H_{28}Br_2N_2P)^+$ 689.03568, 691.03364, 693.03159 found 689.0, 691.0, 692.9.

2.7 Synthesis of *N*-(4-bromobenzylidene)-4-methylbenzenesulfonamide 2.27[104]

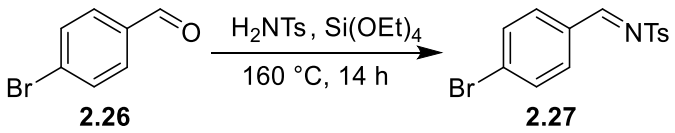

Scheme 2.6 Synthesis of *N*-tosyl substituted *p*-bromobenzaldimine **2.27**.

Tetraethylorthosilicate (1.2 mL, 5.40 mmol) was added to a mixture of *p*-bromobenzaldehyde (1 g, 5.40 mmol) and *p*-toluenesulfonamide **2.26** (0.97 g, 5.68 mmol) in a pressure tube. After overnight stirring at 160 °C, the reaction mixture was dissolved in hot ethyl acetate (50 mL) until the clear solution formed. Then hot *n*-hexane (10 mL) was added until the solution became cloudy. The product crystallized from the solution at room temperature. The white crystals were filtered providing *N*-tosylbenzaldimine **2.27** (1.54 g, 84%). **^{1}H NMR** (400 MHz, $CDCl_3$) δ 2.44 (s, 3H), 7.35 (d, *J* = 8.0 Hz, 2H), 7.63 (d, *J* = 8.5 Hz, 2H), 7.78 (d, *J* = 8.5 Hz, 2H), 7.88 (d, *J* = 8.0 Hz, 2H), 8.98 (s, 1H).

2.8 Procedures for the *aza*-MBH or generic MBH reactions catalyzed by 1.41m, 1.43i, 1.44a and 1.44b [94]

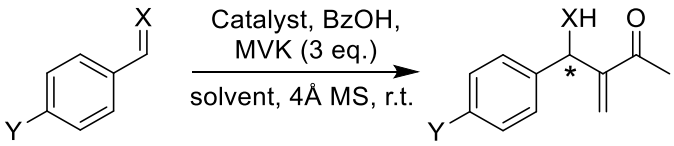

2.27, 2.28 **2.29, 2.30**

X = NTs: Y = Br (**2.27, 2.29**); X = O: Y = NO_2 (**2.28, 2.30**)

Scheme 2.7 *aza*-MBH and generic MBH reactions.

Catalyst **1.41m**, **1.44a**, **1.44b** (10 mol%, 0.002 mmol) or **1.43i** (5 mol%, 0.001 mmol), *p*-bromobenzaldimine **2.27** or *p*-nitrobenzaldehyde **2.28** (0.02 mmol) and benzoic acid (10 mol%, 0.002 mmol for **1.41m**, **1.44a**, and **1.44b** or 5 mol%, 0.001 mmol for **1.43i** in *aza*-MBH) were combined under N_2 in a 1.5 mL teflon capped vial with 4Å molecular sieves. Dichloromethane was added to the mixture (amount, providing C = 0.2 M to imine after addition of MVK solution in dichloromethane). MVK (0.06 mmol) in dichloromethane was added to the mixture. Aliquots (5–10 μL) of the reaction mixture were taken and dried via nitrogen blow down to remove MVK. The residue was redissolved in chloroform-*d* to determine conversion to product **2.29** or **2.30** by ^{1}H NMR and analyzed by chiral HPLC (1:4 *i*-propanol:hexane) to determine *ee*.

3-((4-Bromophenyl)(tosylamino)methyl)but-3-en-2-one 2.29[94]

^{1}H NMR (400 MHz, $CDCl_3$) δ 2.16 (s, 3H), 2.41 (s, 3H), 5.20 (d, *J* = 9.0 Hz, 1H), 5.64 (d, *J* = 9.0 Hz, 1H), 6.06 (s, 1H), 6.10 (s, 1H), 6.99 (d, *J* = 8.0 Hz, 2H), 7.23 (d, *J* = 8.0 Hz, 2H), 7.32 (d, *J* = 8.0 Hz, 2H), 7.63 (d, *J* = 8.0 Hz, 2H). **HPLC**: CHIRALPAK® AD–H column; eluent: *i*-propanol:hexane 1:4. Flow rate: 0.7 mL/min; t_{minor} = 18 min, t_{major} = 21 min. The compound **2.29** was proposed as (*R*)-enriched, based on the literature data[94] where for (*R*)-enriched **2.29** t_{major} = 16.7 min, t_{minor} = 18.8 min at the same conditions using Chiralpak AD column were reported.

3-(hydroxy(4-nitrophenyl)methyl)but-3-en-2-one 2.30[105]

^{1}H NMR (400 MHz, $CDCl_3$) δ 2.36 (s, 3H), 3.25 (d, *J* = 6.0 Hz, 1H), 5.68 (d, *J* = 6.0 Hz, 1H), 6.01 – 6.04 (m, 1H), 6.26 (s, 1H), 7.56 (d, *J* = 9.0 Hz, 2H), 8.20 (d, *J* = 9.0 Hz, 2H).**HPLC**: Whelk-O1 column; eluent: *i*-propanol:hexane 1:4. Flow rate: 0.6 mL/min; t_{major} = 15 min, t_{minor} = 19 min. The compound **2.30** was proposed as (*R*)-enriched, based on the literature data[106] where for (*R*)-enriched **2.30** t_{major} = 28.77 min, t_{minor} = 31.48 min; eluent: *i*-propanol:hexane 1:19; flow rate: 1.0 mL/min; Chiralcel OD-H column were reported.

3. RESULTS AND DISCUSSION

3.1 Synthesis of (*S*)-NOBIN 1.3 from (*S*)-BINOL 2.1

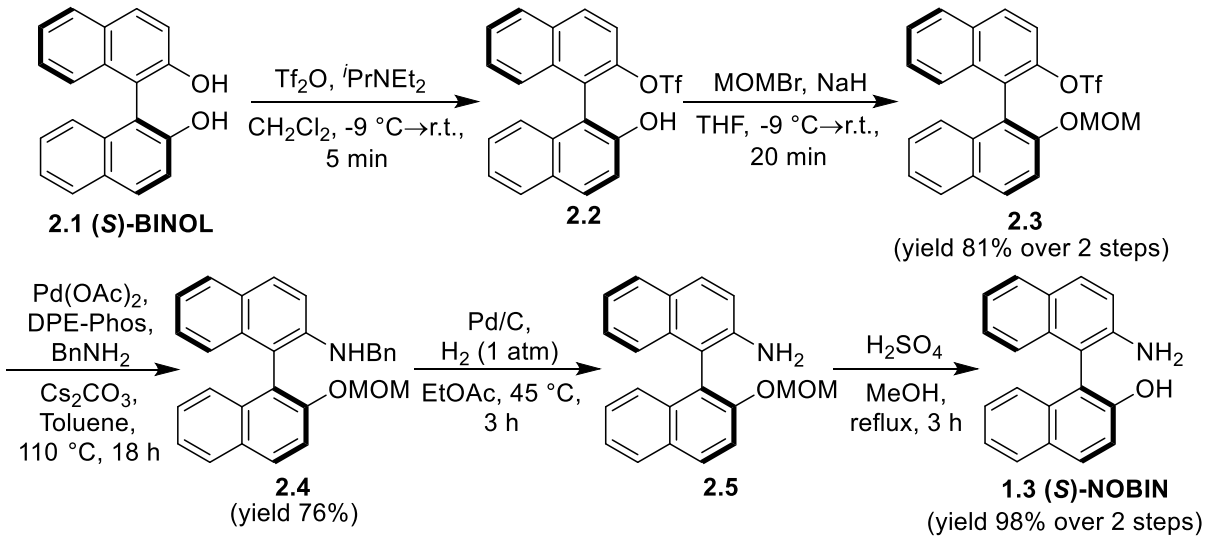

Scheme 3.1 Synthesis of **(*S*)-NOBIN 1.3** from **(*S*)-BINOL 2.1** in five steps with 60% overall yield.

The synthesis of diprotected (*S*)-NOBIN **2.4** was described by Maruoka[46] and used with minor modifications. The synthesis of (*S*)-NOBIN **1.3** from compound **2.4** via two deprotection steps was performed as described in Brückner's method[45] with modifications.[92] Triflation of commercially available (*S*)-BINOL **2.1** by trifluorosulfonic anhydride furnished monotriflate **2.2** in 5 minutes, which was followed by methoxymethyl protection without purification and provides MOM-protected triflate **2.3** in 20 minutes with 81% yield over two steps. The replacement of methoxymethyl chloride by methoxymethyl bromide reduced reaction time from 3 hours to 20 minutes. The undesired side ditriflate **2.11** (Figure 3.1) in the crude mixture with MOM-protected triflate **2.3** interfered with the next Buchwald–Hartwig amination step, reducing the yield of compound **2.4** sharply. Attempts to separate **2.11** from the triflate **2.3** by column chromatography using ethyl acetate/*n*-hexane were unsuccessful but switching to dichloromethane/*n*-hexane (1:2)[92] allowed for the separation of **2.3** from ditriflate **2.11** to ensure conversion in the amination step. In conclusion, the expensive (*S*)-NOBIN **1.3** (Sigma-Aldrich 100 mg – AU$138) was obtained from cheap (*S*)-BINOL **2.1** (Combi-Blocks, Inc. 100 g – US$82) over five steps in overall 60% yield at 3 g scale.

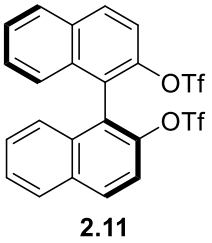

Figure 3.1 Undesired side ditriflate **2.11**.

3.2 Synthesis of aminophosphine 2.10 from (*S*)-NOBIN 1.3

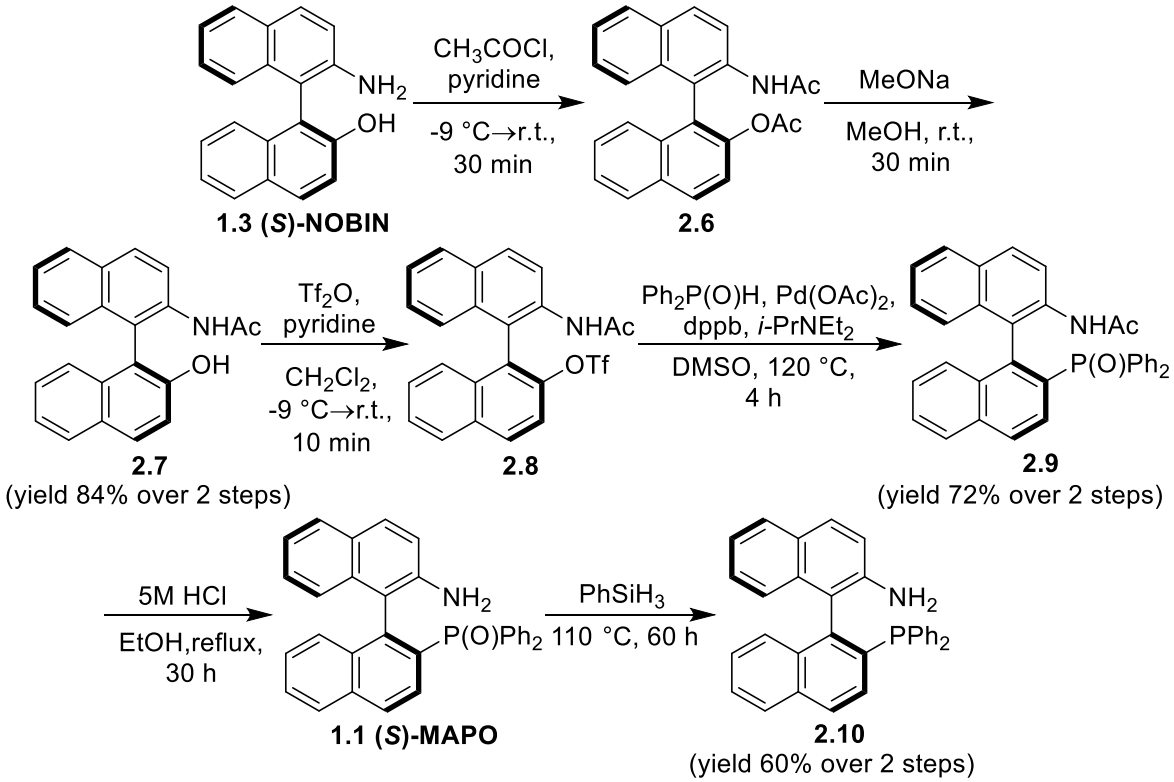

Scheme 3.2 Synthesis of aminophosphine **2.10** from **(*S*)-NOBIN 1.3** in six steps with 36% overall yield.

The synthetic pathway from (*S*)-NOBIN **1.3** to aminophosphine **2.10** was performed by Kočovský's procedure[41] with minor modifications.[92,97] The sequence included acetylation of (S)-NOBIN **1.3** by acetyl chloride and subsequent selective deacetylation of diacetylated product **2.6** by sodium methoxide in methanol that furnished *N*-acetylprotected (*S*)-NOBIN **2.7**. Triflation of **2.7** and phosphonylation of triflate **2.8** by diphenylphosphine oxide provided *N*-acetyl protected (*S*)-MAPO **2.9** in 72% yield over two steps.

In this phosphonylation step, purification of the product from the excess diphenylphosphine oxide was tenuous, and standard eluants such as ethyl acetate/*n*-hexane or ethyl acetate/toluene[93] did not provide optimal separation of **2.9** from diphenylphosphine oxide. The mixture of **2.9** with some diphenylphosphine oxide was allowed to carry through in the next reaction of **2.9** deacetylation and **1.1** phosphine oxide reduction. The deacetylation of *N*-acetylprotected (*S*)-MAPO **2.9** did not show full completion within 6 hours[93] and the time of reaction was increased to 30 hours that provided the complete conversion of starting material **2.9** into (*S*)-MAPO **1.1**. In future, more concentrated acid will be used for this reaction to reduce the reaction time. The final phosphine oxide reduction allowed for the separation of side-products, including diphenylphosphine oxide, by column chromatography and furnished pure aminophosphine **2.10** in 60% isolated yield over two steps at 100 mg scale.

3.3 The optimal synthetic route to aminophosphine 2.10

The 11-step synthetic route from (*S*)-BINOL **2.1** to aminophosphine **2.10** described above is reproducible and scalable. Attempts were made to reach **2.10** from (*S*)-BINOL **2.1** by shorter synthetic routes by converting **2.12**[101] via amination to **2.13** (Scheme 3.3). This might bypass multiple protection-deprotection steps as described previously.

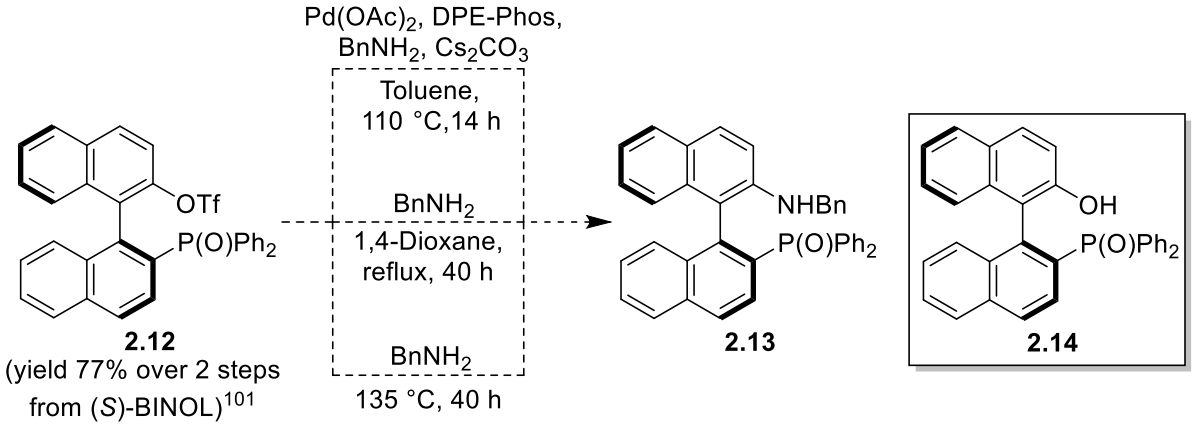

Scheme 3.3 Attempts of the triflate **2.12** amination.

The triflate **2.12** was subjected to Buchwald–Hartwig amination conditions, but only hydrolyzed side product **2.14** (Scheme 3.3) was isolated from the reaction mixture in 63% yield. Nucleophilic aromatic substitution reactions were also attempted[107,108] but did not demonstrate any conversion, which was consistent with the expectation that the lack of an electron-withdrawing group would usually inhibit such mechanisms. The attempts of our research group to reproduce the Staudinger approach[44] towards (*S*)-MAPO **1.1** from (*S*)-BINOL **2.1** have not been fruitful. Moreover, a partial racemisation of 1,1'-binaphthyl system occurred during the Staudinger ligation in our hands. In summary, the combined Maruoka–Brückner–Kočovský route form cheap (*S*)-BINOL **2.1** to aminophosphine **2.10** (Scheme 3.1 and 3.2) remains the most reproducible and scalable method.

3.4 Synthesis of organocatalysts 1.41m, 1.43i, 1.44a, 1.44b.

The synthesis of the new catalysts **1.41m**, **1.43i**, **1.44a**, **1.44b** required the precursor aldehydes **2.19**, **2.23**–**2.25** (Scheme 3.4). The aldehyde **2.19** was synthesized from the commercially available **2.15** over six steps. The preparation of the intermediate aldehyde **2.17** was carried out by the procedure described previously[94] from **2.15** with minor modification in work-up that allowed for the doubling of **2.17** yield. The subsequent bromination by NBS in THF and deprotection by BBr_3 afforded the aldehyde **2.19** in 13 % yield over six steps (Scheme 3.4a).

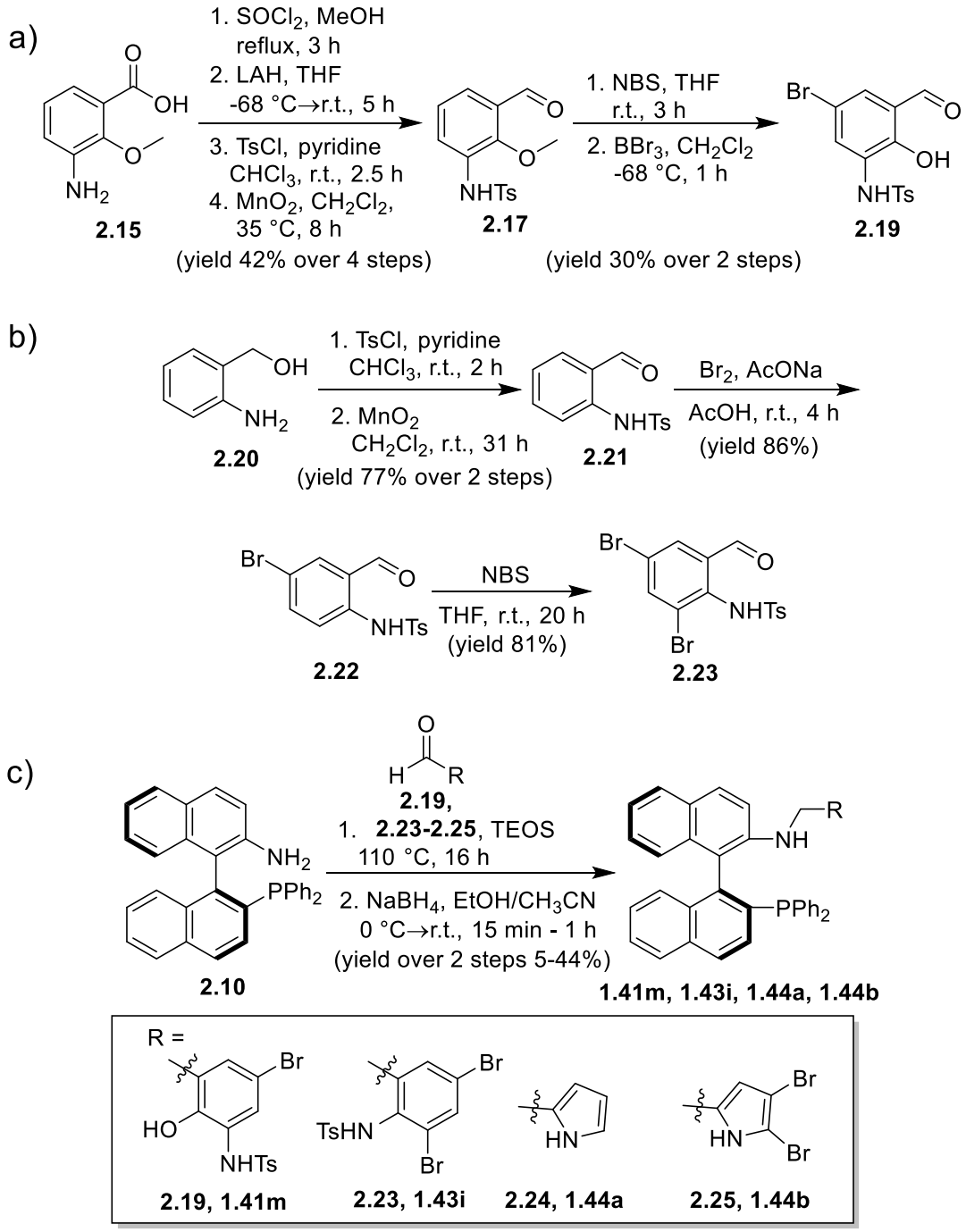

Scheme 3.4 (a) Synthesis of the aldehyde **2.19** from **2.15**. (b) Synthesis of the aldehyde **2.23** from **2.20**. (c) Synthesis of the catalysts **1.41m**, **1.43i**, **1.44a**, **1.44b** from **2.10**.

The aldehyde **2.23** was synthesized from commercially available 2-aminobenzyl alcohol **2.20** (Scheme 3.4b) using known procedures.[94,103] The aldehyde **2.22** was synthesized with the 66% yield over three steps.[94,103] The subsequent bromination of **2.22** by NBS furnished the desired new aldehyde **2.23** in the 81% yield (Scheme 3.4b). The NBS was found to be more experimentally convenient than Br_2 as a brominating agent (easier to control loading, less toxic, easier work-up procedure). The attempts to use higher loading of bromine to achieve the one-pot bromination of both positions in **2.21** were not performed. The downfield shift of N***H***Ts proton signal from δ 7.86 for **2.20** to δ 10.78 or 10.64 for **2.21** and **2.22**

correspondingly in the ^{1}H NMR spectra may be explained by involving this proton into hydrogen bonding.[109] Hypothetically compounds **2.21** and **2.22** can form a 6-member pseudo cycle via the NH•••O hydrogen bond between the proton of N***H***Ts group and newly formed aldehyde oxygen atom. The formation of such 6-member pseudo cycle in compound **2.20** is less likely due to lower electronvegativity of the alcohol oxygen atom in comparison to the carbonyl oxygen atom. Additional NMR investigations at different temperatures and at various concentration of the sample will be performed in the future to test this hypothesis. Aldehydes **2.24** and **2.25** for the synthesis of the pyrrole-type catalysts **1.44a** and **1.44b** were provided by Mr. Ketan Ahire from Prof. Peter Karuso's research lab (Macquarie University). The reductive amination of the aldehydes **2.19**, **2.23**–**2.25** with the aminophosphine **2.10** led to the catalysts **1.41m**, **1.43i**, **1.44a**, **1.44b** formation in 44%, 19%, 5% and 9% yields correspondingly over two steps (Scheme 3.4c). The formation of imine was controlled by a TLC technique that showed a new spot (R_f 0.51; hexane/ethyl acetate 4:1) together with spot of aldehyde **2.25** (there are no the spot of aminophosphine **2.10**) in the synthesis of catalyst **1.44b**, or a new spot (R_f 0.55; hexane/ethyl acetate 4:1) together with spots of starting aminophosphine **2.10** and aldehyde **2.24** in synthesis of the catalyst **1.44a**. These spots disappeared during the reduction by $NaBH_4$. Based on these observations, the conversion of starting aminophosphine **2.10** to imine was full in synthesis of catalyst **1.44b**, and was not full in synthesis of the catalyst **1.44a**. The low yields of catalysts **1.44a** and **1.44b** could be explained by polymerization of pyrrole ring without protection in reaction conditions, which in future could be amended by using Boc-protected pyrrole during catalyst synthesis.[110]

3.5 Catalysis of organocatalyst 1.41m in *aza*-MBH and MBH reactions.

The cooperativity of three functional motifs (phosphine Lewis base, nitrogen Brønsted base and phenolic or NHTs Brønsted acid), as shown in earlier generations of our catalysts, led to fast and enantioselective *aza*-MBH reaction at ambient temperature in the presence of benzoic acid additive.[94-97] The phosphine nucleophile serves as a Lewis base and initiates the *aza*-MBH reaction by addition to MVK forming a zwitterionic intermediate **2.31** (Scheme 3.5). The benzoic acid may be recruited by the exo-amino nitrogen (Brønsted base) to help form, in conjunction with the phenol group (Brønsted acid function), an H-bonding network (transition state **2.32a**) accelerating the aldol addition of *N*-tosylbenzaldimine to the zwitterionic intermediate **2.31** for producing adduct **2.33**. The favoured approach (TS **2.32a)** of the benzaldimine substrate in the aldol step is amenable to efficient H-bonding interactions and may be responsible for the enhancement of reaction rate and *ee* value (Scheme 3.5, favoured TS **2.32a**; unfavoured TS **2.32b**). In our third-generation catalysts[94], an additional Brønsted acid, NHTs, was incorporated to investigate the potential effects of an expanded H-bonding

network that may increase the substrate scope to include aldehydes (generic MBH) (Scheme 3.5, TS **2.34**). While this approach did not improve the proficiency for the *aza*-MBH reaction, it showed moderate activity in a generic MBH test reaction that is generally more difficult to catalyze than the *aza*-MBH reaction. Here, the acidity of the phenolic Brønsted acid function of **1.41m** (Table 3.1, scheme) is further increased, due to a bromine substitution at the *para*-position, in order to examine if this improves catalytic proficiency in this catalyst structure with two Brønsted acids.

The activity of the new catalyst **1.41m** was investigated in *aza*-MBH and generic MBH reactions (Table 3.1, entries 6–9). For ease of comparison, the relevant activity data for catalysts **1.41k**, **1.41i** and **1.41j** are also provided (Table 3.1, entries 1–5, 10). The new catalyst **1.41m** required benzoic acid for activation for rate and *ee* enhancement in both *aza*-MBH and generic MBH test reactions, a feature that is consistently observed in trifunctional catalysis (Table 3.1, entries 6–9). However, the activation by benzoic acid is not pronounced in the case of **1.41m**, compared to that in the case of **1.41k** for *aza*-MBH (Table 3.1, entries 1, 2, 6, 7). Catalyst **1.41m** showed significantly lower reaction rate but similar *ee* values in comparison to **1.41k** and **1.41i** in the *aza*-MBH reaction (Table 3.1, entries 1, 2, 5–7). This suggests that the Brønsted acidity in **1.41m** may be too high, a situation that has been observed in our early studies of acidity tuning in the **1.41i** series[96].

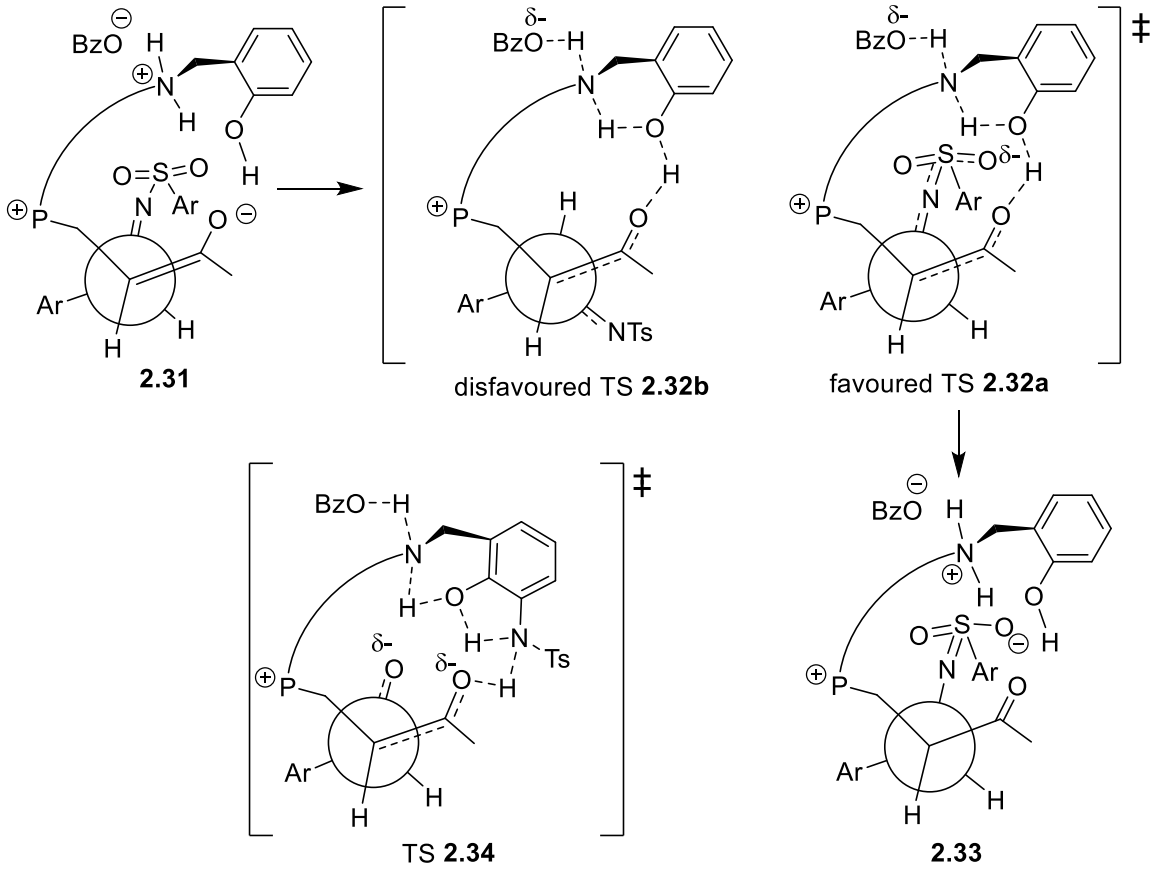

Scheme 3.5 Possible TS structures **2.32a**, **2.32b**, and **2.34**.

Table 3.1 Catalytic activity of catalysts **1.41m**, **1.41i**, **1.41j**, **1.41k** in asymmetric *aza*-MBH and generic MBH reactions.[94,96]

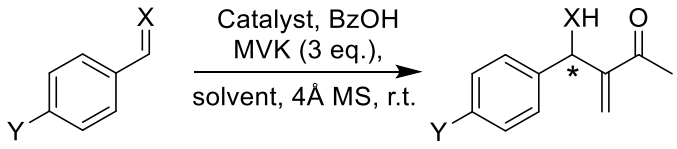

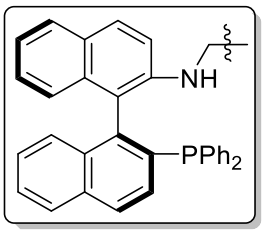

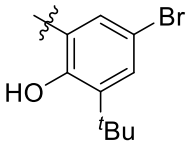

1.41i

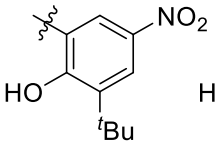

1.41j

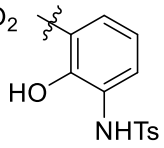

1.41k

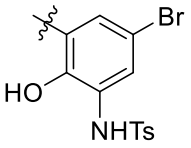

1.41m

Entry	Catalyst	X(Y)	Catalyst [mol%]	BzOH [mol%]	Solvent	Time [h]	Conv(*ee*)[a,b] [%]
1	**1.41k**[94]	NTs(NO_2)	5	5	CH_2Cl_2	0.5	40(88)
2	**1.41k**[94]	NTs(NO_2)	5	0	CH_2Cl_2	0.5	17(*rac*)
3	**1.41k**[94]	O(NO_2)	10	10	Ether	24	75(48)
4	**1.41k**[94]	O(NO_2)	10	0	Ether	24	36(21)
5	**1.41i**[96]	NTs(Br)[d]	10	10	CH_2Cl_2	1	>95(90)
6	**1.41m**	NTs(Br)	10	10	CH_2Cl_2	3	13(92)
7	**1.41m**	NTs(Br)	10	0	CH_2Cl_2	3	0(n.d.)
8	**1.41m**	O(NO_2)	10	10	CH_2Cl_2	24	23(49)
9	**1.41m**	O(NO_2)	10	0	CH_2Cl_2	24	12(20[c])
10	**1.41j**[96]	O(NO_2)[d]	10	10	CH_2Cl_2	24	95(52)

[a]Calculated by ^{1}H NMR spectroscopy. [b]Determined by chiral HPLC analysis. [c]The opposite enantiomer. [d]2 eq. of MVK used.

The generic MBH reaction catalyzed by **1.41m** also demonstrated nearly a three-fold reduction in rate but similar *ee* values compared to that by **1.41k** (Table 3.1, entries 3, 4, 8, 9). It should be noted that generic MBH test reactions catalyzed by **1.41k** were performed in ether while the new catalyst **1.41m** was tested in dichloromethane. Another catalyst **1.41j**, analogous to **1.41k**, was reported to be effective for the same generic MBH reaction in dichloromethane (Table 3.1, entry 10), providing faster rate than **1.41k** but at comparable *ee* values (Table 3.1, entries 3, 10). Therefore, the rate retardation is likely due to the excess Brønsted acidity, rather than solvent effects. In summary, the excess Brønsted acidity of catalyst **1.41m** did not improve catalytic proficiency. However, **1.41m** demonstrated comparable *ee* values to those from **1.41k** and **1.41i**, suggesting that changing the Brønsted acidity by other substituents may improve on the reaction rate.

3.6 Catalysis of organocatalyst 1.43i in *aza*-MBH and MBH reactions.

The third generation of trifunctional NHTs catalysts as reported earlier,[94] compared to previous generations, demonstrated high proficiency in *aza*-MBH with reduced loading levels. However, the proficiency of these catalysts in the generic MBH test reaction was comparable to that of our second generation catalyst.[96] Our earlier attempt to tune the Brønsted acidity of **1.43a** by incorporation of a bromine substituent at the *para*-position to the Brønsted acid (catalyst **1.43e**) did not improve the catalytic proficiency (Table 3.2, entries 2, 6).[93] Here, additional investigations on tuning the Brønsted acidity were performed via testing of catalyst **1.43i** that contains a more acidic Brønsted acid with a second bromine substituent in the *ortho*-position.

The proficiency of the new catalyst **1.43i** was tested in *aza*-MBH and generic MBH reactions (Table 3.2, entries 8–11). For ease of comparison, the relevant activity data for catalysts **1.43a** and **1.43e** are also provided (Table 3.2, entries 1–7).

Table 3.2 Catalytic activity of catalysts **1.43i**, **1.43a**,[94] and **1.43e**[93] in asymmetric *aza*-MBH and generic MBH reactions.

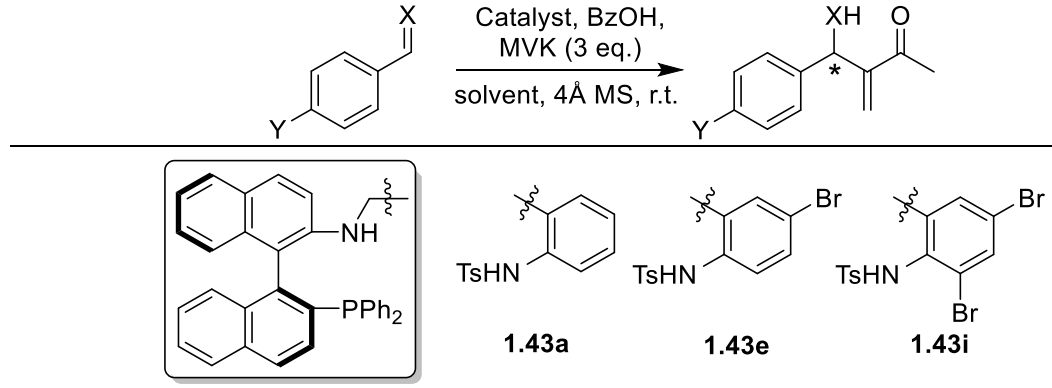

Entry	Catalyst	X(Y)	Catalyst [mol%]	BzOH [mol%]	Solvent	Time [h]	Conv(*ee*)[a,b] [%]
1	**1.43a**[94]	NTs(Br)	2	2	CH_2Cl_2	12	92(81)
2	**1.43a**[94]	NTs(NO_2)	5	5	CH_2Cl_2	0.5	>95(88)
3	**1.43a**[94]	O(NO_2)	10	10	Ether	3	71(47)
4	**1.43a**[94]	O(NO_2)	10	10	CH_2Cl_2	0.5	<5(n.d.)
5	**1.43a**[94]	O(NO_2)	5	10	Ether	3	65(48)
6	**1.43e**[93]	NTs(NO_2)	5	5	CH_2Cl_2	0.5	>95(88)
7	**1.43e**[93]	O(NO_2)	10	10	Ether	3	24(41)
8	**1.43i**	NTs(Br)	5	5	CH_2Cl_2	3	35(40)
9	**1.43i**	NTs(Br)	5	0	CH_2Cl_2	3	<5(n.d.)
10	**1.43i**	O(NO_2)	5	10	CH_2Cl_2	24	18(14[c])

11	**1.43i**	O(NO_2)	5	0	CH_2Cl_2	24	0(n.d.)

[a]Calculated by ^{1}H NMR spectroscopy. [b]Determined by chiral HPLC analysis. [c]The opposite enantiomer.

The activation of catalyst **1.43i** by benzoic acid was pronounced in both *aza*- and generic MBH reactions, again suggesting that the trifunctional catalysis was in operation (Table 3.2, entries 8–11). Catalyst **1.43i**, containing a bulky electron-withdrawing group at the *ortho*-position to the NHTs Brønsted acid, showed low reaction rates and lower *ee* values in comparison to **1.43a** and **1.43e** (Table 3.2, entries 1, 6, 8) and did not provide obvious improvement on rate and enantioselectivity enhancement for the *aza*-MBH reaction.

In the generic MBH test reaction, catalyst **1.43a** was found to be quite active even at a reduced loading level (Table 3.2, entries 3, 5).[94] Catalyst **1.43i** was therefore tested in a generic MBH reaction at a lower loading of 5%, rather than the typical 10%. The rate and *ee* value of catalysis, in this case, were much lower than that by catalysts **1.43a** and **1.43e** (Table 3.2, entries 5, 7, 10). For catalyst **1.43a**, ether was a better solvent for catalysis than dichloromethane (Table 3.2, entries 3, 4).[94] This suggests that **1.43i** should be in future tested in ether as well. Interestingly, while **1.43i** showed low enantioselectivity, the enantiomer in excess had the opposite configuration than that by catalysts **1.43a** and **1.43e**. In summary, the excess Brønsted acidity of catalyst **1.43i** did not improve the proficiency either. It is also possible that a large bromine substituent *ortho* to the NHTs Brønsted acid may be sterically too demanding. This suggests that in future reduction in the excess Brønsted acidity by other smaller substituents may improve on the catalytic proficiency.

3.7 Catalysis of organocatalysts 1.44a and 1.44b in *aza*-MBH and MBH reactions.

The novel pyrrole-containing catalysts **1.44a** and **1.44b** provide a different Brønsted acid from those of previous generations (pyrrole vs. phenol and NHTs). The pyrrole Brønsted acid center has different acidity and spatial orientation compared to that of phenol or NHTs Brønsted acids. The combination of these factors may provide H-bonding interactions that alter catalytic proficiency and substrate scope. The catalyst **1.44b** differs from **1.44a** by the presence of two bromine substituents that modify the Brønsted acidity for comparison.

The activity of the pyrrole catalysts **1.44a** and **1.44b** was investigated in *aza*-MBH and generic MBH reactions (Table 3.3, entries 1–8). For ease of comparison, the relevant activity data for catalysts **1.43a**, **1.43b** and **1.41a** are also provided (Table 3.1, entries 9–12). Both catalysts **1.44a** and **1.44b** demonstrated again significant response of activation to benzoic acid, as the *aza*-MBH reactions without acid activation showed ten times lower conversion with the significant loss in *ee* by nearly 4 and 7 times (Table 3.3, entries 1, 2, 5, 6). The opposite enantiomer was in slight excess in *aza*-MBH reactions without benzoic acid for both

catalysts **1.44a** and **1.44b**. The generic MBH test reactions without benzoic acid also demonstrated much lower proficiency (Table 3.3, entries 3, 4, 7, 8). This positive response of proficiency on acid additive is indicative of trifunctional catalysis.

Catalysts **1.44a** and **1.44b** provided significantly lower reaction rate in *aza*-MBH reactions than our earlier generation catalysts **1.43a** and **1.41a** (Table 3.3, entries 1, 5, 9, 10). The dibromosubstituted pyrrole catalyst **1.44b** demonstrated 84% *ee* that is comparable to the NHTs Brønsted acid catalyst **1.43a** but lower in proficiency than the phenol Brønsted acid catalyst **1.41a** (Table 3.3, entries 5, 9, 10). Catalyst **1.44b** also showed slightly lower reaction rate in comparison to the unsubstituted pyrrole catalyst **1.44a** (Table 3.3, entries 1, 5).

Table 3.3 Catalytic activity of catalysts **1.44a**, **1.44b**, **1.43a**,[94] **1.43b**,[94] and **1.41a**[97] in asymmetric *aza*-MBH and generic MBH reactions.

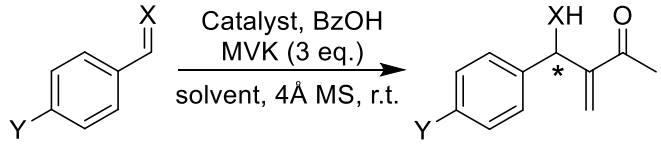

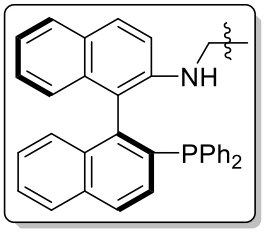

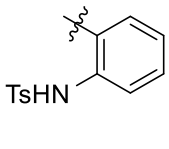

1.43a

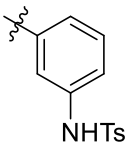

1.43b

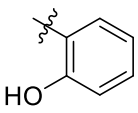

1.41a

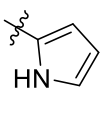

1.44a

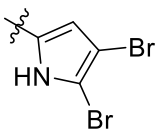

1.44b

Entry	Catalyst	X(Y)	Catalyst [mol%]	BzOH [mol%]	Solvent	Time [h]	Conv(*ee*)[a,b] [%]
1	**1.44a**	NTs(Br)	10	10	CH_2Cl_2	3	76(75)
2	**1.44a**	NTs(Br)	10	0	CH_2Cl_2	3	6(16[c])
3	**1.44a**	O(NO_2)	10	10	CH_2Cl_2	6	11(62)
4	**1.44a**	O(NO_2)	10	0	CH_2Cl_2	6	3(n.d.)
5	**1.44b**	NTs(Br)	10	10	CH_2Cl_2	3	62(84)
6	**1.44b**	NTs(Br)	10	0	CH_2Cl_2	3	5(11[c])
7	**1.44b**	O(NO_2)	10	10	CH_2Cl_2	24	21(65)
8	**1.44b**	O(NO_2)	10	0	CH_2Cl_2	24	7(*rac*)
9	**1.41a**[97]	NTs(Br)[d]	10	50	CH_2Cl_2	3	>95(92)
10	**1.43a**[94]	NTs(Br)	2	2	CH_2Cl_2	12	92(81)
11	**1.43a**[94]	O(NO_2)	10	10	Ether	3	71(47)
12	**1.43b**[94]	O(NO_2)	10	10	Ether	6	95(54)

[a]Calculated by ^{1}H NMR spectroscopy. [b]Determined by chiral HPLC analysis.[c]The opposite enantiomer.
[d]2 eq. of MVK used

The generic MBH test reactions catalyzed by **1.44a** and **1.44b** showed low conversion but with significant enantioselectivity that reached 62% and 65% (*er* 6.2:1) respectively (Table 3.3, entries 3, 7). These represent the highest *ee* values in this generic MBH test reaction amongst the trifunctional organocatalysts tested so far in our group, as compared to catalysts **1.43b** (54% *ee*, *er* 3.4:1) (Table 3.3, entry 3, 7, 12). However, the generic MBH reaction rates by **1.44a** and **1.44b** are low in dichloromethane, compared to the rates by **1.43a** and **1.43b** in ether (Table 3.3, entry 3, 7, 11, 12). This requires future investigation of solvent effects on these pyrrole catalysts.

It is possible that the position of the pyrrole Brønsted acid in the transition state may not be optimal to create efficient H-bonding interactions, which could reduce the reaction rate. Moreover, the acidity of the pyrrole Brønsted acid, which is much lower than that of phenol (pyrrole pK_a 17.5 vs. phenol pK_a 9.95), may also influence the reaction proficiency. However, the improved enantioselectivity of these pyrrole catalysts in the generic MBH test reaction suggests the potential of adding additional Brønsted acid motifs that may improve the catalytic proficiency for generic MBH reactions.

3.8 Conclusions and future directions

In summary, during this research training, the 11-step synthetic route from (*S*)-BINOL **2.1** to aminophosphine **2.10** through (*S*)-NOBIN **1.3** formation was secured and optimized; new phenol, *N*-tosyl and pyrrole Brønsted acid motifs were incorporated into the MAP-structure and tested in *aza*-MBH and generic MBH reactions. The increasing of Brønsted acid acidity in the phenol and *N*-tosyl-containing catalysts did not improve on catalytic proficiency. However, the novel pyrrole-type catalysts provided the enhancement in enantioselectivity in generic MBH tests albeit with lower reaction rates.

Future research in our multifunctional catalyst development may target the synthesis of catalysts **2.35**–**2.43** (Figure 3.2) for testing in *aza*- and generic MBH reactions. The correlation between the reaction rate and the Brønsted acid acidity could be investigated additionally by the testing of the catalyst **2.35**, which has the electron-donating methyl group instead of the weak electron-withdrawing bromine atom in the structure. The influence of tosyl amide moiety could be investigated to ascertain the following factors:

- If the acidity of the phenolic group could be further altered (**2.35**);
- If the NHTs fragment could be altered to be a different Brønsted acid after protonation (**2.36–2.38**);
- If the electronegative oxygen atoms of the sulfonyl fragment could participate as potential H-bonding acceptors (**2.36**);

- If the tosylamide moiety is a bulky group or if π–π interactions from the tosyl group may influence the proficiency (**2.39**).

In addition, new Brønsted acids/bases could be readily introduced by derivatizing from **2.36** to provide catalysts **2.40**–**2.43**. These catalysts will be tested in *aza*- and generic MBH reactions to investigate the effects on catalytic proficiency and reaction scope from new H-bonding interactions in various steric environments.

The strategy of copper chelating by binaphthyl Shiff base analogous of **1.41a** was reported previously and investigated in the copper-catalyzed asymmetric α-chlorination and hydroxylation of β-keto esters.[71,72] Catalysts **2.40**–**2.43** may be amenable to copper-catalyzed *aza*-MBH and generic MBH reactions by hybrid catalysis.

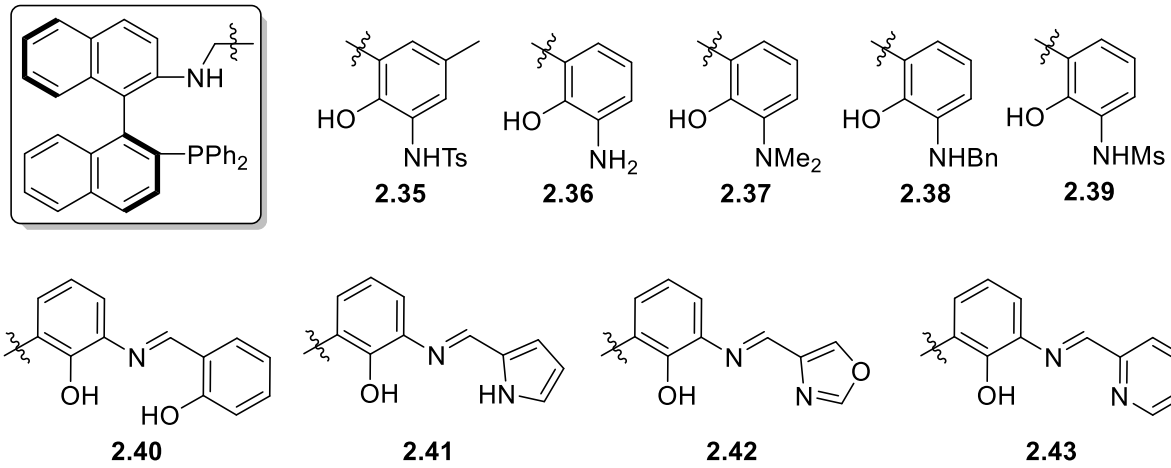

Figure 3.2 Development of new multifunctional catalysts with phenol Brønsted acids.

The presence of two bromine atoms in catalyst **1.43i** structure made the Brønsted acid too acidic for proficient catalysis. However, the *ortho*-positioned bromine atom can be used for further modifications by cross-coupling reactions. Therefore, catalyst **2.44** (Figure 3.3), which contains an electron-donating methyl group instead of a bromine atom, can be synthesized and tested in MBH reactions in the future. This can also bypass the issue cross-coupling regioselectivity with only one bromine substituent. The next step in the development of these tosylamide catalysts may include metal binding fragments such as the pyrrole **2.45**, oxazole **2.46** and pyridine **2.47** rings at the position *ortho* to the Brønsted acid.

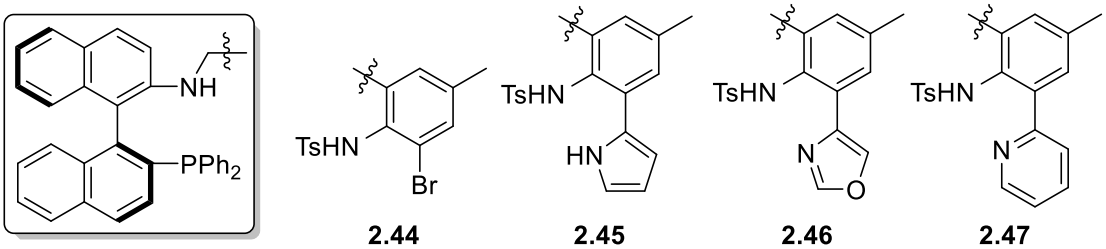

Figure 3.3 Development of new multifunctional catalysts with NHTs Brønsted acids.

The insertion of a pyrrole ring as a Brønsted acid function into the MAP scaffold produced multifunctional catalysts **1.44a** and **1.44b** that showed reasonable proficiency in both *aza*- and generic MBH reactions. Moreover, these catalysts provided the highest enantioselectivity in the generic MBH test reactions in comparison to our earlier generations of catalysts with phenol and NHTs Brønsted acids. The mechanism of these catalysts remains unclear and new control catalysts **2.48** and **2.49** (Figure 3.4) will be synthesized and tested in MBH reactions for understanding the potential role of the Brønsted base and Brønsted acid fragments. The catalyst **2.48** without the nitrogen Brønsted base may show the influence of this motif on catalysis proficiency in this system. Likewise, the catalyst **2.49** will not have the Brønsted acid function for ascertaining its role in catalytic proficiency.

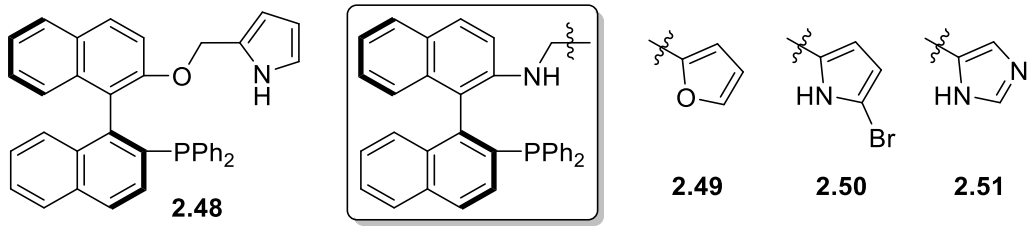

Figure 3.4 Development of new multifunctional catalysts with pyrrole Brønsted acids.

A monobromo substituted catalyst **2.50** (Figure 3.4) will be synthesized as an intermediate catalyst for further modification by cross-coupling reactions for producing new multifunctional catalysts. It will also be interesting to test the imidazolyl catalyst **2.51** (Figure 3.4) that has a more acidic Brønsted acid (imidazole pK_a 14.2 vs. pyrrole pK_a 17.5). The imidazole fragment also has the second nitrogen atom that could be protonated by an acid additive that may alter the H-bonding interactions of the imidazole ring (Figure 3.5a). Moreover, the additional amount of acid in reactions catalyzed by pyrrole and furan containing catalysts **1.44a**, **1.44b**, **2.48**–**2.50** will be investigated due to the ability of an acid additive to protonate pyrrole nitrogen center (Figure 3.5b) that may also have an influence to the proficiency of the catalysts to expand the substrate scope.

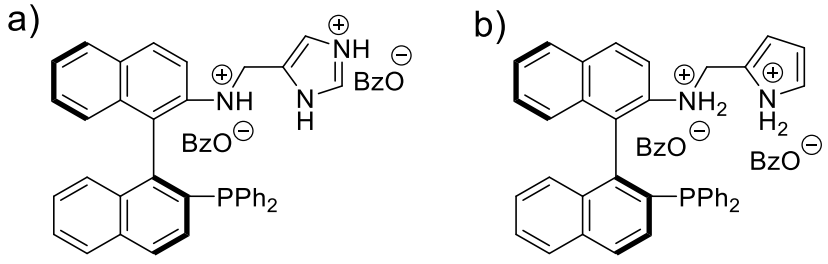

Figure 3.5 Probable imidazole-containing catalyst **2.51** (a) and pyrrole-containing catalyst **1.44a** (b) structures in the presence of the benzoic acid double excess.

In conclusion, the overall aim of future work will be on new catalysts that could incorporate new functionalities, such as a Lewis acidic metal center or another Brønsted acid/base, into the catalysis for hybrid or organized catalysis. This may increase the proficiency and also

expand the substrate scope of these MBH reactions. In addition, cascade reactions will also be investigated in which these organocatalysts could catalyze the MBH reaction and also serve as ligands in subsequent catalytic cycles for converting the MBH product further into other highly functionalized structures.

REFERENCES

(1) Ojima, I. *Catalytic asymmetric synthesis*; 3rd ed.; John Wiley: Hoboken, N.J., 2010.

(2) Dalko, P. I. *Enantioselective organocatalysis : reactions and experimental procedures*; Wiley-VCH ; John Wiley distributor: Weinheim Chichester, 2007.

(3) Gotor, V.; Alfonso, I.; García-Urdiales, E. *Asymmetric organic synthesis with enzymes*; Wiley-VCH: Weinheim, 2008.

(4) Bates, R. *Organic synthesis using transition metals*; 2nd ed.; Wiley: Chichester, West Sussex, 2012.

(5) Drauz, K.; Gröger, H.; May, O. *Enzyme catalysis in organic synthesis : a comprehensive handbook*; 3rd, completely rev. and enl. ed.; Wiley-VCH: Weinheim, Germany, 2012.

(6) Pellissier, H. *Chem. Rev.* **2013**, *113*, 442.

(7) Maruoka, K. *Asian J. Org. Chem.* **2014**, *3*, 319.

(8) Lykourinou, V.; Hanafy, A. I.; da Silva, G. F. Z.; Bisht, K. S.; Larsen, R. W.; Livingston, B. T.; Angerhofer, A.; Ming, L.-J. *Eur. J. Inorg. Chem.* **2008**, 2584.

(9) Babtie, A.; Tokuriki, N.; Hollfelder, F. *Curr. Opin. Chem. Biol.* **2010**, *14*, 200.

(10) Kenny, R.; Liu, F. *Eur. J. Org. Chem.* **2015**, 5304.

(11) Liu, F. *Chirality* **2013**, *25*, 675.

(12) Giacalone, F.; Gruttadauria, M.; Agrigento, P.; Noto, R. *Chem. Soc. Rev.* **2012**, *41*, 2406.

(13) Nicewicz, D. A.; MacMillan, D. W. C. *Science* **2008**, *322*, 77.

(14) Baer, K.; Kraußer, M.; Burda, E.; Hummel, W.; Berkessel, A.; Gröger, H. *Angew. Chem., Int. Ed.* **2009**, *48*, 9355.

(15) Rulli, G.; Duangdee, N.; Baer, K.; Hummel, W.; Berkessel, A.; Gröger, H. *Angew. Chem., Int. Ed.* **2011**, *50*, 7944.

(16) Ward, T. R.; Pordea, A. In *Comprehensive chirality*; Carreira, E. M., Yamamoto, H., Eds.; Elsevier: Amsterdam, 2012, p 516.

(17) Ma, J.; Ding, X.; Hu, Y.; Huang, Y.; Gong, L.; Meggers, E. *Nat. Commun.* **2014**, *5*.

(18) Held, F.; Grau, D.; Tsogoeva, S. *Molecules* **2015**, *20*, 16103.

(19) Serdyuk, O. V.; Zamfir, A.; Hampel, F.; Tsogoeva, S. B. *Adv. Synth. Catal.* **2012**, *354*, 3115.

(20) List, B.; Arseniyadis, S. *Asymmetric organocatalysis*; Springer: Heidelberg ; New York, 2010.

(21) Schenker, S.; Zamfir, A.; Freund, M.; Tsogoeva, S. B. *Eur. J. Org. Chem.* **2011**, 2209.

(22) Shibasaki, M.; Matsunaga, S. In *Privileged chiral ligands and catalysts*; Wiley-VCH Verlag GmbH & Co. KGaA: 2011, p 295.

(23) Hatano, M.; Ishihara, K. *Asian J. Org. Chem.* **2014**, *3*, 352.

(24) Ma, G.; Sibi, M. P. *Chem. Eur. J.* **2015**, *21*, 11644.

(25) Che, C. M.; Huang, J. *Coord. Chem. Rev.* **2003**, *242*, 97.

(26) Kočovský, P.; Vyskočil, Š.; Smrčina, M. *Chem. Rev.* **2003**, *103*, 3213.

(27) Lee, S. J.; Lin, W. *Acc. Chem. Res.* **2008**, *41*, 521.

(28) Hannedouche, J.; Collin, J.; Trifonov, A.; Schulz, E. *J. Organomet. Chem.* **2011**, *696*, 255.

(29) Turlington, M.; Pu, L. *Synlett* **2012**, *23*, 649.

(30) Parmar, D.; Sugiono, E.; Raja, S.; Rueping, M. *Chem. Rev.* **2014**, *114*, 9047.

(31) Akiyama, T.; Mori, K. *Chem. Rev.* **2015**, *115*, 9277.

(32) Lv, J.; Luo, S. *Chem. Commun.* **2013**, *49*, 847.

(33) Jing, C.; Xing, D.; Hu, W. *Org. Lett.* **2015**, *17*, 4336.
(34) Wu, H.; He, Y.-P.; Gong, L.-Z. In *Cooperative catalysis*; Wiley-VCH Verlag GmbH & Co. KGaA: 2015, p 171.
(35) Kitamura, M.; Ohkuma, T.; Inoue, S.; Sayo, N.; Kumobayashi, H.; Akutagawa, S.; Ohta, T.; Takaya, H.; Noyori, R. *J. Am. Chem. Soc.* **1988**, *110*, 629.
(36) Bräse, S.; de Meijere, A.; de Meijere, A.; Diederich, F. *Metal-catalyzed cross-coupling reactions*, 2004.
(37) Meijere, A. d.; Diederich, F. o. *Metal-catalyzed cross-coupling reactions*; 2nd, completely rev. and enl. ed.; Wiley-VCH: Weinheim, 2004.
(38) Surry, D. S.; Buchwald, S. L. *Angew. Chem., Int. Ed.* **2008**, *47*, 6338.
(39) Seayad, J.; List, B. *Org. Biomol. Chem.* **2005**, *3*, 719.
(40) Vyskočil, Š.; Smrčina, M.; Kočovský, P. *Tetrahedron Lett.* **1998**, *39*, 9289.
(41) Vyskočil, Š.; Smrčina, M.; Hanuš, V.; Polášek, M.; Kočovský, P. *J. Org. Chem.* **1998**, *63*, 7738.
(42) Hamada, T.; Buchwald, S. L. *Org. Lett.* **2002**, *4*, 999.
(43) Aranyos, A.; Old, D. W.; Kiyomori, A.; Wolfe, J. P.; Sadighi, J. P.; Buchwald, S. L. *J. Am. Chem. Soc.* **1999**, *121*, 4369.
(44) Botman, P. N. M.; David, O.; Amore, A.; Dinkelaar, J.; Vlaar, M. T.; Goubitz, K.; Fraanje, J.; Schenk, H.; Hiemstra, H.; van Maarseveen, J. H. *Angew. Chem., Int. Ed.* **2004**, *43*, 3471.
(45) Sälinger, D.; Brückner, R. *Synlett* **2009**, *2009*, 109.
(46) Ooi, T.; Ohmatsu, K.; Maruoka, K. *J. Am. Chem. Soc.* **2007**, *129*, 2410.
(47) Wang, Y.; Guo, H.; Ding, K. *Tetrahedron: Asymmetry* **2000**, *11*, 4153.
(48) Wang, Y.; Li, X.; Ding, K. *Tetrahedron Lett.* **2002**, *43*, 159.
(49) Kawamura, M.; Kiyotake, R.; Kudo, K. *Chirality* **2002**, *14*, 724.
(50) Taylor, A. M.; Altman, R. A.; Buchwald, S. L. *J. Am. Chem. Soc.* **2009**, *131*, 9900.
(51) Hamada, T.; Chieffi, A.; Åhman, J.; Buchwald, S. L. *J. Am. Chem. Soc.* **2002**, *124*, 1261.
(52) Chieffi, A.; Kamikawa, K.; Åhman, J.; Fox, J. M.; Buchwald, S. L. *Org. Lett.* **2001**, *3*, 1897.
(53) Rousseaux, S.; García-Fortanet, J.; Del Aguila Sanchez, M. A.; Buchwald, S. L. *J. Am. Chem. Soc.* **2011**, *133*, 9282.
(54) García-Fortanet, J.; Kessler, F.; Buchwald, S. L. *J. Am. Chem. Soc.* **2009**, *131*, 6676.
(55) Kuwabe, S.-i.; Torraca, K. E.; Buchwald, S. L. *J. Am. Chem. Soc.* **2001**, *123*, 12202.
(56) Shen, X.; Jones, G. O.; Watson, D. A.; Bhayana, B.; Buchwald, S. L. *J. Am. Chem. Soc.* **2010**, *132*, 11278.
(57) Herrbach, A.; Marinetti, A.; Baudoin, O.; Guénard, D.; Guéritte, F. *J. Org. Chem.* **2003**, *68*, 4897.
(58) Yin, J.; Buchwald, S. L. *J. Am. Chem. Soc.* **2000**, *122*, 12051.
(59) Morimoto, T.; Mochizuki, N.; Suzuki, M. *Tetrahedron Lett.* **2004**, *45*, 5717.
(60) Yuan, Z.-L.; Jiang, J.-J.; Shi, M. *Tetrahedron* **2009**, *65*, 6001.
(61) Uozumi, Y.; Hayashi, T. *J. Am. Chem. Soc.* **1991**, *113*, 9887.
(62) Kočovský, P.; Vyskočil, Š.; Císařová, I.; Sejbal, J.; Tišlerová, I.; Smrčina, M.; Lloyd-Jones, G. C.; Stephen, S. C.; Butts, C. P.; Murray, M.; Langer, V. *J. Am. Chem. Soc.* **1999**, *121*, 7714.
(63) Lloyd-Jones, G. C.; Stephen, S. C.; Murray, M.; Butts, C. P.; Vyskočil, Ŝ.; Kočovský, P. *Chem. Eur. J.* **2000**, *6*, 4348.
(64) Fairlamb, I. J. S.; Lloyd-Jones, G. C.; Vyskočil, Š.; Kočovský, P. *Chem. Eur. J.* **2002**, *8*, 4443.

(65) Gouriou, L.; Lloyd-Jones, G. C.; Vyskočil, Š.; Kočovský, P. *J. Organomet. Chem.* **2003**, *687*, 525.
(66) Wang, Y.; Li, X.; Sun, J.; Ding, K. *Organometallics* **2003**, *22*, 1856.
(67) Yamamura, T.; Nakatsuka, H.; Tanaka, S.; Kitamura, M. *Angew. Chem., Int. Ed.* **2013**, *52*, 9313.
(68) Hu, X.; Chen, H.; Zhang, X. *Angew. Chem., Int. Ed.* **1999**, *38*, 3518.
(69) Sun, Y.-W.; Jiang, J.-J.; Zhao, M.-X.; Wang, F.-J.; Shi, M. *J. Organomet. Chem.* **2011**, *696*, 2850.
(70) Jiang, J.-J.; Shi, M. *Tetrahedron: Asymmetry* **2007**, *18*, 1376.
(71) Jiang, J.-J.; Huang, J.; Wang, D.; Yuan, Z.-L.; Zhao, M.-X.; Wang, F.-J.; Shi, M. *Chirality* **2011**, *23*, 272.
(72) Jiang, J.-J.; Huang, J.; Wang, D.; Zhao, M.-X.; Wang, F.-J.; Shi, M. *Tetrahedron: Asymmetry* **2010**, *21*, 794.
(73) Qi, M.-J.; Ai, T.; Shi, M.; Li, G. *Tetrahedron* **2008**, *64*, 1181.
(74) Guan, X.-Y.; Jiang, Y.-Q.; Shi, M. *Eur. J. Org. Chem.* **2008**, 2150.
(75) Jiang, Y.-Q.; Shi, Y.-L.; Shi, M. *J. Am. Chem. Soc.* **2008**, *130*, 7202.
(76) Wang, D.; Yang, Y.-L.; Jiang, J.-J.; Shi, M. *Org. Biomol. Chem.* **2012**, *10*, 7158.
(77) Wei, Y.; Ma, G.-N.; Shi, M. *Eur. J. Org. Chem.* **2011**, 5146.
(78) Wei, Y.; Shi, M. In *Comprehensive enantioselective organocatalysis*; Wiley-VCH Verlag GmbH & Co. KGaA: 2013, p 899.
(79) Sasai, H.; Takizawa, S. In *Comprehensive chirality*; Carreira, E. M., Yamamoto, H., Eds.; Elsevier: Amsterdam, 2012, p 234.
(80) Oishi, T.; Oguri, H.; Hirama, M. *Tetrahedron: Asymmetry* **1995**, *6*, 1241.
(81) Masson, G.; Housseman, C.; Zhu, J. *Angew. Chem., Int. Ed.* **2007**, *46*, 4614.
(82) Guillena, G.; Ramon, D. J.; Yus, M. In *Catalysis: Volume 24*; The Royal Society of Chemistry: 2012; Vol. 24, p 223.
(83) Shi, Y.-L.; Shi, M. *Adv. Synth. Catal.* **2007**, *349*, 2129.
(84) Ma, G.-N.; Cao, S.-H.; Shi, M. *Tetrahedron: Asymmetry* **2009**, *20*, 1086.
(85) Yang, Y.-L.; Pei, C.-K.; Shi, M. *Org. Biomol. Chem.* **2011**, *9*, 3349.
(86) Deng, H.-P.; Wei, Y.; Shi, M. *Eur. J. Org. Chem.* **2011**, 1956.
(87) Deng, H.-P.; Shi, M. *Eur. J. Org. Chem.* **2012**, 183.
(88) Deng, H.-P.; Wei, Y.; Shi, M. *Org. Lett.* **2011**, *13*, 3348.
(89) Hu, F.-L.; Wei, Y.; Shi, M. *Chem. Commun.* **2014**, *50*, 8912.
(90) Zhang, X.-N.; Deng, H.-P.; Huang, L.; Wei, Y.; Shi, M. *Chem. Commun.* **2012**, *48*, 8664.
(91) Zhang, X.-N.; Shi, M. *ASC Catal.* **2013**, *3*, 507.
(92) Anstiss, C.; Karuso, P.; Richardson, M.; Liu, F. *Molecules* **2013**, *18*, 2788.
(93) Anstiss, C. *Macquarie University* **2011**.
(94) Anstiss, C.; Liu, F. *Tetrahedron* **2010**, *66*, 5486.
(95) Anstiss, C.; Garnier, J.-M.; Liu, F. *Org. Biomol. Chem.* **2010**, *8*, 4400.
(96) Garnier, J.-M.; Liu, F. *Org. Biomol. Chem.* **2009**, *7*, 1272.
(97) Garnier, J.-M.; Anstiss, C.; Liu, F. *Adv. Synth. Catal.* **2009**, *351*, 331.
(98) Caputo, C. A.; Jones, N. D. *Dalton Trans.* **2007**, 4627.
(99) Han, Y.-Y.; Wu, Z.-J.; Chen, W.-B.; Du, X.-L.; Zhang, X.-M.; Yuan, W.-C. *Org. Lett.* **2011**, *13*, 5064.
(100) Smrčina, M.; Vyskočil, Š.; Polívková, J.; Poláková, J.; Sejbal, J.; Hanus, V.; Polášek, M.; Verrier, H.; Kočovský, P. *Tetrahedron: Asymmetry* **1997**, *8*, 537.
(101) Shi, M.; Chen, L.-H.; Li, C.-Q. *J. Am. Chem. Soc.* **2005**, *127*, 3790.
(102) Bernárdez, R.; Suárez, J.; Fañanás-Mastral, M.; Varela, J. A.; Saá, C. *Org. Lett.* **2016**, *18*, 642.
(103) Nishiguchi, A.; Ikemoto, T.; Ito, T.; Miura, S.; Tomimatsu, K. *Heterocycles* **2007**, *71*, 1183.
(104) Love, B. E.; Raje, P. S.; Williams Ii, T. C. *Synlett* **1994**, *1994*, 493.

(105) López-Iglesias, M.; Busto, E.; Gotor, V.; Gotor-Fernández, V. *Adv. Synth. Catal.* **2011**, *353*, 2345.
(106) Yuan, K.; Zhang, L.; Song, H.-L.; Hu, Y.; Wu, X.-Y. *Tetrahedron Lett.* **2008**, *49*, 6262.
(107) Joseph, B.; Béhard, A.; Lesur, B.; Guillaumet, G. *Synlett* **2003**, *2003*, 1542.
(108) Schio, L.; Lemoine, G.; Klich, M. *Synlett* **1999**, *1999*, 1559.
(109) Silverstein, R. M.; Webster, F. X.; Kiemle, D. J. *Spectrometric identification of organic compounds*; 7th ed.; John Wiley & Sons: Hoboken, NJ, 2005.
(110) Handy, S. T.; Sabatini, J. J.; Zhang, Y.; Vulfova, I. *Tetrahedron Lett.* **2004**, *45*, 5057.

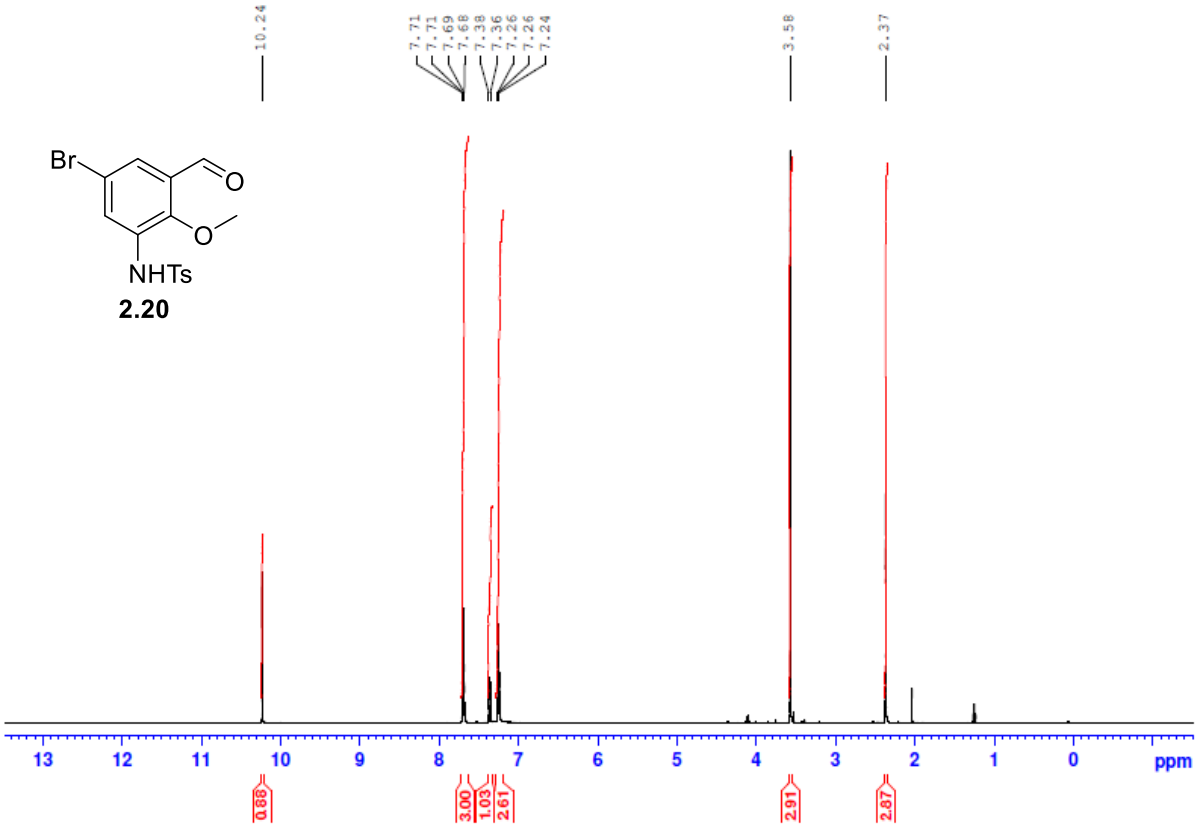

Figure SI-1 ^{1}H NMR spectrum in $CDCl_3$ for aldehyde **2.20**.

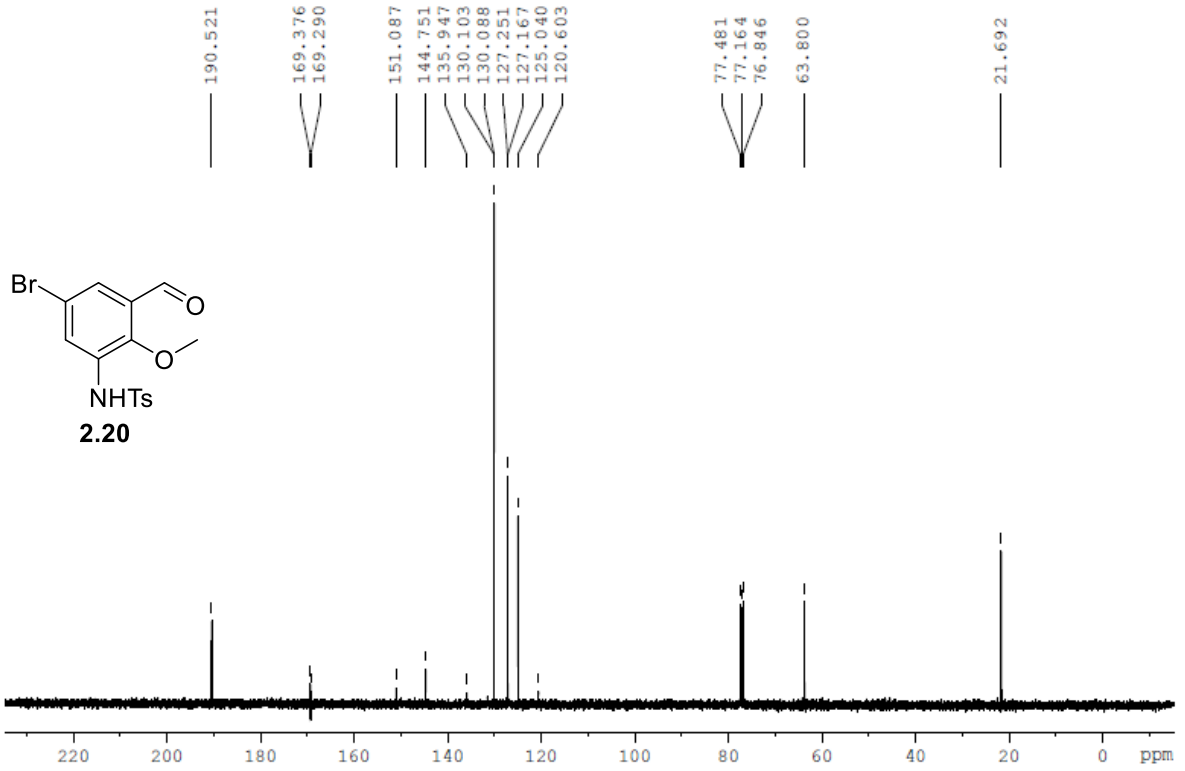

Figure SI-2 ^{13}C NMR spectrum in $CDCl_3$ for aldehyde **2.20**.

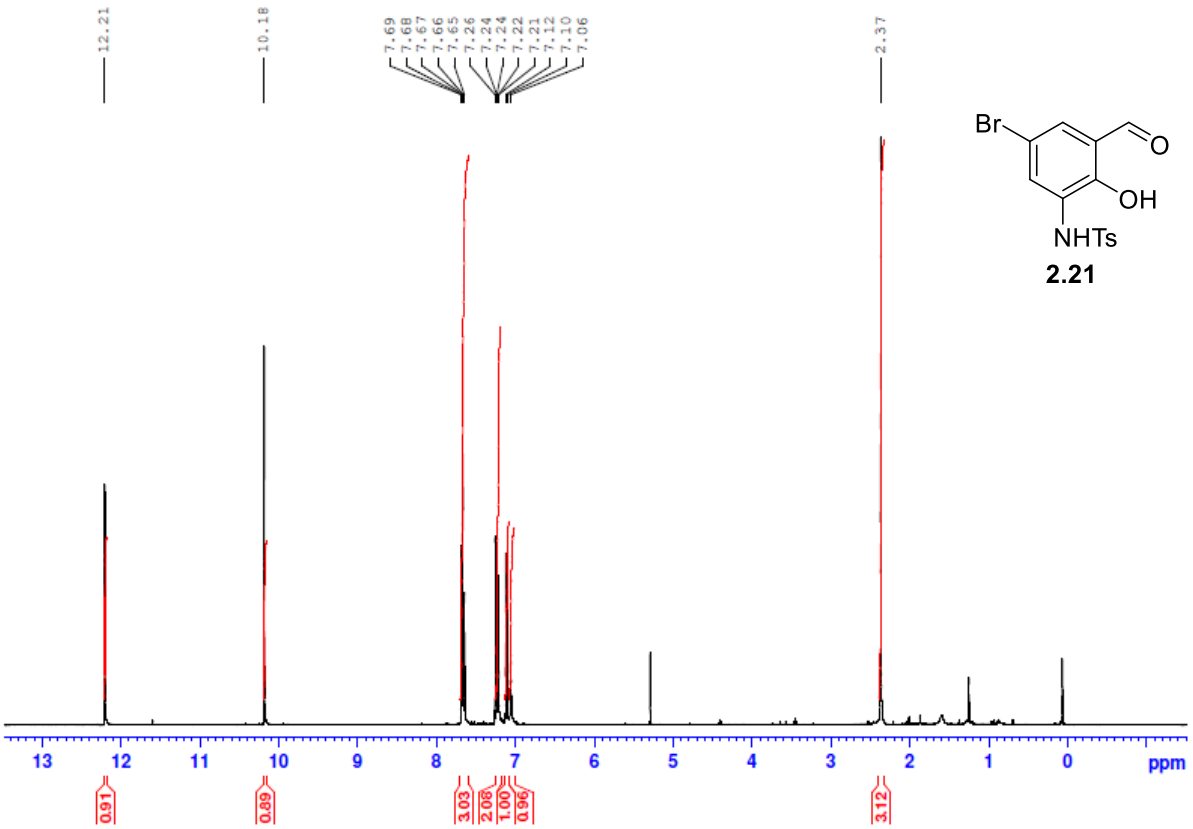

Figure SI-3 ^{1}H NMR spectrum in $CDCl_3$ for aldehyde **2.21.**

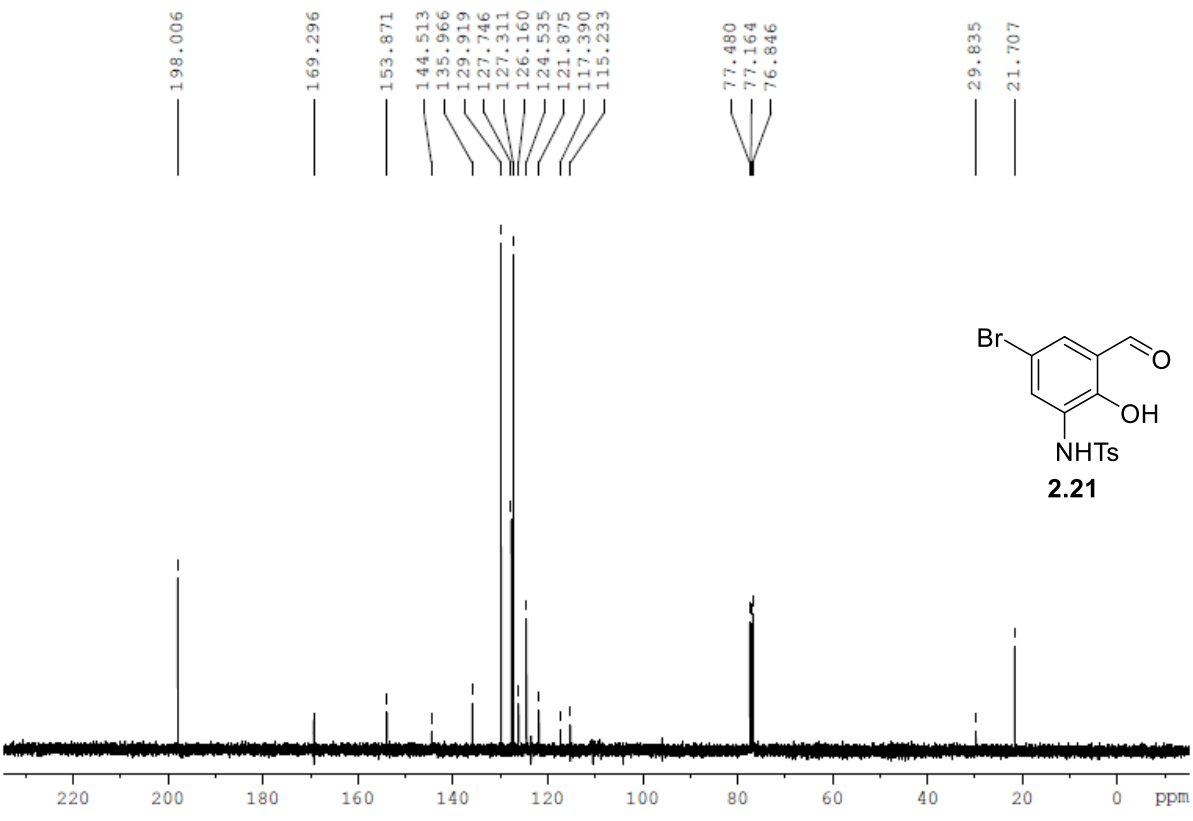

Figure SI-4 ^{13}C NMR spectrum in $CDCl_3$ for aldehyde **2.21**.

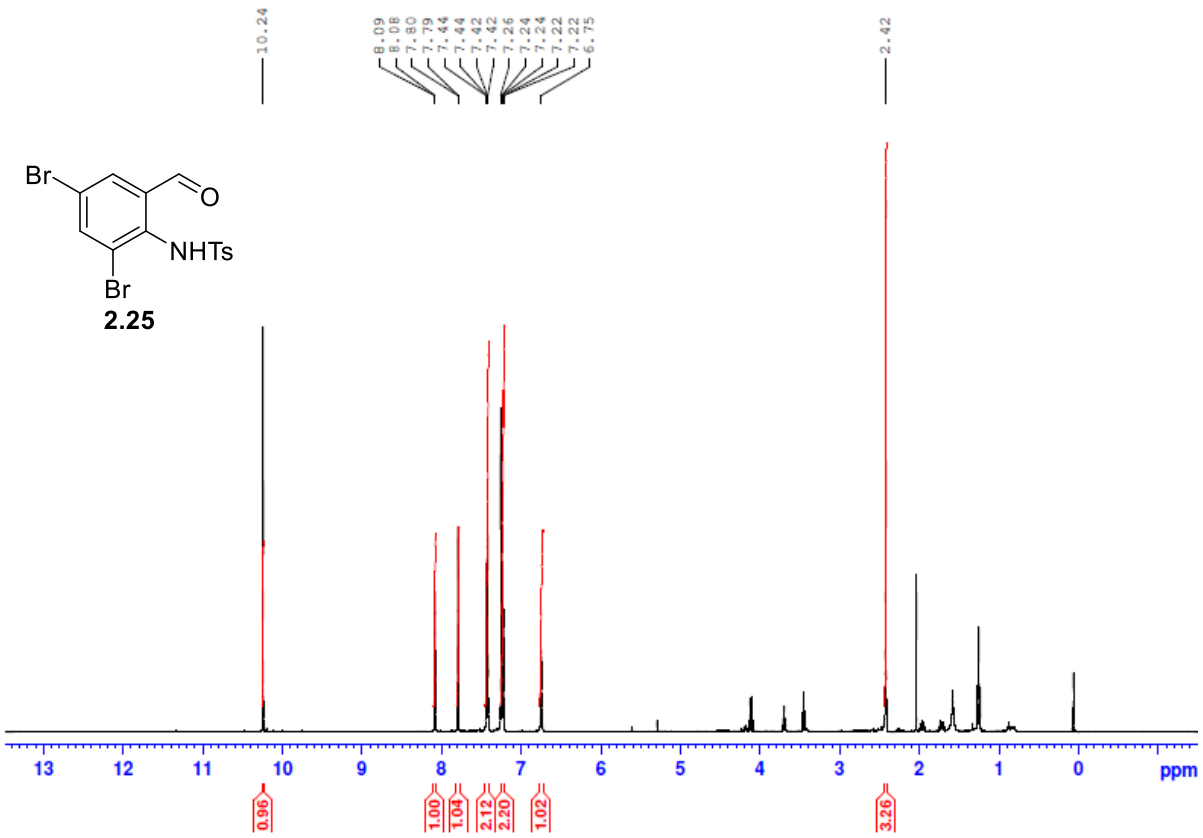

Figure SI-5 ^{1}H NMR spectrum in $CDCl_3$ for aldehyde **2.25**.

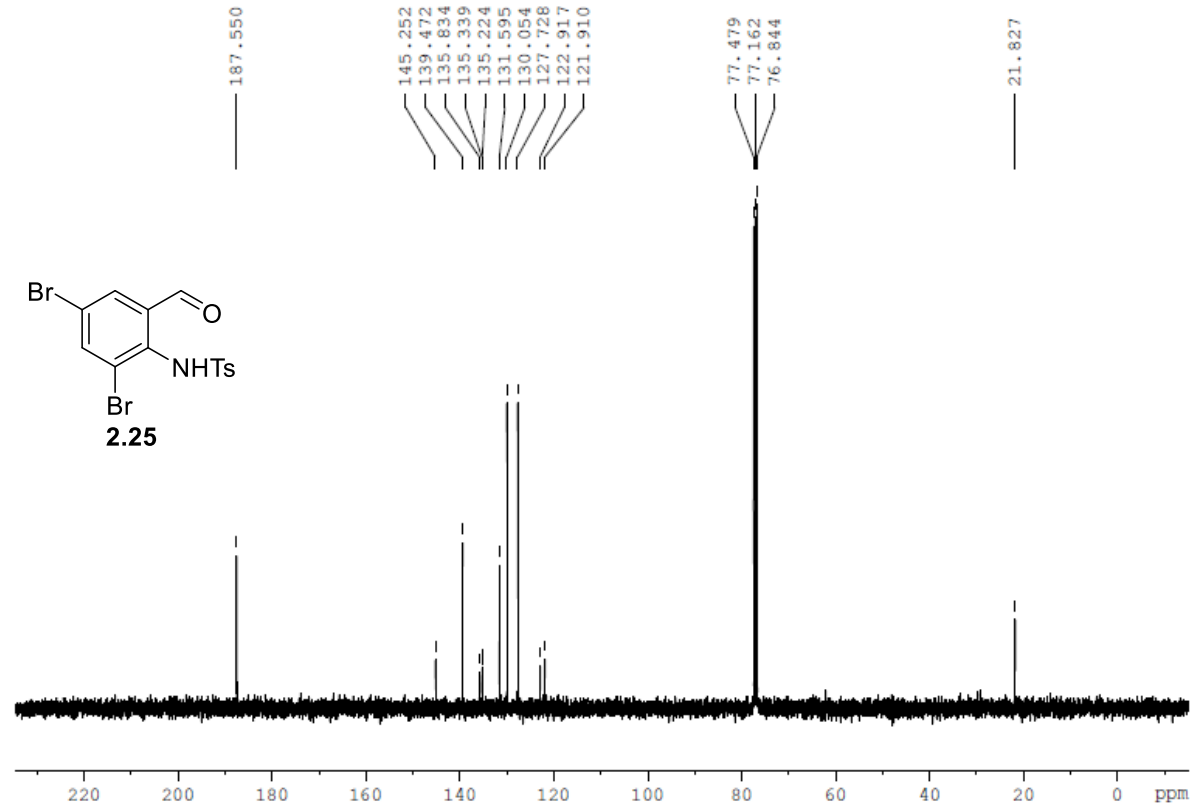

Figure SI-6 ^{13}C NMR spectrum in $CDCl_3$ for aldehyde **2.25**.

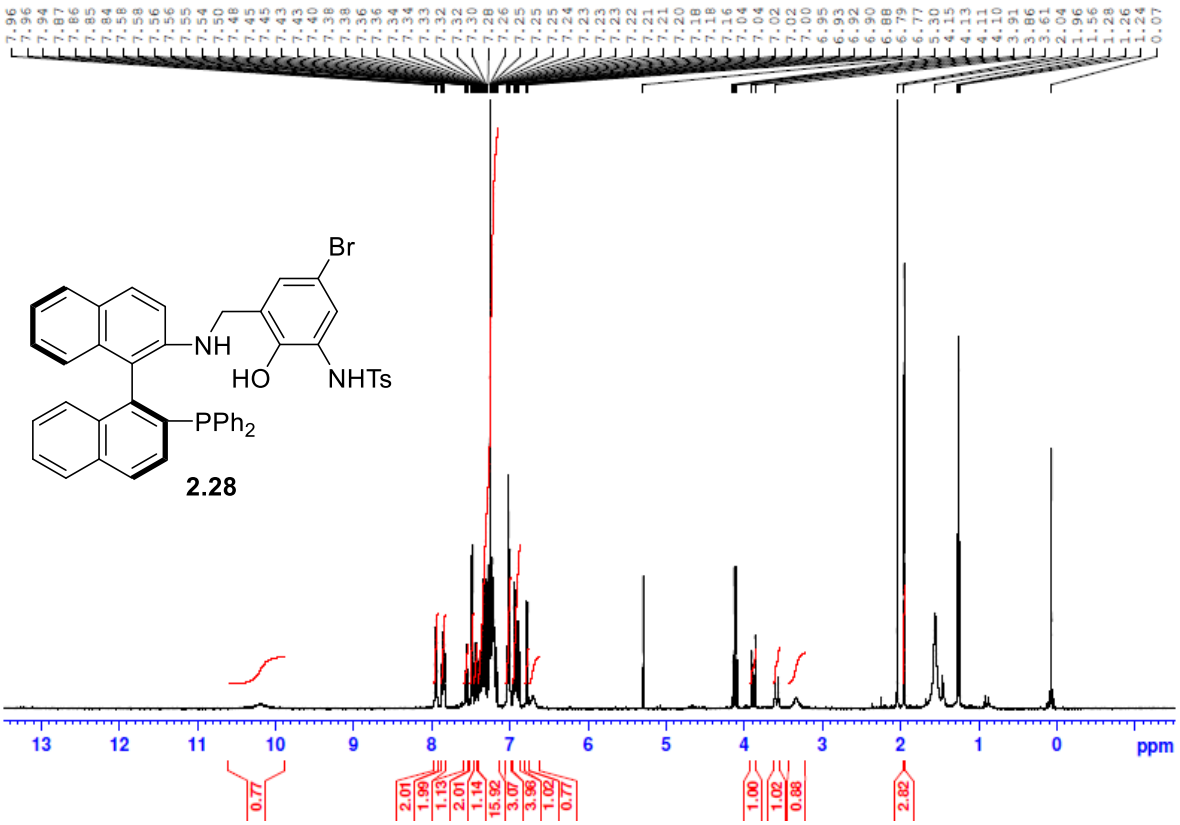

Figure SI-7 ^{1}H NMR spectrum in $CDCl_3$ for catalyst **2.28**.

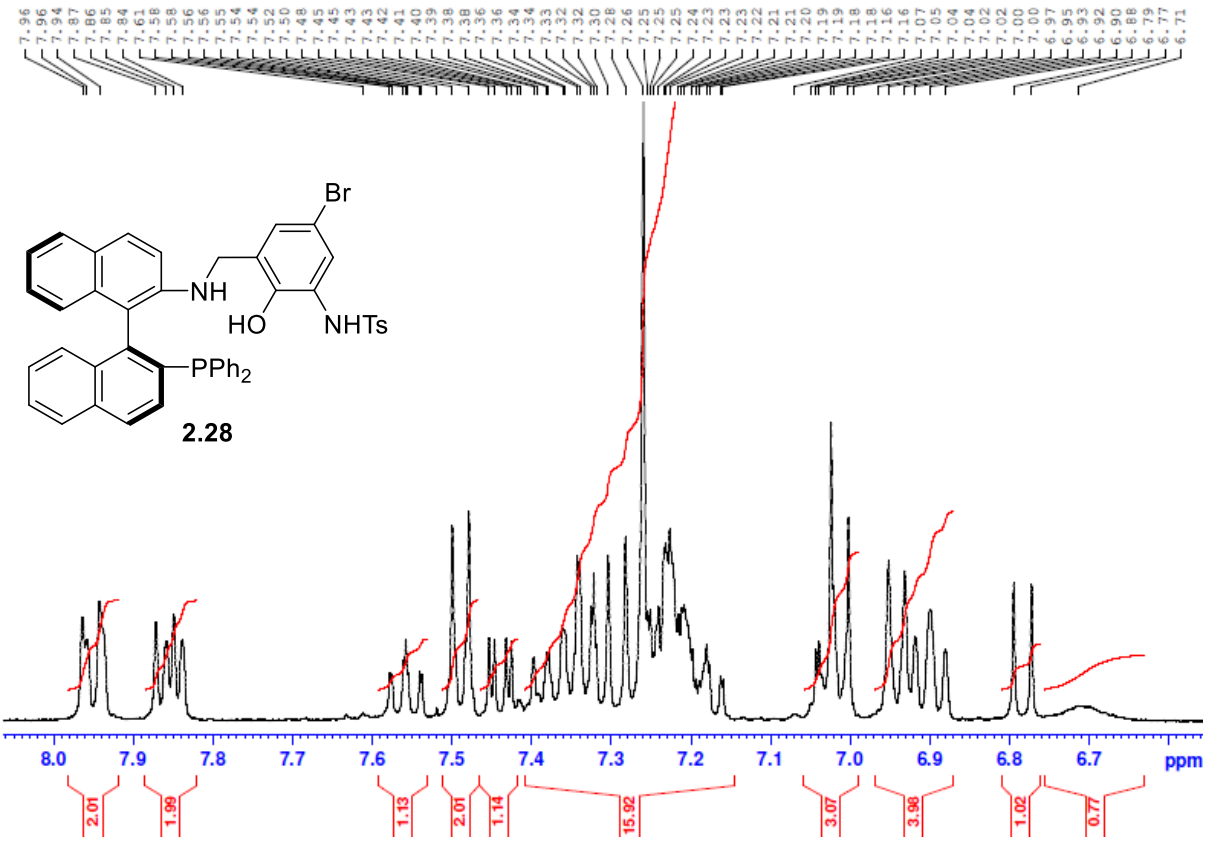

Figure SI-8 Aromatic region of the ^{1}H NMR spectrum in $CDCl_3$ for catalyst **2.28**.

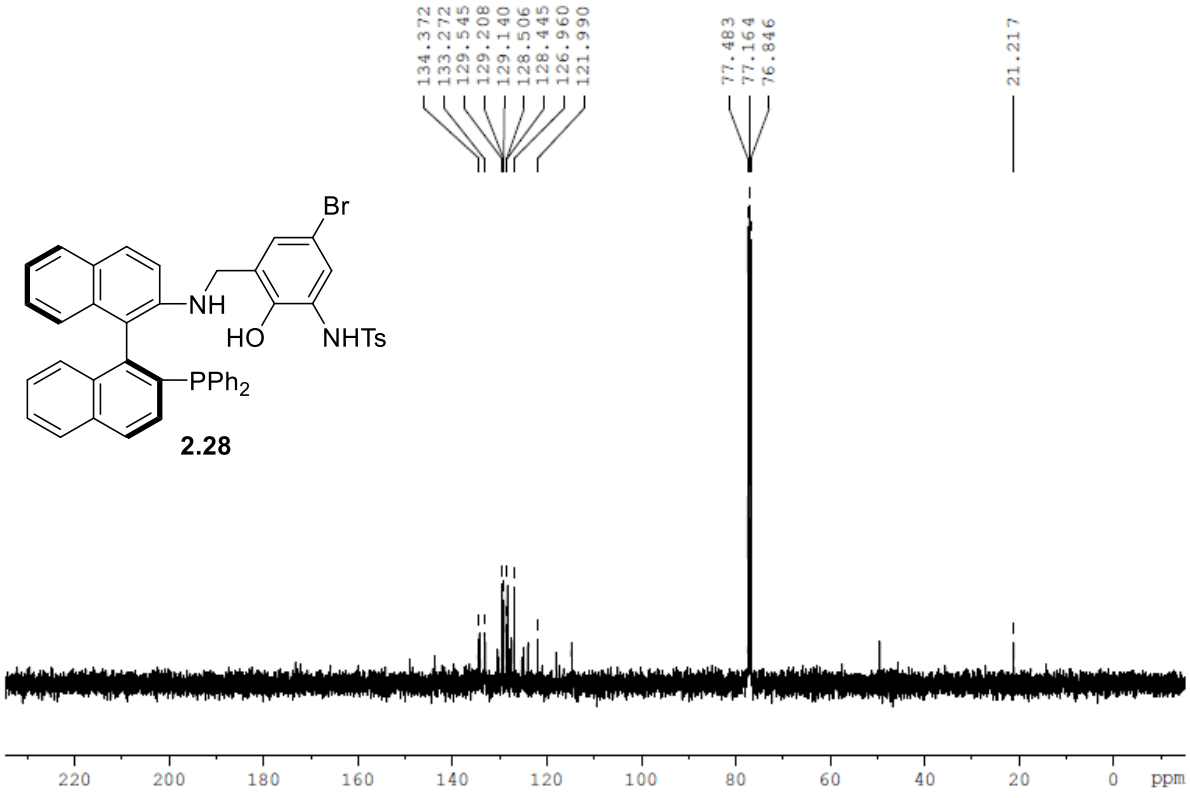

Figure SI-9 ^{13}C NMR spectrum in $CDCl_3$ for catalyst **2.28**.

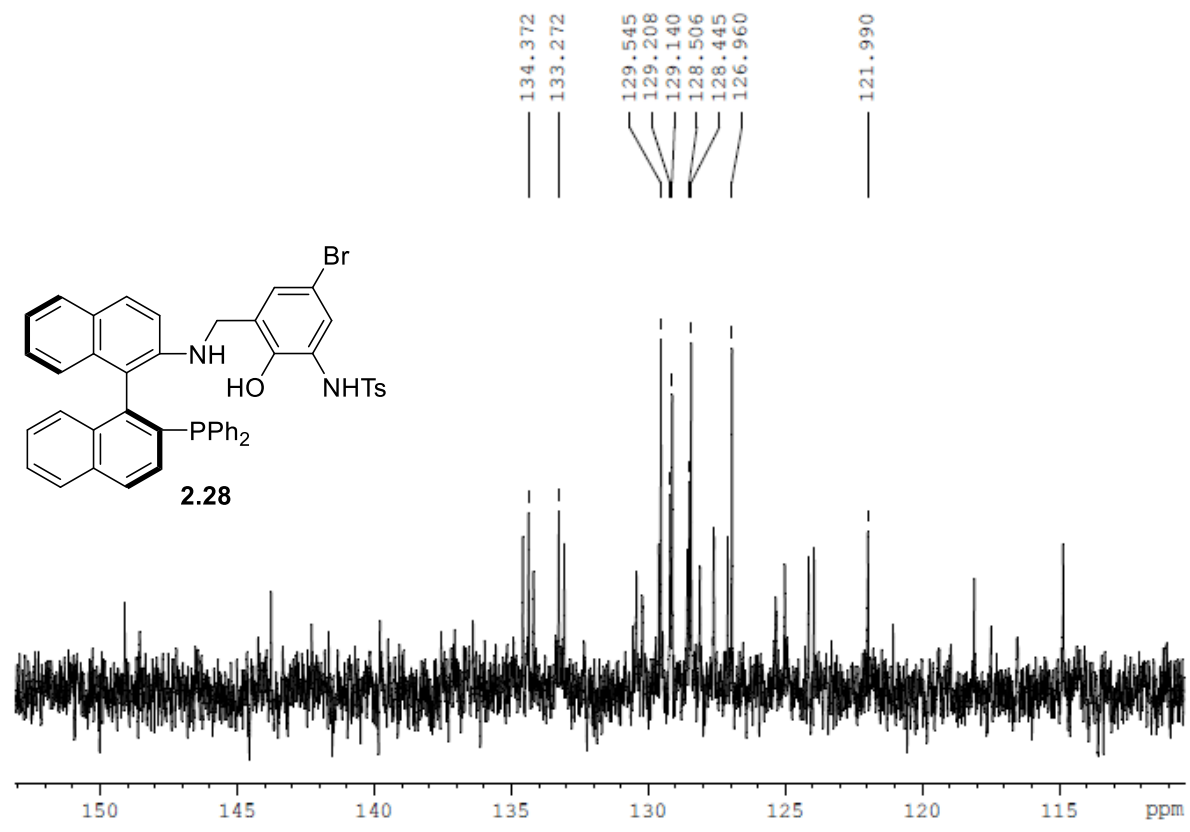

Figure SI-10 Aromatic region of the ^{13}C NMR spectrum in $CDCl_3$ for catalyst **2.28**.

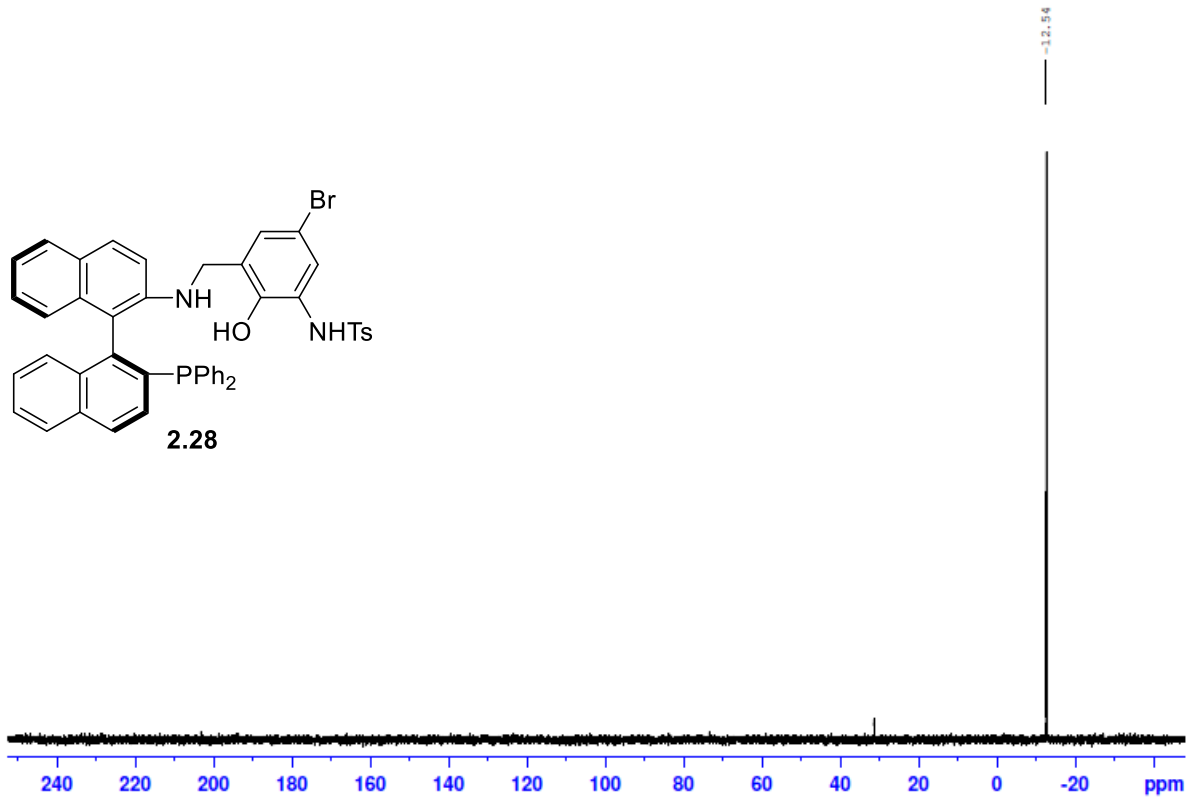

Figure SI-11 ^{31}P NMR spectrum in $CDCl_3$ for catalyst **2.28**.

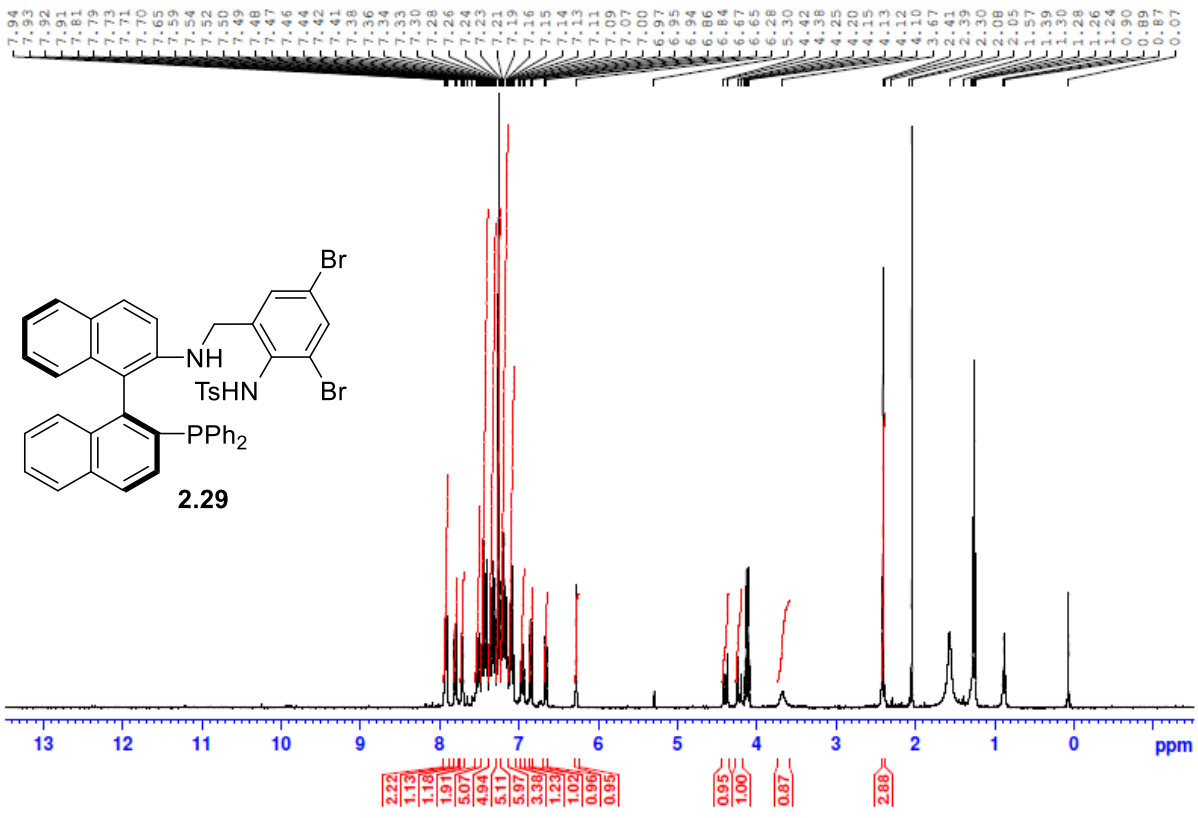

Figure SI-12 ^{1}H NMR spectrum in $CDCl_3$ for catalyst **2.29**.

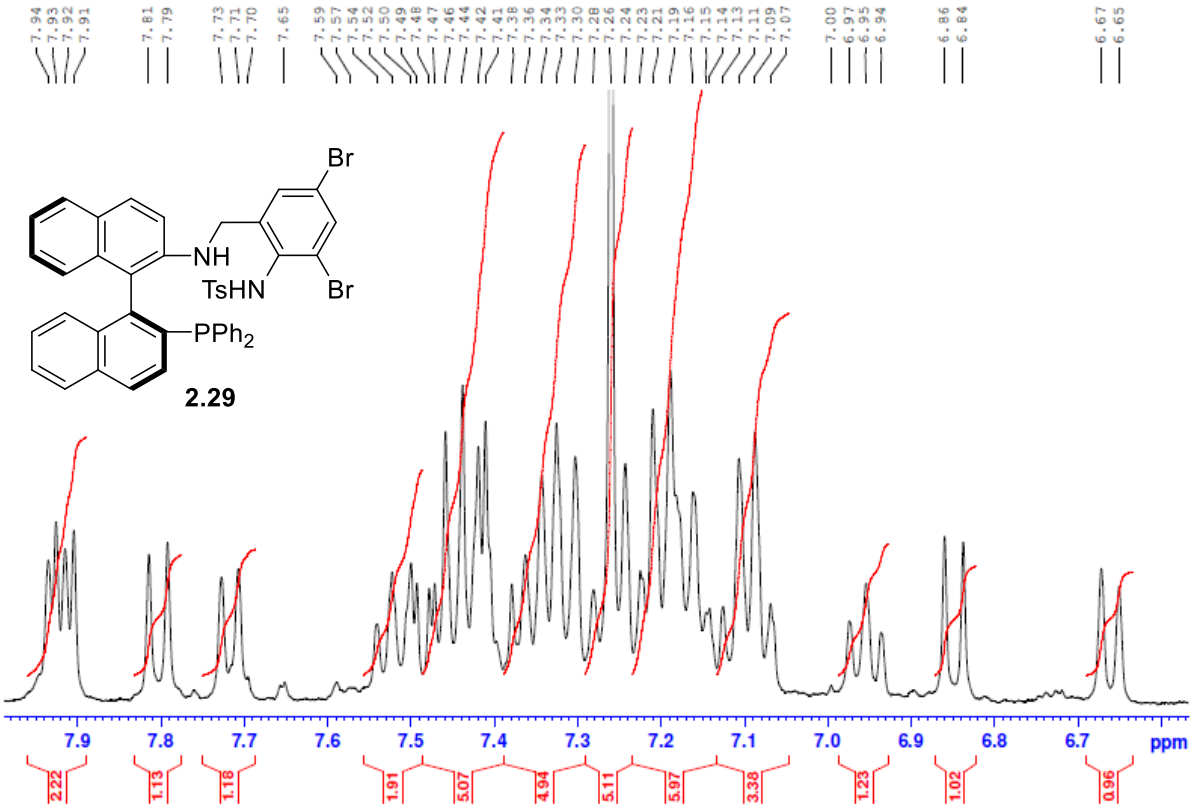

Figure SI-13 Aromatic region of the ^{1}H NMR spectrum in $CDCl_3$ for catalyst **2.29**.

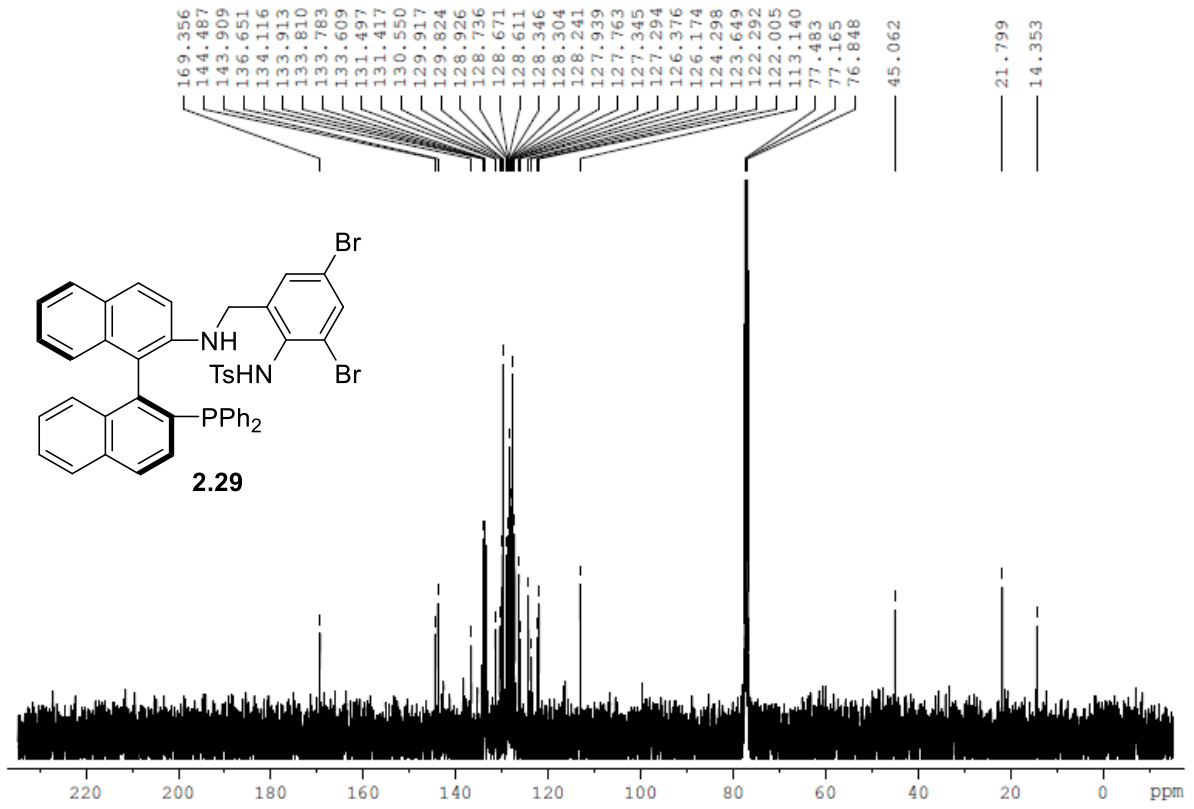

Figure SI-14 ^{13}C NMR spectrum in $CDCl_3$ for catalyst **2.29**.

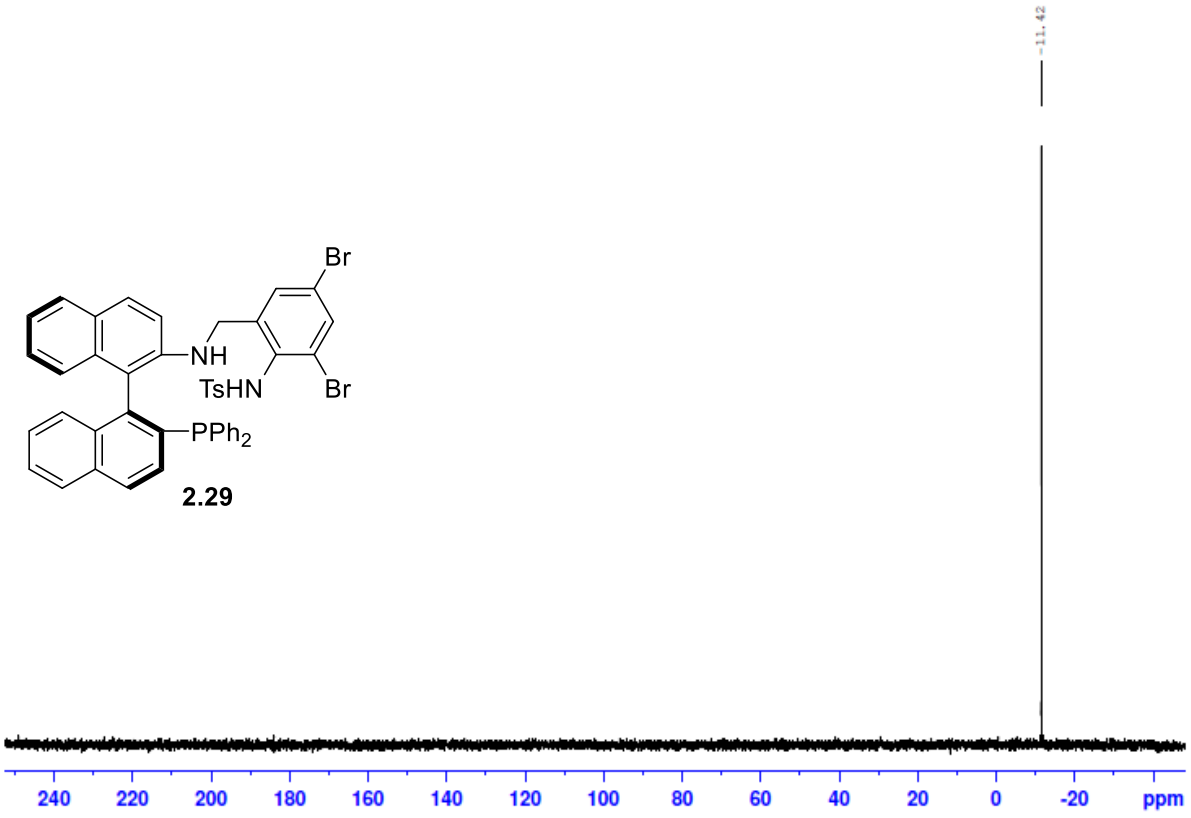

Figure SI-15 ^{31}P NMR spectrum in $CDCl_3$ for catalyst **2.29**.

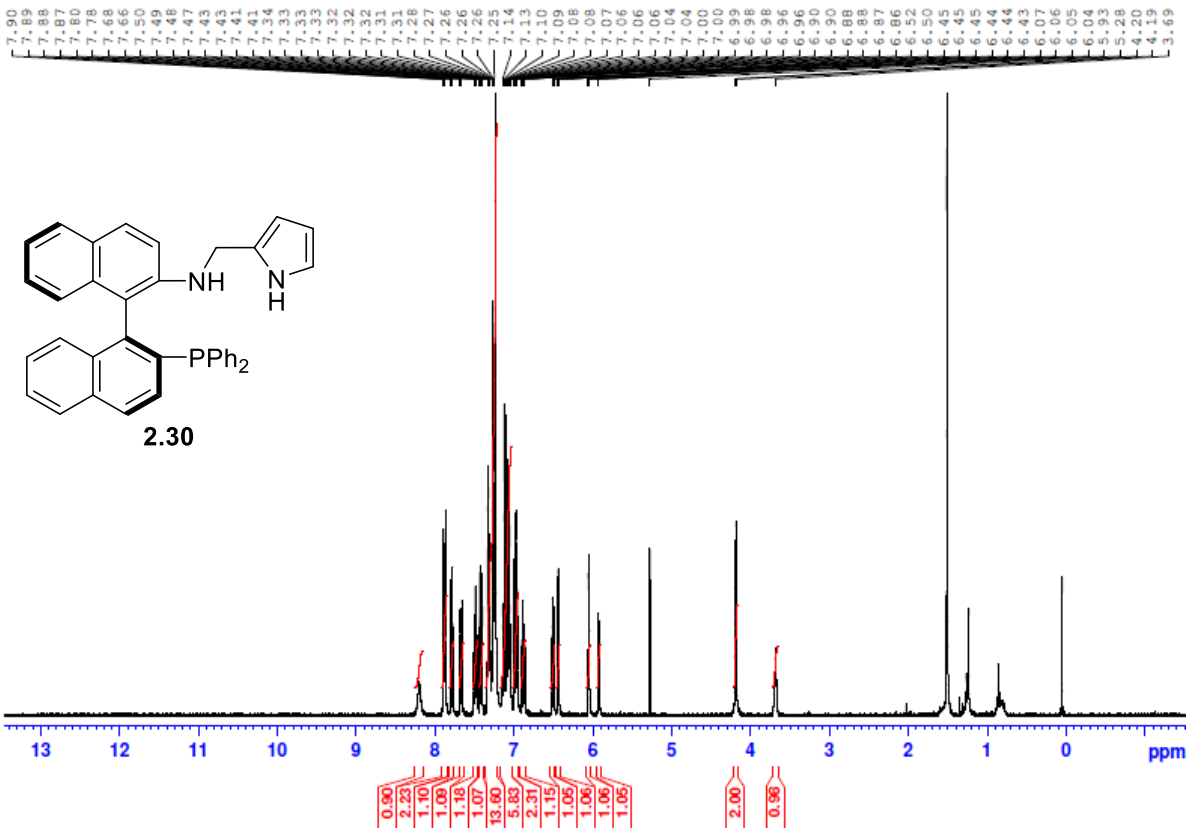

Figure SI-16 ^{1}H NMR spectrum in $CDCl_3$ for catalyst **2.30**.

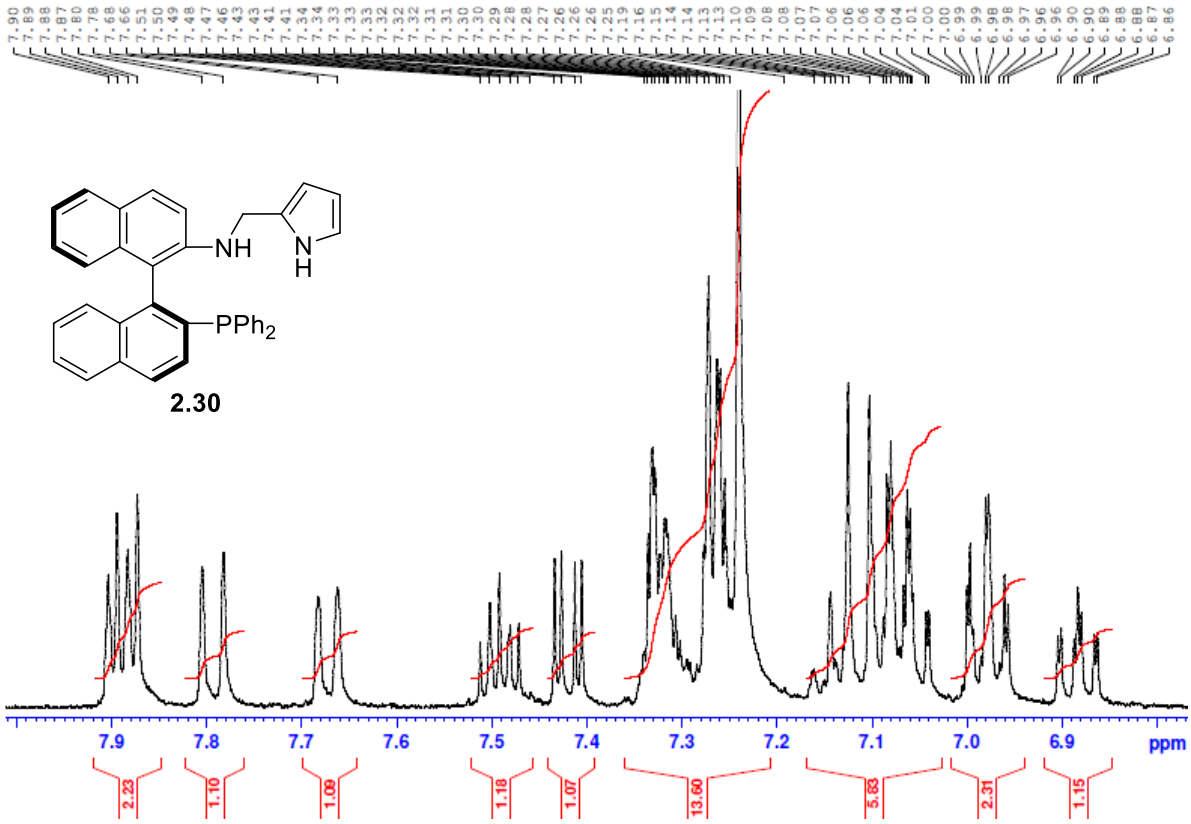

Figure SI-17 Aromatic region of the ^{1}H NMR spectrum in $CDCl_3$ for catalyst **2.30**

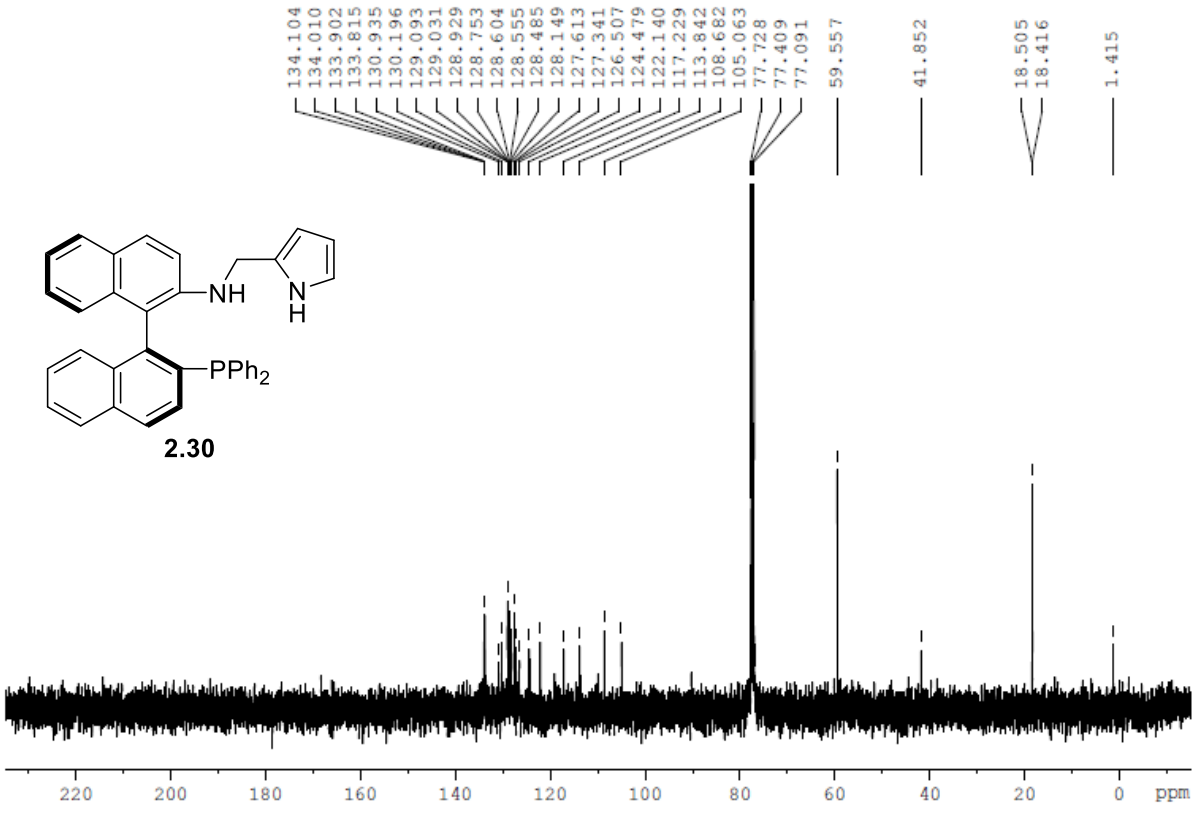

Figure SI-18 ^{13}C NMR spectrum in $CDCl_3$ for catalyst **2.30**

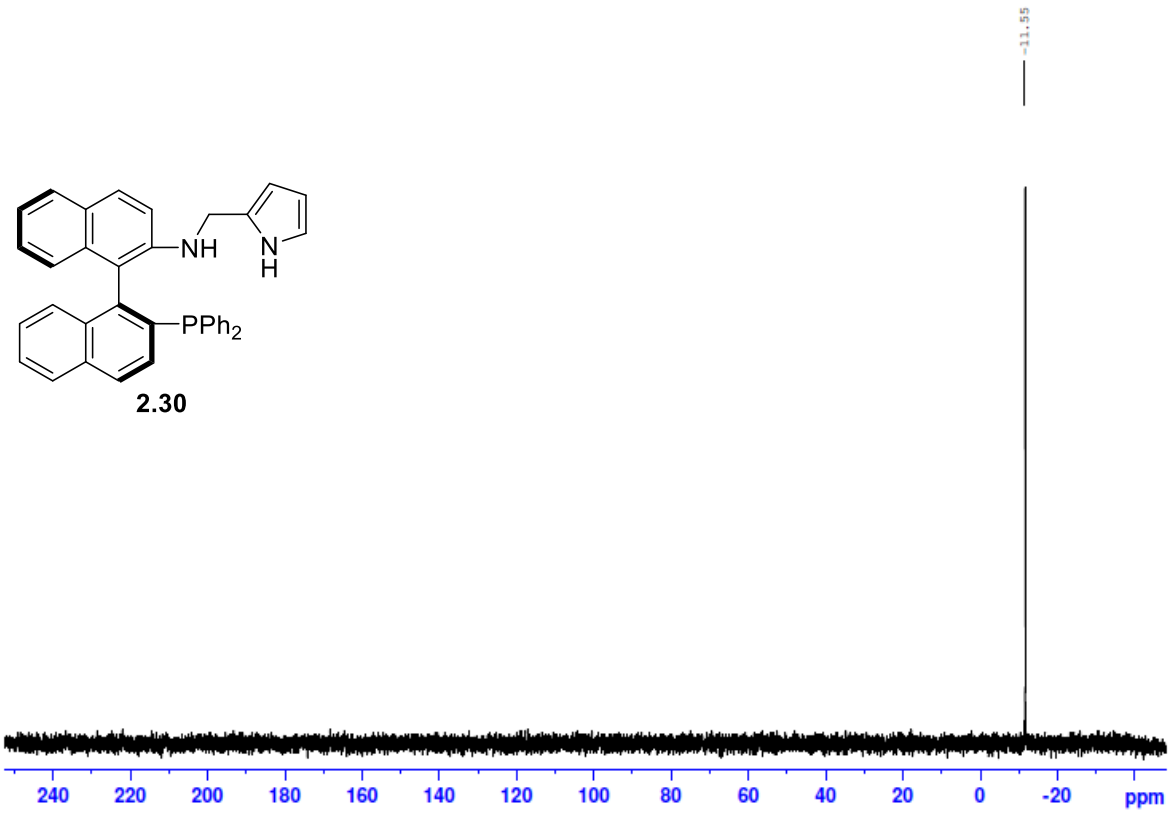

Figure SI-19 ^{31}P NMR spectrum in $CDCl_3$ for catalyst **2.30**

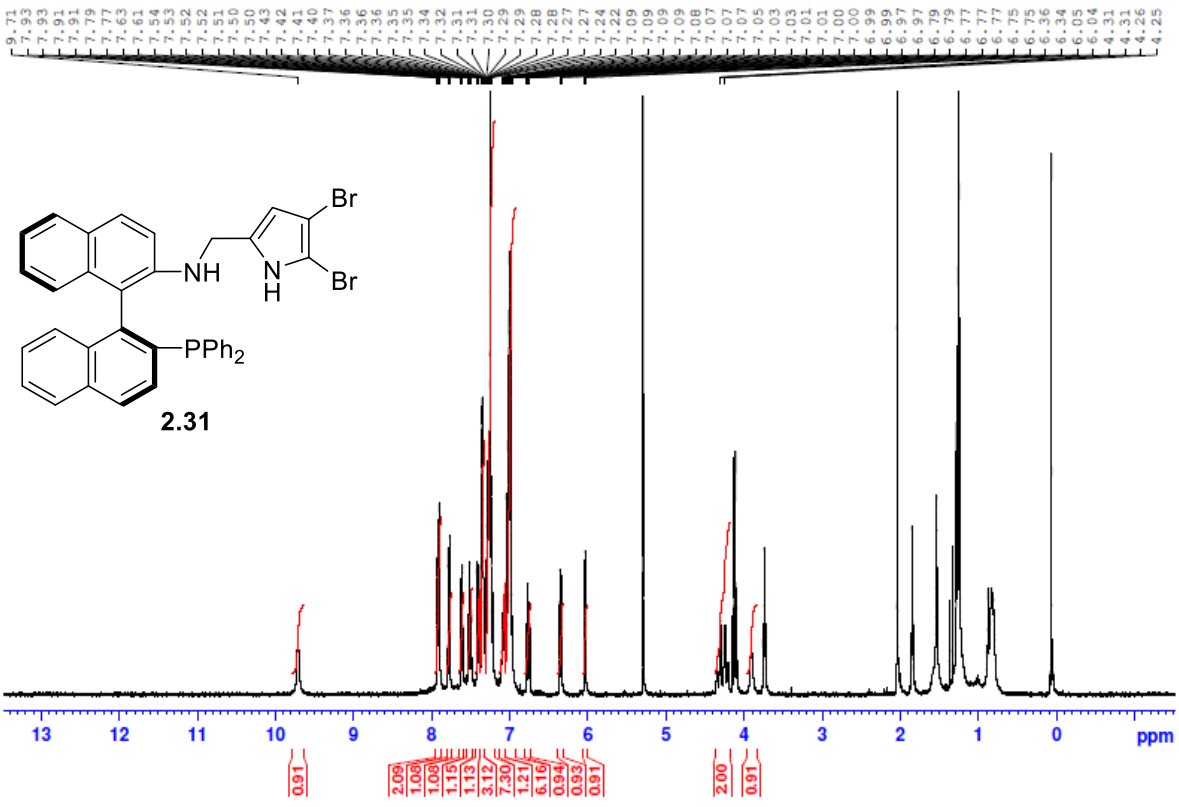

Figure SI-20 ^{1}H NMR spectrum in $CDCl_3$ for catalyst **2.31**

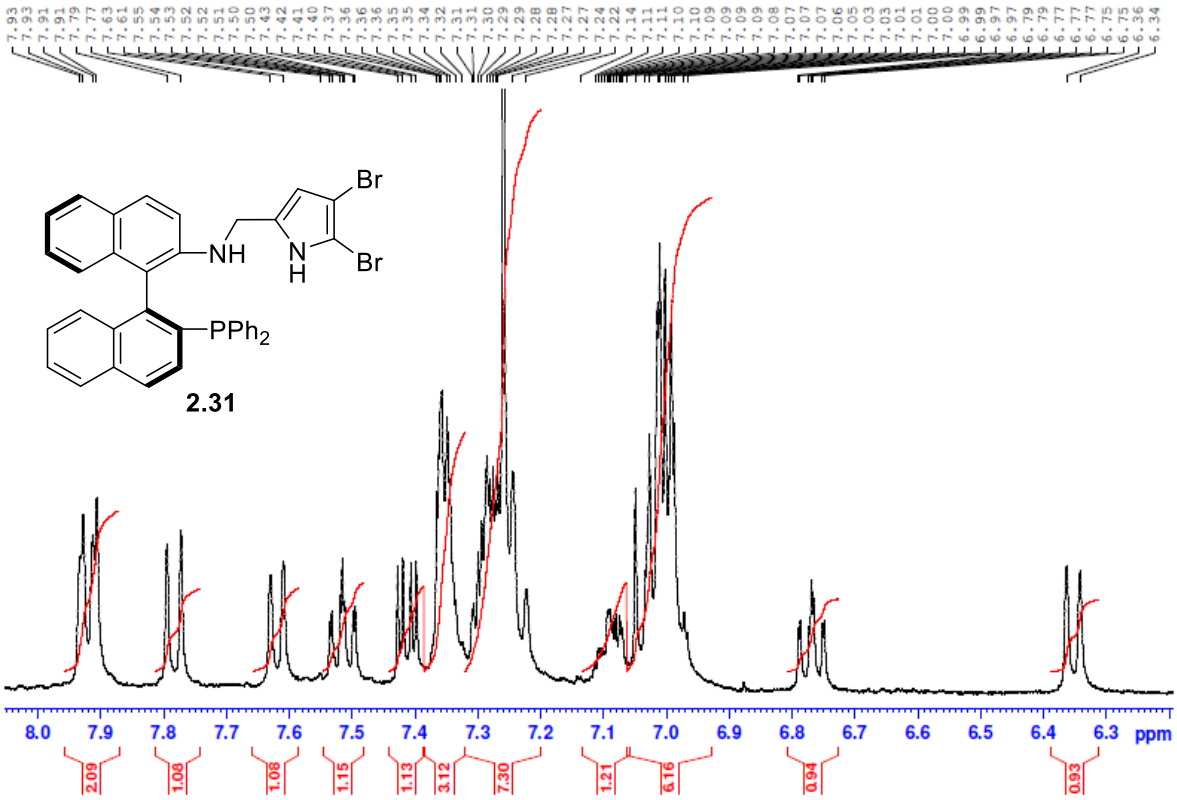

Figure SI-21 Aromatic region of the ^{1}H NMR spectrum in $CDCl_3$ for catalyst **2.31**

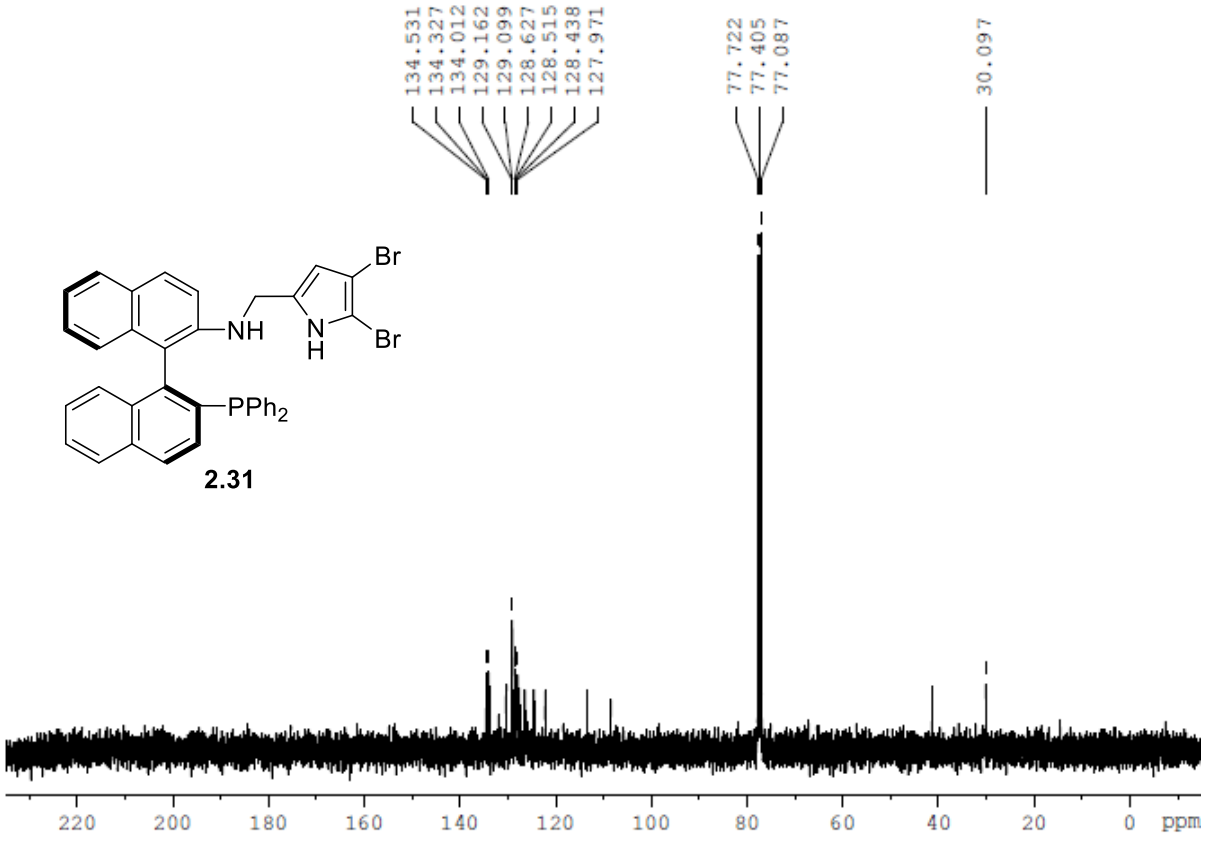

Figure SI-22 ^{13}C NMR spectrum in $CDCl_3$ for catalyst **2.31**

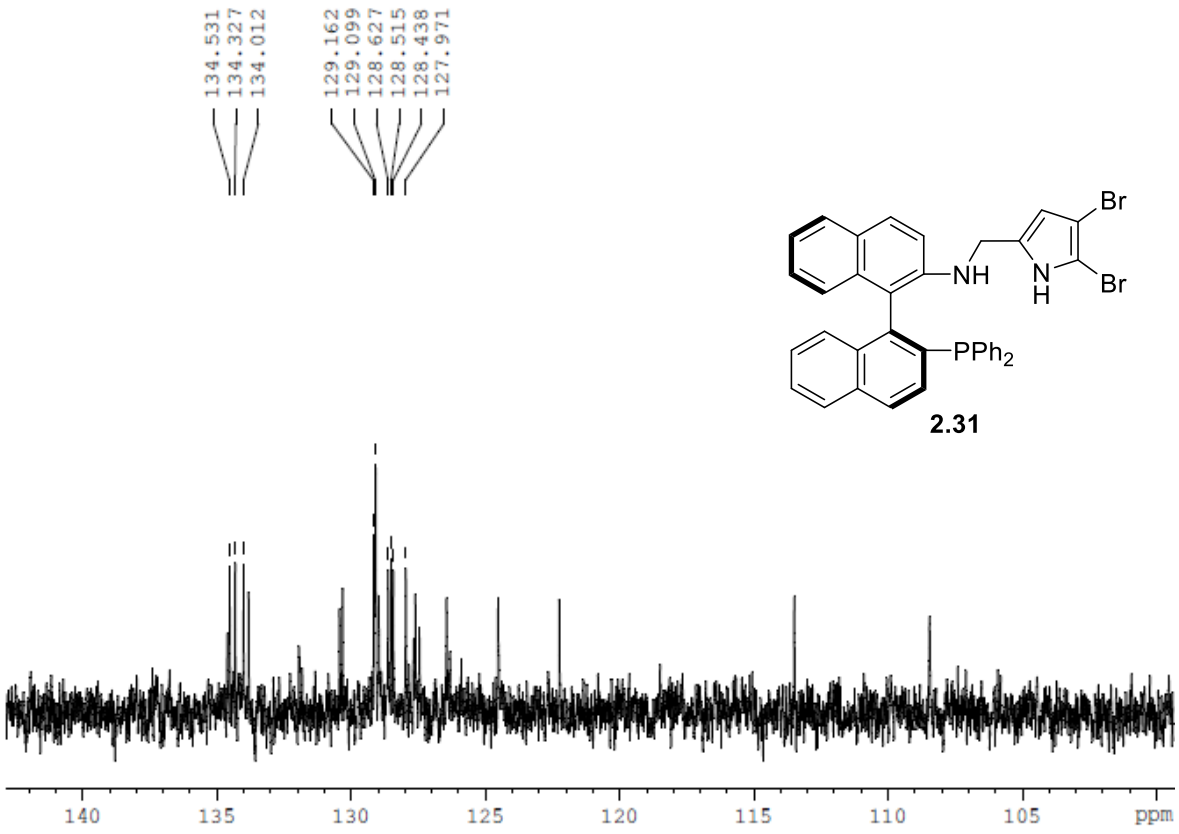

Figure SI-23 Aromatic region of the ^{13}C NMR spectrum in $CDCl_3$ for catalyst **2.31**

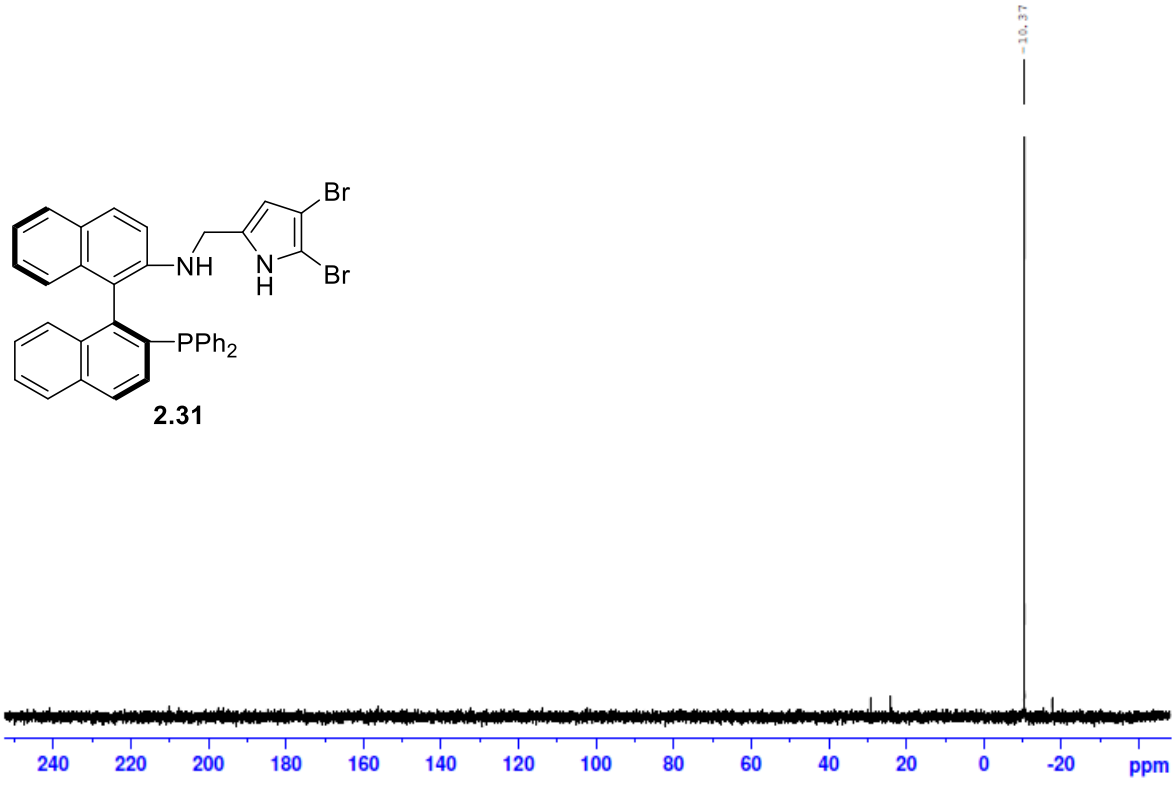

Figure SI-24 ^{31}P NMR spectrum in $CDCl_3$ for catalyst **2.31**